Magnetic Resonance Imaging of Monocyte Infiltration in an Animal Model of Multiple Sclerosis

Raoul Oude Engberink

The work described in this thesis was performed at the Image Sciences Institute, University Medical Center Utrecht and at the Department of Molecular Cell Biology and Immunology, VU Medical Center, Amsterdam.

Cover: MR image of a phantom made of clay, which represents a myelinated axon under attack by clusters of monocytes.

Cover Design: Raoul Oude Engberink and Erwin Blezer

Produced by: F&N Boekservice/Eigen Beheer

ISBN 978907867537 2

Magnetic Resonance Imaging of Monocyte Infiltration in an Animal Model of Multiple Sclerosis

Visualisatie van Monocyten Infiltratie in een Diermodel van Multiple Sclerose met Magnetic Resonance Imaging

(met een samenvatting in het Nederlands)

Proefschrift

ter verkrijging van de graad van doctor aan de Universiteit Utrecht op gezag van de rector magnificus, prof.dr. J.C. Stoof, ingevolge het besluit van het college voor promoties in het openbaar te verdedigen op donderdag 24 april 2008 des middags te 16.15 uur

door

Raoul David Oude Engberink

geboren op 11 juni 1978 te Leiden

Promotoren:	Prof.dr.ir. M.A. Viergever Prof.dr. C.D. Dijkstra
Co-promotoren:	Dr.ir. E.L.A. Blezer Dr. H.E. de Vries

Financial support by the Dutch MS Research Foundation for the publication of this thesis is gratefully acknowledged.

Additional financial support for the publication of this thesis was kindly provided by Philips Medical Systems, Guerbet Nederland B.V., J.E. Jurriaanse Stichting, Röntgen Stichting Utrecht, Bayer Schering Pharma, Harlan Nederland and by ImagO; Research School for Biomedical Image Sciences.

Voor mijn ouders

Contents

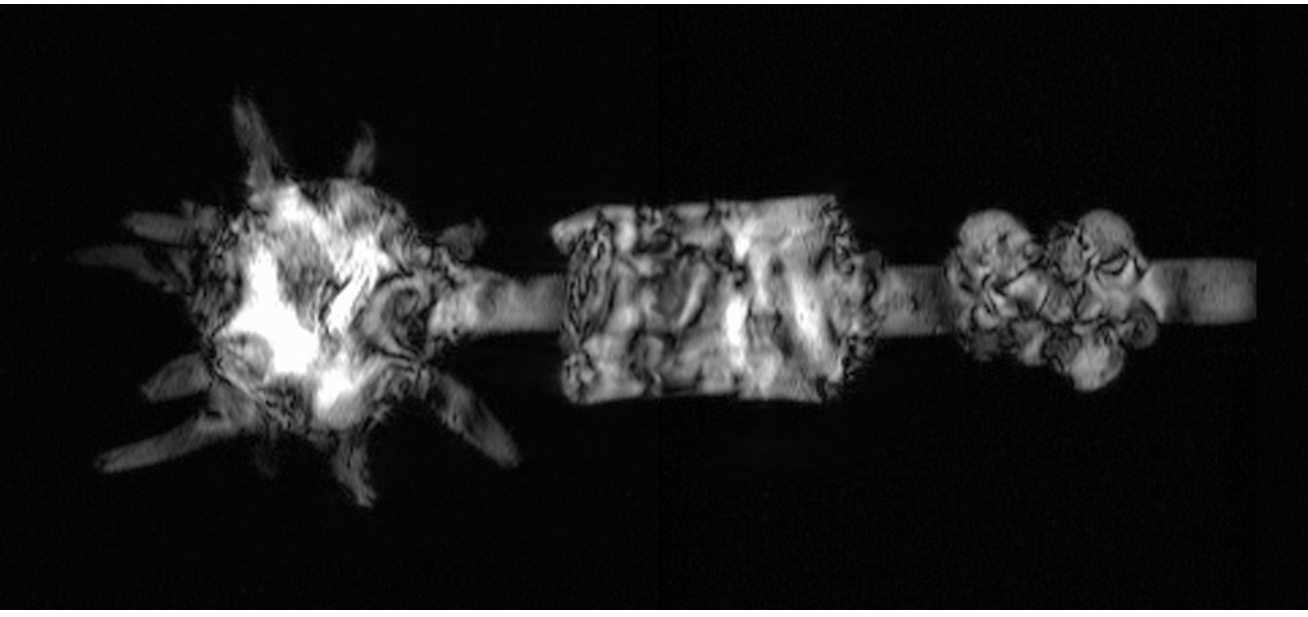

General Introduction

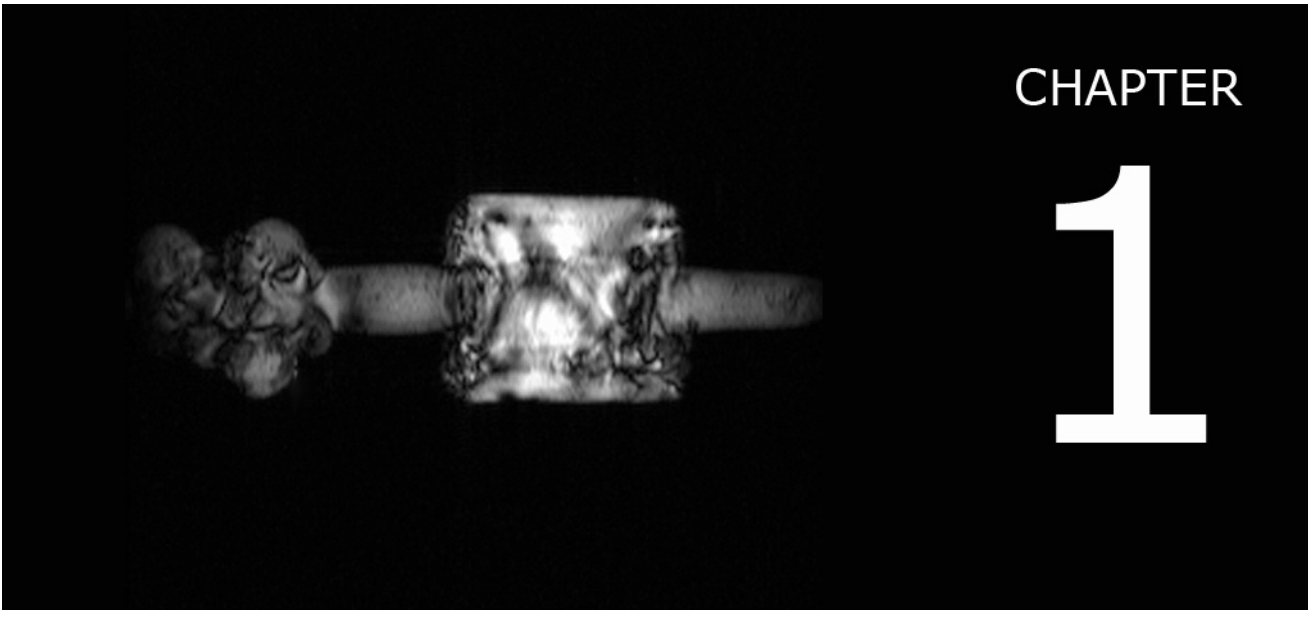

1. Inflammation in the central nervous system

1.1 The importance to study CNS inflammation

The central nervous system (CNS) has long been considered to be an immune privileged site without immune surveillance. This view was supported by the presence of a highly specialized endothelial barrier between blood and brain (the blood-brain-barrier; BBB) which forms tight junctions and prevents uncontrolled influx of molecules and cells into the CNS (Barker and Billingham, 1977). However, experimental evidence from animal studies has challenged this point of view by demonstrating immune cell reactivity in the CNS (Wekerle et al., 1986)(Hickey et al., 1991). It is now clear that immune cells can enter the CNS and generate an inflammatory response. Although the primary purpose of the inflammatory response is the elimination of pathogens, it is nowadays also recognized as a major contributor to the severity of a number of CNS disorders like multiple sclerosis (MS), stroke and Alzheimer's disease (Allan and Rothwell, 2003). There, prolonged neuroinflammation is initiated which is detrimental for the surrounding tissue (Nguyen et al., 2002). Research described in this thesis aims to visualize neuroinflammation at the cellular level, with a focus on monocytes and MS pathology.

1.2 Multiple Sclerosis

MS is an autoimmune disease of the CNS and is characterized by immune cell infiltration, demyelination, axonal damage and progressive neurological disability (Pender and Greer, 2007). A general consensus exists that breakdown of the BBB is an early event in MS leading to the formation of acute inflammatory lesions (Stone et al., 1995). Although the primary cause of MS remains unknown, the most widely accepted view on the pathogenesis of the disease involves a cellular immune response that targets myelin components in the CNS (for a detailed review see: (Lassmann, 1998; Steinman, 1996). Pathological hallmarks, as observed in post-mortem material, are the focal plaques of demyelination in the white matter where inflammation is dominated by presence of lymphocytes and monocytes (Charcot, 1880; Lassmann et al., 2007). Initial T-cell priming may orchestrate an immune attack through the subsequent recruitment of leukocytes.

Especially monocyte-derived-macrophages are suggested to play an important role in lesion development and the breakdown of myelin (Fig 1). This view is based upon previous studies in humans that found incorporated myelin components in infiltrated monocyte-derived-macrophages. Moreover, their presence was related to disease activity and the extent of axonal damage (Bruck et al., 1995; Bruck et al., 1996). Therefore, inhibi-

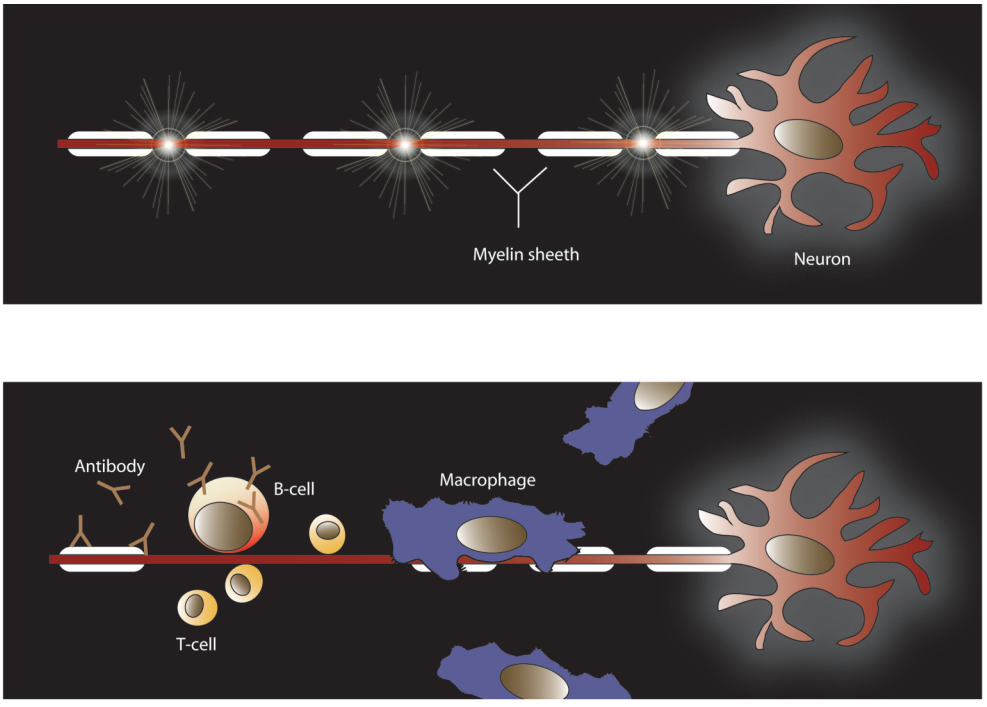

Figure 1: Cartoon of cell recruitment and resulting demyelination. The upper panel represents a healthy neuron conducting electrical impulses. The lower panel represents pathological events during demyelination. Note the breakdown of the protective myelin sheet, which is vital for the physiological function of neurons.

tion of monocyte infiltration is considered an attractive therapeutic strategy to limit the inflammatory response. A number of treatment studies in MS patients have focused on diminishing migratory capacity of peripheral blood mononuclear cells by immunomodulation (Corsini et al., 1997; Floris et al., 2002; Pender and Wolfe, 2002). More recently, the crucial function of inflammation in MS was demonstrated by the beneficial clinical effect of natalizumlab therapy that directly blocks the cell adhesion molecule family alpha-4 integrins (Niino et al., 2006; Polman et al., 2006).
The trigger that drives the inflammatory response remains elusive but is likely to involve both environmental factors and genetic factors that predispose to autoimmunity in general (Compston and Coles, 2002; Giovannoni and Ebers, 2007). The existing view on the pathogenesis of MS is still changing and identification of infectious agents as well as immune cell trafficking in and out of the CNS are under current investigation. In this view, the role of lymphoid organs is of particular interest because immune responses are the result of antigen recognition and priming of T-cells in these structures. Especially the cervical lymph nodes (CLN) that are in fact the first draining site of the brain may play a role in the maintenance and

expansion of local autoimmune responses in MS (Fabriek et al., 2005; Weller, 1998). Much of the evidence that supports the role for an autoimmune-mediated response in the pathogenesis of MS comes from the ability to immunize experimental animals with proteins derived from CNS myelin that result in similar neuropathologic features as those of MS.

1.3 Experimental autoimmune encephalomyelitis: Animal model to study monocyte migration

Important findings on immune cell-mediated inflammation have been obtained in the animal model for MS, experimental autoimmune encephalomyelitis (EAE). EAE is induced in various laboratory animals through immunization with myelin components or transfer of encephalitogenic T-cells. As a result EAE has clinical and histopathological similarities to MS (Owens and Sriram, 1995; Raine, 1984). However, it is important to underline the key difference between EAE and MS: in EAE active immunization or transfer of T-cells cause autoimmunity whereas in MS the cause of autoimmunity is unknown and the animal model does not reflect the complete pathological spectrum of MS.
In this thesis we use the acute EAE model which is induced in Lewis rats by active immunization with myelin components (myelin basic protein) together with a strong adjuvant (Gold et al., 2000; van der Goes and Dijkstra, 2001). The disease in this specific model is characterized by a highly reproducible mono-phasic disease course that mimics important pathological events in MS like increased BBB permeability and cellular infiltration. The importance of monocytes in inflammation and especially in lesion development was demonstrated in this model. Depletion of monocytes from the circulation led to a reduction or even a complete absence of neurological deficits, whereas T-cells still gained access to the brain (Brosnan et al., 1981; Huitinga et al., 1990; Tran et al., 1998). A critical step for monocytes that contribute to inflammation and lesion development is their migration over the BBB. Therefore, it is essential to investigate how and when these cells gain access to the CNS. Previously, in our lab the initial steps of monocyte adhesion to and the migration across brain endothelium were investigated (Floris et al., 2002; Floris et al., 2003). To elaborate on the role of monocytes during CNS inflammation we focused on the visualization of monocyte infiltration in vivo in a longitudinal fashion.

Summarizing, experimental evidence has emphasized the crucial role of monocytes in neuroinflammation and extensive research has been performed to elucidate the molecular mechanisms that facilitate monocyte entry in the CNS. However, since much of our current knowledge comes from histological studies, little is known on the time-window in which monocytes cross the BBB and exploit their destructive properties. Histol-

ogy can only provide us with a snapshot view of cellular localization. The ability of tracking monocytes longitudinally would be of great interest for these studies and helps understanding the cellular pathology of neuroinflammation. To study the dynamic processes of cell migration, there is an emerging need to develop non-invasive imaging strategies that allow monitoring these processes in vivo.

2. Magnetic resonance imaging in neuroinflammation

2.1 Imaging strategy

To monitor cell migration in vivo non-invasively, it is essential to have specific labeling techniques and sensitive imaging strategies. Currently, a few in vivo cell imaging modalities exist: (1) nuclear (Bogdanov and Weissleder, 1998), (2) optical (Benaron, 1994; Contag et al., 1998) and (3) magnetic resonance imaging (MRI), each with their particular advantages and disadvantages. In numerous applications, MRI is preferred over other modalities because of its high anatomical resolution and its multifunctionality. In principle, one can monitor anatomy, metabolism, physiology and function with the same technique. MRI is used both in an experimental as a clinical setting which facilitates bench to bedside implementation. Taken together, MRI is a promising candidate to study monocyte trafficking in vivo.

It is not within the scope of this thesis to provide a complete technical insight, but merely a simplified overview on the use of MRI to study biological processes in vivo. Detailed information on the physics part of nuclear magnetic resonance and its role in MRI has been described in several textbooks (see for example: The Basics of MRI by Joseph P. Hornak, available online at www.cis.rit.edu/htbooks/mri/). The understanding of nuclear spin was one of the major steps in physics that has ultimately led to the full potential of MRI. Our body consists of billions of small magnetic spheres (nuclear spins of hydrogen nuclei) which are specifically oriented when placed in an external magnetic field resulting in a net magnetic moment. Exposing the body to radio frequency (RF) wavelengths will disturb this magnetic moment. Subsequently, after turning off this RF exposure, excited protons will return to their original orientation and this process of relaxation causes a typical MR signal. It was soon recognized that this MR signal was dependent on the biological environment of the hydrogen nuclei. Nowadays MR imaging systems are capable of producing soft tissue contrast images that are superior to other imaging techniques.

2.2 Magnetic resonance imaging of pathological tissue

MRI has become a powerful tool to visualize pathological processes in a non-invasive manner in experimental models of brain disorders (reviewed in Dijkhuizen and Nicolay, 2003). In a clinical setting, early studies showed that MRI is a sensitive method to detect different types of cerebral infarcts in stroke patients (Kertesz et al., 1987). Moreover, MRI has developed into an important tool to diagnose MS patients by visualization of contrast changes in the CNS indicative for neuropathological changes (Filippi et al., 2002; Gebarski et al., 1985; McDonald et al., 2001). Contrast agents were developed to improve the sensitivity and specificity of MRI. For example Gadolinium (Gd) complexed to chelating agents like diethylenetriamine penta-acetic (Gd-DTPA; 550Da) can be applied intravenously and after extravasation, Gd-DTPA will influence tissue relaxation properties (Daldrup-Link and Brasch, 2003) (Weinmann et al., 1984). Typically, Gd-DTPA enhanced MRI is used to study BBB integrity during neuroinflammation as it can leak though an impaired BBB. Especially for MS research, this technique is routinely used for diagnosis, establishment of disease severity and detection of active inflammatory lesions in the CNS (Barkhof et al., 1992; Grossman et al., 1986).

2.3 Cellular magnetic resonance imaging

Recently, MRI has been extended with the concept of cellular imaging. Specific procedures have been developed to label cells of interest with MR contrast agents. Gd-DTPA, as described in the previous paragraph, is not incorporated by cells and therefore provides no cell-specific information. However, a different type of contrast agent, the superparamagnetic particles of iron oxides (SPIO), has been successfully applied for cellular MRI (Bulte and Kraitchman, 2004). SPIO consist of an iron oxide core coated

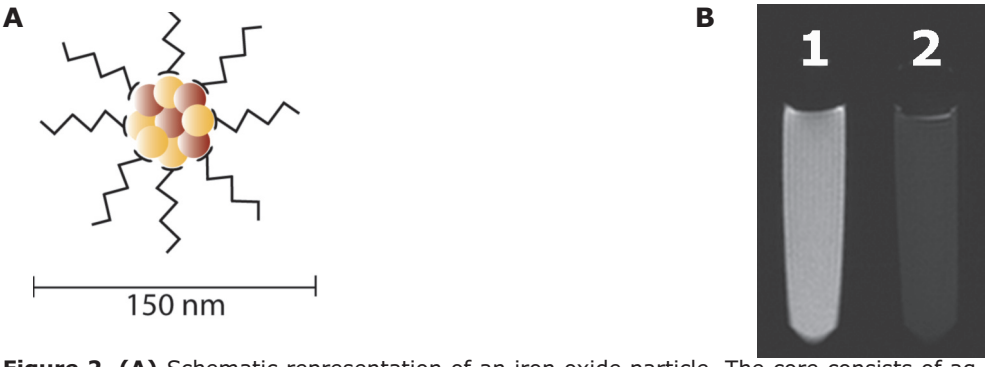

Figure 2. (A) Schematic representation of an iron oxide particle. The core consists of aggregates of iron oxides, Fe_2O_3 and Fe_3O_4 coated by dextran chains. **(B)** T_2-weighted MR image of two plastic vials. Vial 1 contains an agar-gel solution and vial 2 contains the same solution mixed with iron oxide particles. The presence of iron oxide particles decreases MR signal intensity and is detected as hypointense area on T_2-weighted images.

with dextran and vary in size from nanometer to micrometer (Fig 2A). SPIO with a diameter smaller than 50nm are usually termed ultra small SPIO (USPIO). Iron oxide particles predominantly shorten the T_2 and T_2* relaxation times of protons in their proximity (Renshaw et al., 1986), visualized as areas of signal loss on a $T_2^{(*)}$-weighted MR image (Fig 2B).

2.4 Cell tracking methods

Since iron oxide particles induce changes in MR signal intensity, labeling cells with these contrast agents provides the opportunity to visualize cells with MRI. In this thesis, we explored the use of iron oxide particles to label monocytes and study their migration in vivo. In theory, cell tracking methods using iron oxide particles can be divided into two main approaches: (1) the contrast agent is administered intravenously after which it is generally believed that monocytes incorporate the iron oxide particles in circulation. (2) Monocytes are isolated first, labeled ex vivo and re-introduced in the organism (Fig 3).

With respect to the first approach, the larger sized SPIO have primarily been developed as specific contrast agents for liver and spleen (Stark et al., 1988; Weissleder, 1994). After administration, they accumulate in the mononuclear phagocytic system of liver (Kupffer cells) and spleen. The half-life in circulation for these compounds is therefore relatively low. In

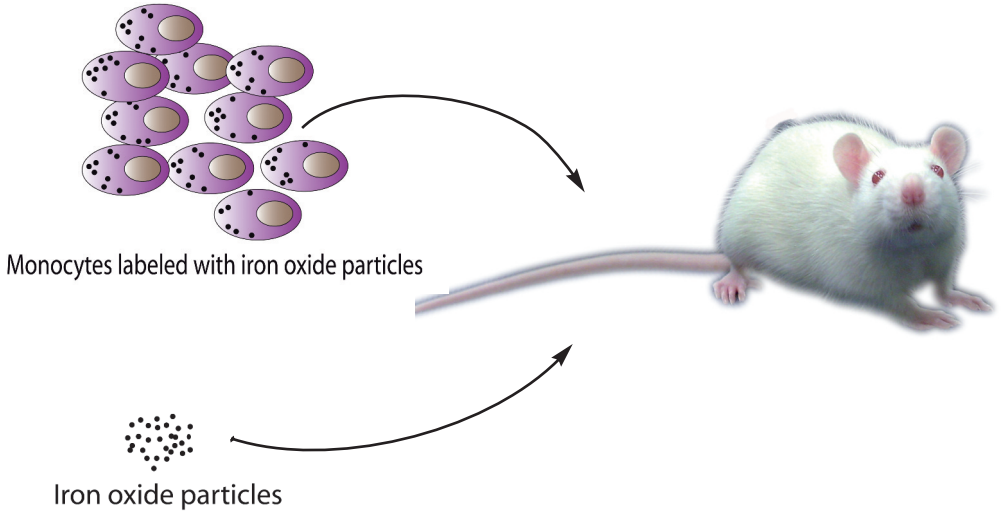

Figure 3: Graphical representation of two methods to perform cellular imaging in an experimental setting: Injection of monocytes labeled with iron oxide particles versus the direct injection of the MR contrast agents. MR imaging at later time points may reveal changes in signal intensity in the CNS at inflammatory sites.

contrast, the smaller sized USPIO have a much longer blood half-life as they do not accumulate in these organs as fast as larger particles. Therefore, USPIO are used as contrast agents for lymph nodes and bone marrow (Weissleder et al., 1990). Due to their prolonged half-life, USPIO have also been applied to study the macrophage activity in experimental models of neuroinflammation (Bulte and Kraitchman, 2004; Corot et al., 2006). Previously, we and others have shown in EAE that USPIO injections resulted in decreased signal intensities in the brain 24h after administration, indicative for cellular infiltration (Dousset et al., 1999; Floris et al., 2004). However, next to the migration of peripherally labeled cells several other uptake mechanisms during neuroinflammation have to be considered, like leakage into the brain parenchyma over an impaired BBB and non-specific labeling of other cell types.
The second approach to visualize monocytes in vivo, i.e. ex vivo labeling and subsequent re-injection of labeled monocytes may be more specific. It is crucial in this type of experiments to develop an efficient labeling strategy that results in a high amount of contrast agent per cell to ensure optimal MR detection. In addition, it is important that the labeling procedure and the incorporated contrast agent do not influence the physiological functions of the cell. Therefore, a first step towards cellular MRI is the design of a labeling strategy that results in a proper balance between iron incorporation and cell function.

3. Aim and outline

The research described in this thesis focused on MRI as non-invasive imaging modality to visualize monocyte infiltration in the CNS during neuroinflammatory conditions. The goal was to unravel the time window of monocyte migration in an animal model of neuroinflammation, which would be of great therapeutic interest to monitor the effectiveness of anti-inflammatory drugs and optimize timing of administration.
To detect monocytes with MRI it is essential to label the cells with a significant amount of contrast agent without affecting physiological function. Therefore, **chapter 2** describes the procedures to label human monocytes efficiently and testing USPIO and SPIO with or without chemical adjuvants. Labeling efficiency was quantified by MRI and biological assays were performed to assess monocyte function. This resulted in an optimized protocol to label human monocytes, which was subsequently adapted to label freshly isolated rat monocytes in **chapter 3**. There, we established proof of principle for in vivo cell tracking of SPIO-labeled monocytes in a rat model of local neuroinflammation. Following intravenous injection, infiltration of SPIO-labeled monocytes was monitored longitudinally towards a

focal lesion in the cortex. Moreover, the time window of signal changes in the inflammatory area as a result of labeled monocytes was compared to signal changes following injection of the free label.
Although successful in animals with a relatively large and well-defined lesion, we were not able to detect the migration of SPIO-labeled monocytes in EAE rats applying similar labeling and re-injection procedures. Therefore, in **chapter 4** we describe a novel labeling technique, magneto-electroporation (MEP). We investigated if MEP improves uptake of iron oxide particles by monocytes and thereby facilitates the detection of small infiltrates of monocytes distributed over brain and spinal cord in EAE rats. Infiltration of monocytes, labeled with iron oxide particles using MEP, was monitored at different stages of the disease course and validated by ex vivo high resolution MRI and histology.

In contrast to isolating monocytes, ex vivo labeling and subsequent re-injection, a different approach is the injection of free particles into circulation. However, much is unknown concerning cerebral USPIO uptake and distribution in vivo. There are various ways that iron oxide particles can enter the brain parenchyma through an impaired BBB. To shed some light on USPIO kinetics in vivo, we investigated in **chapter 5** USPIO entrance and persistence in the CNS of EAE rats. Brain and spinal cord were imaged directly after intravenous USPIO administration and correlated to USPIO positive areas at later time points. In addition, a potential mechanism for USPIO efflux out of the brain was studied by simultaneous imaging of the cervical lymph nodes.
Inspired by the ability of USPIO to detect inflammatory lesions and given their clinical safety, **chapter 6** describes signal changes in the brains of MS patients following intravenous USPIO injections. We studied whether USPIO positive areas can reveal different stages of lesion development in humans.
Chapter 7 summarizes results obtained from the initial monocyte labeling studies to in vivo application. Important pitfalls are discussed for cell tracking studies in general and where we stand now concerning bedside implementation.

REFERENCES

Allan SM, Rothwell NJ. Inflammation in central nervous system injury. Philos Trans R Soc Lond B Biol Sci 2003; 358: 1669-77.

Barker CF, Billingham RE. Immunologically privileged sites. Adv Immunol 1977; 25: 1-54.

Barkhof F, Scheltens P, Frequin ST, Nauta JJ, Tas MW, Valk J, et al. Relapsing-remitting multiple sclerosis: sequential enhanced MR imaging vs clinical findings in determining disease activity. AJR Am J Roentgenol 1992; 159: 1041-7.

Benaron DA. Optical imaging reborn with technical advances. Diagn Imaging (San Franc) 1994; 16: 69-76.

Bogdanov A, Jr., Weissleder R. The development of in vivo imaging systems to study gene expression. Trends Biotechnol 1998; 16: 5-10.

Brosnan CF, Bornstein MB, Bloom BR. The effects of macrophage depletion on the clinical and pathologic expression of experimental allergic encephalomyelitis. J Immunol 1981; 126: 614-20.

Bruck W, Porada P, Poser S, Rieckmann P, Hanefeld F, Kretzschmar HA, et al. Monocyte/macrophage differentiation in early multiple sclerosis lesions. Ann Neurol 1995; 38: 788-96.

Bruck W, Sommermeier N, Bergmann M, Zettl U, Goebel HH, Kretzschmar HA, et al. Macrophages in multiple sclerosis. Immunobiology 1996; 195: 588-600.

Bulte JW, Kraitchman DL. Iron oxide MR contrast agents for molecular and cellular imaging. NMR Biomed 2004; 17: 484-99.

Charcot JM. Lecons sur les maladies du systeme nerveux faites a la Salpetriere. Tome 1. Vol Bureau du Progres Medical: V.A. Delahaye et Co., 1880: Paris.

Compston A, Coles A. Multiple sclerosis. Lancet 2002; 359: 1221-31.

Contag PR, Olomu IN, Stevenson DK, Contag CH. Bioluminescent indicators in living mammals. Nat Med 1998; 4: 245-7.

Corot C, Robert P, Idee JM, Port M. Recent advances in iron oxide nanocrystal technology for medical imaging. Adv Drug Deliv Rev 2006; 58: 1471-504.

Corsini E, Gelati M, Dufour A, Massa G, Nespolo A, Ciusani E, et al. Effects of beta-IFN-1b treatment in MS patients on adhesion between PBMNCs, HUVECs and MS-HBECs: an in vivo and in vitro study. J Neuroimmunol 1997; 79: 76-83.

Daldrup-Link HE, Brasch RC. Macromolecular contrast agents for MR mammography: current status. Eur Radiol 2003; 13: 354-65.

Dijkhuizen RM, Nicolay K. Magnetic resonance imaging in experimental models of brain disorders. J Cereb Blood Flow Metab 2003; 23: 1383-402.

Dousset V, Delalande C, Ballarino L, Quesson B, Seilhan D, Coussemacq M, et al. In vivo macrophage activity imaging in the central nervous system detected by magnetic resonance. Magn Reson Med 1999; 41: 329-33.

Fabriek BO, Zwemmer JN, Teunissen CE, Dijkstra CD, Polman CH, Laman JD, et al. In vivo detection of myelin proteins in cervical lymph nodes of MS patients using ultrasound-guided fine-needle aspiration cytology. J Neuroimmunol 2005; 161: 190-4.

Filippi M, Dousset V, McFarland HF, Miller DH, Grossman RI. Role of magnetic resonance imaging in the diagnosis and monitoring of multiple sclerosis: consensus report of the White Matter Study Group. J Magn Reson Imaging 2002; 15: 499-504.

Floris S, Blezer EL, Schreibelt G, Dopp E, van der Pol SM, Schadee-Eestermans IL, et al. Blood-brain barrier permeability and monocyte infiltration in experimental allergic encephalomyelitis: a quantitative MRI study. Brain 2004; 127: 616-27.

Floris S, Ruuls SR, Wierinckx A, van der Pol SM, Dopp E, van der Meide PH, et al. Interferon-beta directly influences monocyte infiltration into the central nervous system. J Neuroimmunol 2002; 127: 69-79.

Floris S, van den Born J, van der Pol SM, Dijkstra CD, De Vries HE. Heparan sulfate proteoglycans modulate monocyte migration across cerebral endothelium. J Neuropathol Exp Neurol 2003; 62: 780-90.

Gebarski SS, Gabrielsen TO, Gilman S, Knake JE, Latack JT, Aisen AM. The initial diagnosis of multiple sclerosis: clinical impact of magnetic resonance imaging. Ann Neurol 1985; 17: 469-74.
Giovannoni G, Ebers G. Multiple sclerosis: the environment and causation. Curr Opin Neurol 2007; 20: 261-8.
Gold R, Hartung HP, Toyka KV. Animal models for autoimmune demyelinating disorders of the nervous system. Mol Med Today 2000; 6: 88-91.
Grossman RI, Gonzalez-Scarano F, Atlas SW, Galetta S, Silberberg DH. Multiple sclerosis: gadolinium enhancement in MR imaging. Radiology 1986; 161: 721-5.
Hickey WF, Hsu BL, Kimura H. T-lymphocyte entry into the central nervous system. J Neurosci Res 1991; 28: 254-60.
Huitinga I, van Rooijen N, de Groot CJ, Uitdehaag BM, Dijkstra CD. Suppression of experimental allergic encephalomyelitis in Lewis rats after elimination of macrophages. J Exp Med 1990; 172: 1025-33.
Kertesz A, Black SE, Nicholson L, Carr T. The sensitivity and specificity of MRI in stroke. Neurology 1987; 37: 1580-5.
Lassmann H. Neuropathology in multiple sclerosis: new concepts. Mult Scler 1998; 4: 93-8.
Lassmann H, Bruck W, Lucchinetti CF. The immunopathology of multiple sclerosis: an overview. Brain Pathol 2007; 17: 210-8.
McDonald WI, Compston A, Edan G, Goodkin D, Hartung HP, Lublin FD, et al. Recommended diagnostic criteria for multiple sclerosis: guidelines from the International Panel on the diagnosis of multiple sclerosis. Ann Neurol 2001; 50: 121-7.
Nguyen MD, Julien JP, Rivest S. Innate immunity: the missing link in neuroprotection and neurodegeneration? Nat Rev Neurosci 2002; 3: 216-27.
Niino M, Bodner C, Simard ML, Alatab S, Gano D, Kim HJ, et al. Natalizumab effects on immune cell responses in multiple sclerosis. Ann Neurol 2006; 59: 748-54.
Owens T, Sriram S. The immunology of multiple sclerosis and its animal model, experimental allergic encephalomyelitis. Neurol Clin 1995; 13: 51-73.
Pender MP, Greer JM. Immunology of multiple sclerosis. Curr Allergy Asthma Rep 2007; 7: 285-92.
Pender MP, Wolfe NP. Prevention of autoimmune attack and disease progression in multiple sclerosis: current therapies and future prospects. Intern Med J 2002; 32: 554-63.
Polman CH, O'Connor PW, Havrdova E, Hutchinson M, Kappos L, Miller DH, et al. A randomized, placebo-controlled trial of natalizumab for relapsing multiple sclerosis. N Engl J Med 2006; 354: 899-910.
Raine CS. Biology of disease. Analysis of autoimmune demyelination: its impact upon multiple sclerosis. Lab Invest 1984; 50: 608-35.
Renshaw PF, Owen CS, McLaughlin AC, Frey TG, Leigh JS, Jr. Ferromagnetic contrast agents: a new approach. Magn Reson Med 1986; 3: 217-25.
Stark DD, Weissleder R, Elizondo G, Hahn PF, Saini S, Todd LE, et al. Superparamagnetic iron oxide: clinical application as a contrast agent for MR imaging of the liver. Radiology 1988; 168: 297-301.
Steinman L. Multiple sclerosis: a coordinated immunological attack against myelin in the central nervous system. Cell 1996; 85: 299-302.
Stone LA, Smith ME, Albert PS, Bash CN, Maloni H, Frank JA, et al. Blood-brain barrier disruption on contrast-enhanced MRI in patients with mild relapsing-remitting multiple sclerosis: relationship to course, gender, and age. Neurology 1995; 45: 1122-6.
Tran EH, Hoekstra K, van Rooijen N, Dijkstra CD, Owens T. Immune invasion of the central nervous system parenchyma and experimental allergic encephalomyelitis, but not leukocyte extravasation from blood, are prevented in macrophage-depleted mice. J Immunol 1998; 161: 3767-75.
van der Goes A, Dijkstra CD. Models for demyelination. Prog Brain Res 2001; 132: 149-63.
Weinmann HJ, Brasch RC, Press WR, Wesbey GE. Characteristics of gadolinium-DTPA complex: a potential NMR contrast agent. AJR Am J Roentgenol 1984; 142: 619-24.
Weissleder R. Liver MR imaging with iron oxides: toward consensus and clinical practice. Ra-

diology 1994; 193: 593-5.
Weissleder R, Elizondo G, Wittenberg J, Rabito CA, Bengele HH, Josephson L. Ultrasmall superparamagnetic iron oxide: characterization of a new class of contrast agents for MR imaging. Radiology 1990; 175: 489-93.
Wekerle H, Schwab M, Linington C, Meyermann R. Antigen presentation in the peripheral nervous system: Schwann cells present endogenous myelin autoantigens to lymphocytes. Eur J Immunol 1986; 16: 1551-7.
Weller RO. Pathology of cerebrospinal fluid and interstitial fluid of the CNS: significance for Alzheimer disease, prion disorders and multiple sclerosis. J Neuropathol Exp Neurol 1998; 57: 885-94.

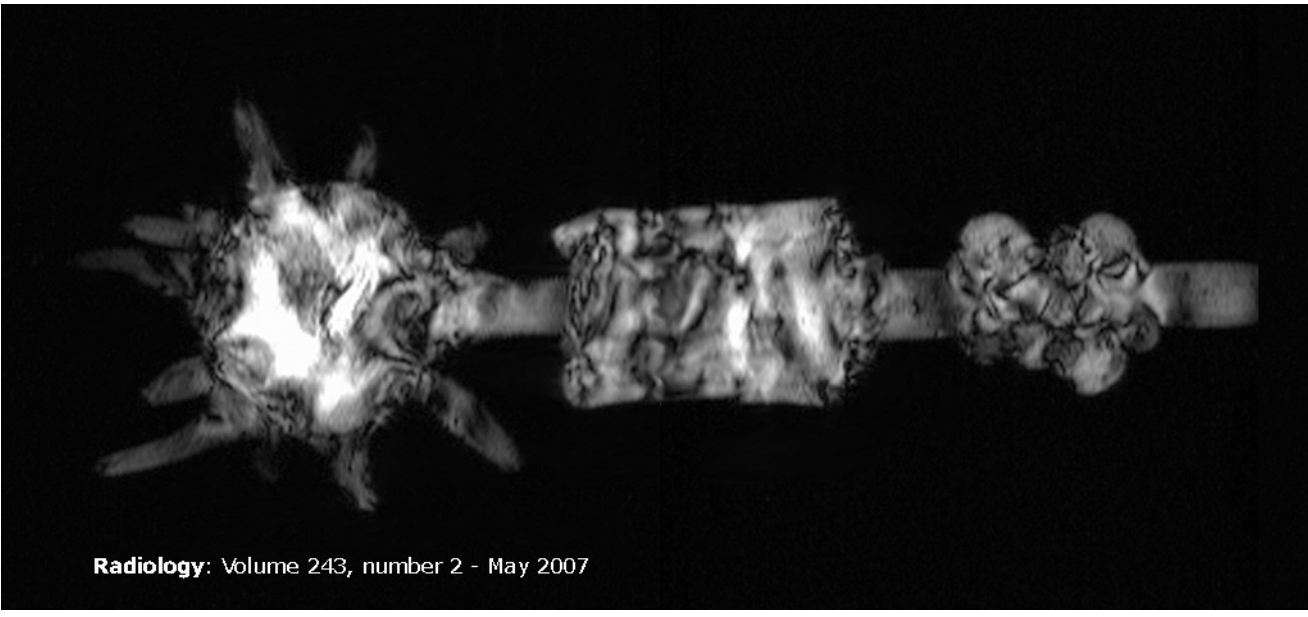

Radiology: Volume 243, number 2 - May 2007

Comparison of SPIO and USPIO for In Vitro Labeling of Human Monocytes with Respect to MR Detection and Cell Function

R.D. Oude Engberink[1], S.M.A. van der Pol[2], E. Döpp[2], H.E. de Vries[2], E.L.A. Blezer[1]

[1]Image Sciences Institute, University Medical Center Utrecht
[2]Molecular Cell Biology and Immunology, VU Medical Center Amsterdam

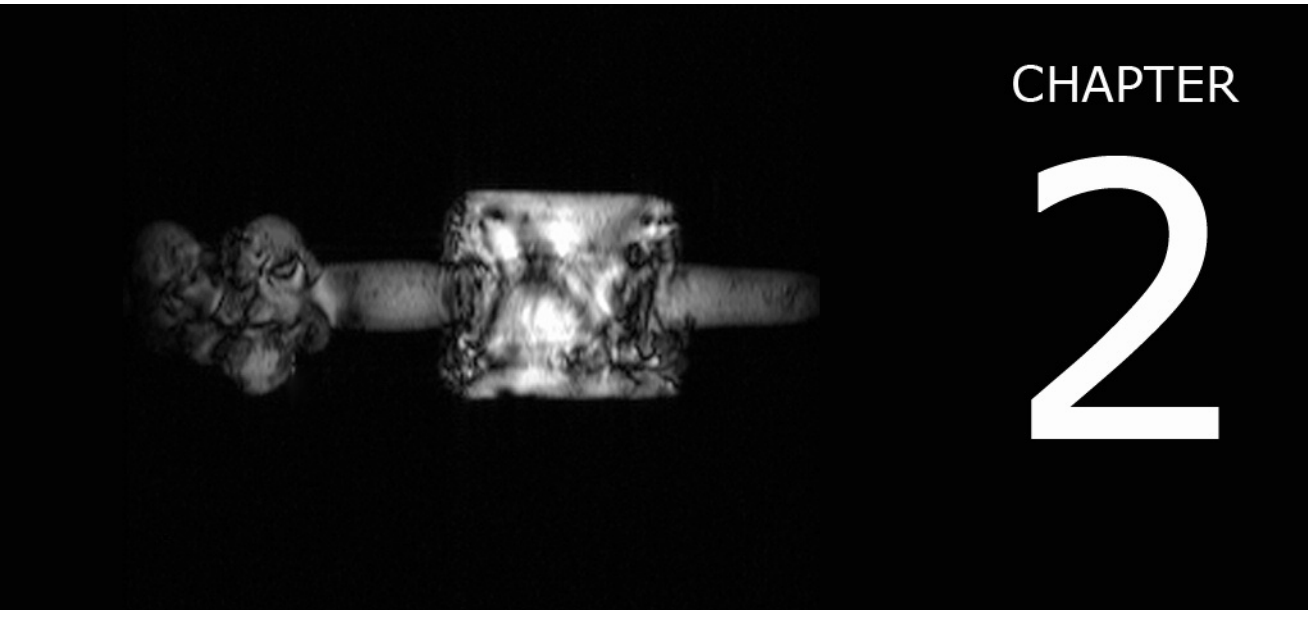

ABSTRACT

PURPOSE: To label human monocytes with superparamagnetic particles of iron oxide (SPIO) and compare labeling efficiency with that of ultra small SPIO (USPIO) and evaluate the effect of iron incorporation on cell viability, migratory capacity and pro-inflammatory cytokine production.

MATERIALS AND METHODS: Our study was approved by the Ethics Committee of VU Medical Center, the Netherlands. Freshly isolated human monocytes were labeled with two differently sized iron oxide particles, USPIO (30nm) and SPIO (150nm) for 1.5h in culture medium containing 0.1 - 3.7mg Fe/ml. Labeling efficiency was determined by relaxation time MRI (4.7 T) and by Prussian blue staining for the presence of intracellular iron. Cell viability was monitored and the migratory capacity of monocytes after labeling was studied by an in vitro assay using a monolayer of brain endothelial cells. Levels of the pro-inflammatory cytokines, interleukin (IL)-1 and -6 were measured by means of ELISA 24h after labeling. Data were analyzed with student's *t*-tests or two-way analysis of variance followed by a multiple-comparison procedure.

RESULTS: R_2 relaxation rates increased for cell samples incubated with SPIO whereas incubation with the highest concentration of USPIO, R_2 was not affected. Labeling monocytes with SPIO (1mg Fe/ml) resulted in a R_2 relaxation rate of 13±0.8 s^{-1} (7±0.2 s^{-1} for vehicle-treated cells; $P<0.05$) and had no effect on cell viability. Based on T_2 relaxation times, we were able to calculate the in vitro MR detection limit of 58 labeled monocytes/0.05 µl. Migration of labeled monocytes was not different from vehicle-treated cells. Intracellular iron had no effect on the production of IL-1 and IL-6 24h after labeling.

CONCLUSION: In vitro labeling of human monocytes is effective using SPIO, not USPIO. Incubation with SPIO (1mg Fe/ml) results in efficient labeling detectable on MR images and does not affect cellular viability and activation markers such as cell migration and cytokine production.

INTRODUCTION

Neuroinflammation is an important event in neurological diseases like stroke, Alzheimers disease and multiple sclerosis. The infiltration of monocytes into the central nervous system plays a dominant role (Al-Omaishi et al., 1999; Bruck et al., 1996; de Vries et al., 1997). Non-invasive visualization of monocyte trafficking provides insight into the pathological aspects of neuroinflammatory conditions and may possibly provide a valuable tool to monitor cell directed intervention strategies aimed to inhibit cell entry into the central nervous system.

The development of new contrast agents like superparamagnetic particles of iron oxide (SPIO) extended the use of magnetic resonance imaging (MRI) to cellular imaging (Weissleder et al., 1990). Prior studies have evaluated the use of intravenously administered ultra small SPIO (USPIO) as MR contrast agents for imaging macrophage activity in animal models of neuroinflammation (Dousset et al., 1999; Floris et al., 2004; Rausch et al., 2003). However, transport to and uptake of USPIO in the central nervous system and its cellular compartments remain unclear. As a result, hypointense areas as seen on $T_2^{(*)}$-weighted images of the affected areas may not only represent infiltrates of macrophages but also reflect leakage of USPIO across the blood-brain barrier or nonspecific uptake by subsets of immune cells.

Investigators in some studies have reported on labeling stimulated (in macrophage medium or endotoxin activated) (Sipe et al., 1999; Zelivyanskaya et al., 2003) and unstimulated (Metz et al., 2004) human monocytes with SPIO, showing uptake of iron particles and MR relaxivities of labeled cells. These studies suggested that in vitro labeling of target cells with SPIO is an interesting concept for in vivo tracking of monocytes /macrophages. It is important that the labeling procedure allows in vivo detection of a small number of cells and that the incorporation of contrast agents does not affect cell function. Optimal MR detection of pre-labeled monocytes requires a biological balance between iron incorporation and cell function. We hypothesized that labeling efficiency and the effect on cell function are dependent on particle size, concentration and incubation time. The purpose of our study was to label human monocytes with SPIO and compare labeling efficiency with that of USPIO and evaluate the effect of iron incorporation on cell viability, migratory capacity and pro-inflammatory cytokine production.

MATERIALS AND METHOD

Isolation of primary monocytes

Human monocytes were isolated from buffycoats of four healthy donors (Sanquin blood bank, Netherlands). Informed consent was obtained from each donor and the study was approved by the Ethics Committee of VU Medical Center, the Netherlands. Whole blood samples of 15 ml were layered on 12.5 ml lymphocyte separation medium (Lymphoprep™, Fresenius Kabi Norge AS) and centrifuged (40min, 400g, 18°C). The mononuclear interphase cells were isolated and washed with phosphate-buffered saline (PBS, pH 7.4). Finally, monocytes were purified by positive selection using immunomagnetic beads coated with a monoclonal antibody (mAb) directed against the monocytic CD14 molecule (MACS-CD14; Milteny Biotec).

MR contrast agent: USPIO versus SPIO

Two differently-sized iron oxides with superparamagnetic properties were compared (USPIO, Sinerem versus SPIO, Endorem®; kindly provided by Guerbet, France). The authors had control of all data and information submitted for publication. SPIO are composed of an iron oxide crystalline core coated with dextran T-10, with a mean hydrodynamic diameter of 150nm supplied in suspension at a concentration of 11.2mg Fe/ml. USPIO are similar dextran-coated iron oxides but with a mean hydrodynamic diameter of 30nm (Benderbous et al., 1996; Jung, 1995; Wang et al., 2001), supplied as lyophilized powder.

Monocyte labeling

Monocytes (n=4) were incubated in the absence (vehicle-treated) or presence of SPIO and USPIO at 37°C. Iron concentrations in culture medium (supplemented RPMI-1640) were adjusted to 0.1, 0.5, 1.0 and 3.7mg Fe/ml. The concentration of cells in the medium was $2x10^6$ cells/ml. The effects of incubation time (n=3) and the presence of transfection agents (TAs, n=3) were investigated for cell samples incubated with SPIO at a standard concentration of 1mg Fe/ml. After 0.5, 1.5, 3 and 6h, monocytes were processed for in vitro MRI and viability measurements. In separate experiments both iron oxide particles (1mg Fe/ml) were pre-incubated at room temperature with three different TAs: a multicomponent lipid-based reagent (Fugene™ 6 at a 0.1% v/v ratio for 60min; Roche Diagnostics), Poly-L-lysine (1µg/ml w/v, 60min; Sigma) and Superfect® (0.025% v/v, 10min; Qiagen). After pre-incubation, the (U)SPIO-TA mixture was added directly to the cell samples. Following the incubation period of 1.5h, cell samples were washed 3 times in cold PBS and centrifuged for 8min at 1190 rpm.

In vitro MRI

Labeling efficiency was determined by T_1 and T_2 relaxation time MRI performed on a 4.7T horizontal bore spectrometer (Varian Instruments, Palo Alto, USA). Relaxation times were measured from agarose-gel (0.4%) suspensions containing free label (n=2) and all samples of labeled monocytes described in the previous paragraph ($0.5x10^6$ cells per 250µl) in 96-well plates. The following MRI data sets were collected (field of view = 4 x 4 cm; matrix = 128 x 128; receiver bandwidth = 42.5 kHz; number of transitions = 2): T_1-maps were a result of a mono-exponential fit of 7 saturation recovery, single-slice T_1 weighted spin-echo images with increasing repetition times (1x 20mm, TR/TE = 55 - 3000/18 ms). T_2-maps were a result of a mono-exponential fit of 10 spin-echo images with increasing echo times (9x 0.5mm, TR=3200ms, TE=17.5, 35, 52.5, 70, 87.5, 105, 122.5, 140, 157.5 and 175ms). For relaxation time analysis, regions of interest (circular, 7.5mm in diameter) were placed in the center of a well and special care was taken to exclude areas with air- susceptibility artifacts. Quantitative T_1 values were obtained using the single slice. Quantitative T_2 values were obtained by averaging the middle 5 regions of interest in the phantom volume. These procedures generated the most stable relaxation time values with minimum noise levels.

In vitro detection limit

Monocytes were incubated in the presence of SPIO at 1mg Fe/ml for 1.5h. T_2 relaxation times were measured of 4 concentrations labeled monocytes in agar phantoms. An exponential equation ($y = e^x$) describes the decrease in T_2 (variable y) as a function of increasing cell numbers (variable x). We chose the T_2 value of vehicle-treated cells (minus two times standard deviation) as minimum relaxation time that can be detected in this specific phantom. Solving the equation for $y = T_2$ (vehicle minus two times standard deviation) results in the minimum number of cells that must be present in this volume to give rise to a substantial MR signal intensity.

Histochemical detection of SPIO and USPIO

Immediately after labeling, cell samples were washed and cytospots were prepared on glass slides with centrifugation (68rpm, 5min) and air dried. The presence of SPIO and USPIO was detected by Prussian blue staining of iron and cell spots were counterstained with nuclear fast red. Briefly, cell spots were fixed in acetone and incubated with a 1:1 v/v mixture of 2% potassium ferrous cyanide (kalium-hexacyanoferrat [II]) and 2N HCL for 30min. Glass slides were rinsed in distilled water and counterstained with nuclear fast red for 5min. The presence of iron oxide particles was qualitatively assessed with a microscope by estimating iron positive cells from a total of approximately 150 cells.

Cell activation assays

Cell viability was determined for all samples by trypan blue exclusion assays as described in the paragraph about monocyte labeling. Dead cells were counted with the microscope in a total area of 25mm^2 (approximately 150 cells) using a calibrated counting chamber.

Monocyte migration was monitored using a time-lapse video-microscopy migration assay (Floris et al., 2002; Hendriks et al., 2004; Van der Goes et al., 2001). Briefly, 7.5x10^5 monocytes suspended in serum-free culture medium were added to brain endothelial monolayers (established from rat brain endothelial cell line GP8/3) grown in 96-well plates, and allowed to migrate for 4h. Monocyte migration (n=4 for all samples) was carried out for labeled (SPIO; 1mg Fe/ml) and vehicle-treated monocytes. Freshly isolated monocytes served as a negative control and monocytes stimulated with lipopolysaccharide (LPS, 100ng/ml) for 24h served as a positive control. The level of migration was quantified as the percentage of migrated cells of the total number of monocytes present within a field of 200μm^2.

Major histocompatibility complex (MHC) class II receptor expression on labeled monocytes was tested by using flow cytometric analysis (n=3) of labeled cells (SPIO; 1mg Fe/ml) compared with vehicle-treated cells after 24h. Cells were incubated with mouse-anti-human HLA-DR (1μg/ml) for 1h at 4^{o}C. Binding of these monoclonal antibodies was detected using phycoerythrin-coupled rabbit-anti-mouse F(ab)$_2$ (1μg/ml). Omission of the primary antibody served as negative control. Fluorescence intensity was determined using a FACScan flow cytometer (Becton & Dickinson, San Jose, USA).

Production of pro-inflammatory cytokines interleukin (IL)-1 and IL-6 was measured 24h after labeling (SPIO; 1mg Fe/ml, n=5) using standard ELISA protocols. Briefly, 96-well ELISA plates were coated with 1mg/ml mouse-anti-human IL-1β or IL-6 diluted in PBS (pH 7.4, 100ml/well). Following overnight incubation at 4°C, plates were washed in PBS with 0.1% Tween and blocked with PBS containing 0.5% bovine serum albumin (37°C, 1h). After washing, diluted serum samples (1:1, 1:10, 1:100 v/v ratios) were added to the plates in duplicate and incubated for 1h at 37°C in the presence of detecting antibodies, 0.5 mg/ml mouse-anti-human IL-1B-biotine and IL-6-biotine. After washing, samples were incubated with peroxidase-labeled streptavidin (Vector Laboratories) to enhance the detecting antibodies. After final washing, binding of secondary antibodies was detected by adding the substrate tetramethylbenzidine. After 10-20min, the reaction was stopped using 1M H_2SO_4 and optical density in the wells was measured in an ELISA plate reader at 450nm. Freshly isolated monocytes served as a negative control and monocytes stimulated with LPS (100ng/ml) for 24h served as a positive control.

Statistical Analysis

The effects of increasing iron concentrations on relaxation rates and cell viability were evaluated by two-way analysis of variance, followed by a multiple-comparison procedure (Student-Newman-Keuls test) using statistical software (Sigmastat, version 3.11, 2004). The effects of incubation time, presence of TAs and cell activity assays were analyzed by using student's *t*-tests. A difference with $P < .05$ was considered statistically significant.

RESULTS

In vitro MR imaging: MR properties of free label

R_1 relaxation rate is similar for both iron oxide particles (Fig 1A) and shows a linear detection up to 20µg Fe/ml (r_1 = 0.035 s^{-1} $µg^{-1}$ ml). No substantial differences were observed for R_2 relaxation rates (Fig 1B), but in this case linear detection is up to 10µg Fe/ml (r_2 USPIO=1.58 and r_2 SPIO=1.55 s^{-1} $µg^{-1}$ ml). Because r_2 relaxivity was 50 times more sensitive for the presence of small amounts of iron, T_2 relaxation time MRI was used in all subsequent experiments.

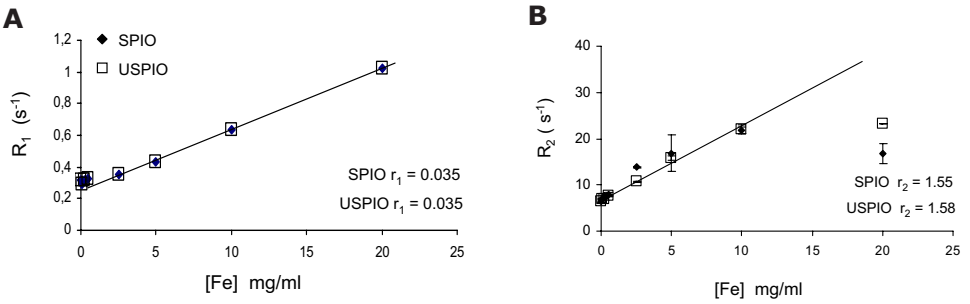

Figure 1 Graphs show **(A)** R_1 and **(B)** R_2 relaxation rates determined at 4.7T for increasing concentrations of USPIO (□) and SPIO (◆). Linear regression analyses were performed to calculate relaxivity values r_1 and r_2 (s^{-1} $µg^{-1}$ ml).

In vitro MR imaging: monocyte labeling

A typical T_2-map of monocytes in a 96-well plate (Fig 2A) shows the difference in signal intensity loss between vehicle-treated cells and cells incubated with SPIO versus USPIO for similar iron concentrations. Corresponding R_2 relaxation rates show the effects of different iron concentrations on labeling efficiency (Fig 2B). Cells incubated with SPIO resulted in increasing R_2 relaxation rate for increasing iron concentrations; R_2 of monocytes labeled with 1mg Fe/ml SPIO was 13±0.8 s^{-1} (vehicle-treated monocytes; R_2=7±0.2 s^{-1}). In contrast, cells incubated with USPIO at maximal iron concentration (3.7mg Fe/ml) did not show a significant increase in R_2 as compared to vehicle-treated cells (P= .18). Relaxation rates of agar phantoms containing vehicle-treated monocytes were not different from empty agar phantoms (P= .57, data not shown).

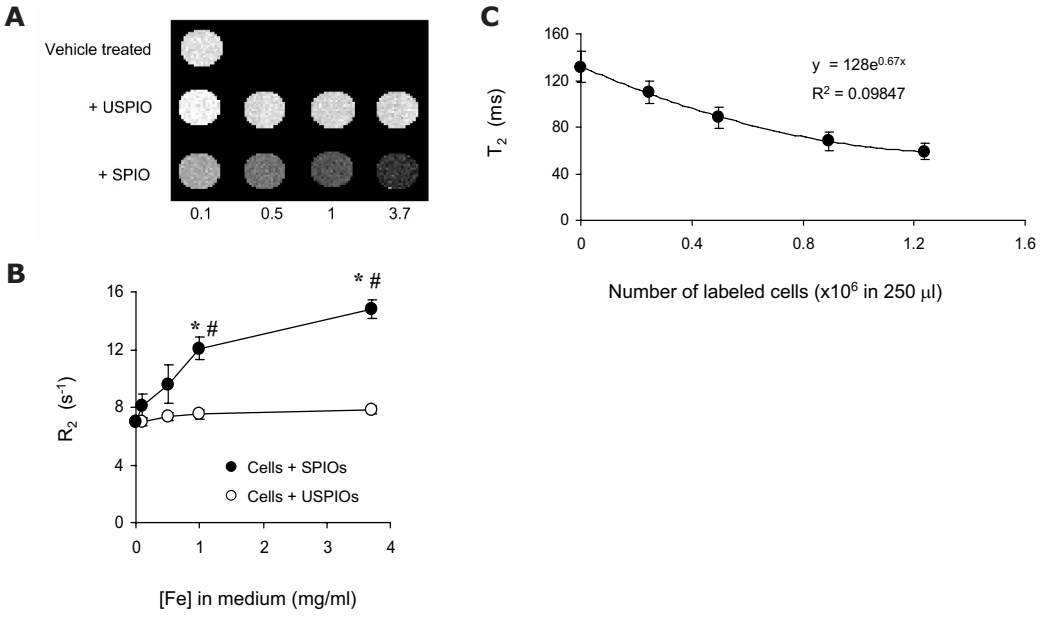

Figure 2 In vitro MR image of monocytes in an agar-gel suspension, labeled at varying iron concentrations. **(A)** Typical T_2 relaxation time image of SPIO and USPIO-labeled monocytes in a 96-wells plate. The vehicle-treated sample contained unlabeled monocytes. **(B)** Graph shows R_2 relaxation rates of cell samples. **(C)** Graph shows T_2 relaxation times of increasing concentrations of SPIO-labeled monocytes. Data in B and C are presented as mean ± standard error of the mean.

* = P< .05 versus vehicle-treated cells,

= P< .05 versus USPIO-labeled cells.

In vitro MR imaging: incubation time and TAs

In regard to the effect of increasing incubation times up to 6h on MR detection and cell viability for monocytes incubated in the presence of SPIO 1mg Fe/ml (Table 1), incubation times longer than 1.5h did not further increase R_2 (P= .009 for 1.5h versus 0.5h and P= .16 for 3h versus 1.5h). Increased cell death was observed after 6h incubation. Pre-incubation of both iron oxide particles (1mg Fe/ml) with previously described TAs did not enhance R_2 relaxation rate of labeled monocytes.

Table 1

Effect of incubation time and TAs on R_2

A: R_2 for SPIO-labeled Monocytes as a Function of Incubation Time

Time (h)	R_2 for SPIO (s^{-1})		Viabilty (%)
0	6.9 ± 0.2		86
0,5	11.1 ± 0.1	*	91
1,5	12.6 ± 0.2	*	86
3	13.5 ± 0.6		83
6	12.5 ± 0.1		69

B: R_2 for Monocytes Incubated with Iron Oxides after Preincubation with TAs

TA	R_2 for SPIO (s^{-1})	R_2 for USPIO (s^{-1})
None	13.1 ± 0.8	7.5 ± 0.3
Poly-L-lysine	12.7 ± 0.4	7.3 ± 0.4
FuGene 6	11.2 ± 0.8	7.5 ± 0.3
Superfect	11.5 ± 1	7.6 ± 0.1

Note - R_2 for monocytes labeled in the presence of SPIO was increased up to 1.5h of incubation time. The iron concentration for iron oxide particles was 1mg Fe/ml. Unless otherwise indicated, values are the mean ± standard error of the mean.

* $P < .05$ versus previous time point.

In vitro MR imaging: detection limit

Based on the plot for T_2 relaxation times of increasing numbers of labeled monocytes (Fig 2C), voxel size (0.3x0.3x0.5mm^3 or approximately 0.05 l) and phantom volume (250 µl), we calculated a MR detection limit of 58 labeled monocytes per 0.05µl. T_2 relaxation time of vehicle-treated monocytes minus two times standard deviation (y = 105ms) was used in the trend line equation to solve 'x' as the minimum number of cells that could be detected theoretically in a T_2 relaxation time image of this specific phantom.

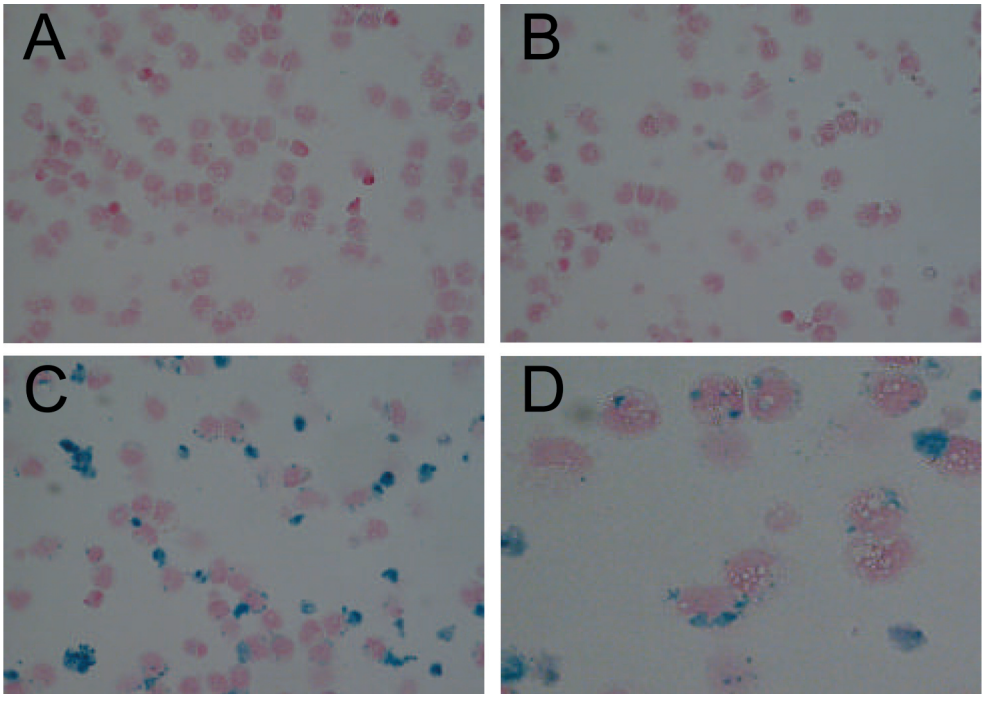

Figure 3. Detection of iron oxide particles in monocytes with Prussian blue staining. SPIO and USPIO are blue and cell nuclei are red. (A) vehicle-treated monocytes. (B) Monocytes incubated with USPIO; 1mg Fe/ml. (C) Monocytes incubated with SPIO; 1mg Fe/ml. (D) Higher magnification of SPIO-labeled monocytes. (Original magnification; x40 [A-C] and x100 [D]).

Histochemical detection of SPIO and USPIO

vehicle-treated monocytes showed no positive staining for iron (Fig 3A). Approximately 1% of the monocytes incubated in the presence of USPIO (1mg Fe/ml) contained intracellular iron (Fig 3B). In contrast, 70-80% of monocytes incubated with SPIO (1mg Fe/ml) showed intracellular iron present in the cytosol of the monocytes (Fig 3C, 3D). Qualitative analysis of cell samples incubated in the presence of SPIO with a concentration higher than 2mg Fe/ml, revealed an extracellular clustering of SPIO particles.

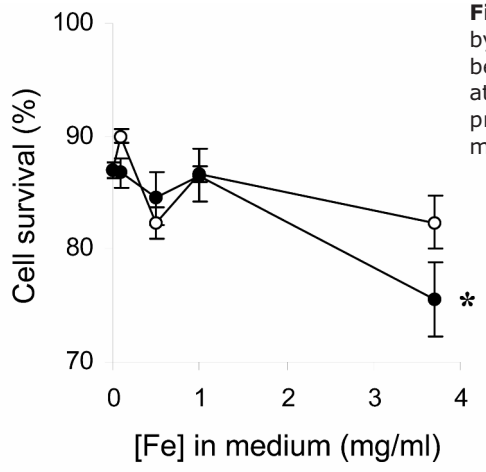

Figure 4. Graph shows cell viability measured by using trypan blue exclusion for monocytes labeled in the presence of USPIO (□) or SPIO (●) at varying iron concentrations for 1.5h. Data are presented as mean ± standard error of the mean. * = P< .05 versus vehicle-treated cells.

Effect of iron incorporation on monocyte function

No decrease in monocyte viability was observed after SPIO and USPIO incubation up to a concentration of 1mg Fe/ml (Fig 4). SPIO incubation at a concentration of 3.7mg Fe/ml significantly declined cell viability to 76±3.3% (P= .015 versus vehicle-treated cells). Cell viability after USPIO incubation (3.7mg Fe/ml) decreased to 83±2.3% (P= .08 versus vehicle-treated cells).

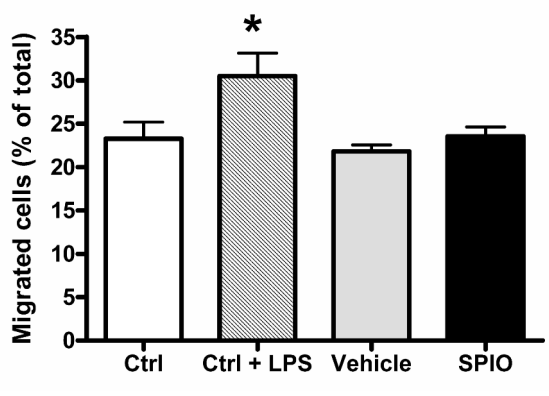

Figure 5. Following SPIO labeling at a concentration of 1mg Fe/ml, monocytes were allowed to migrate across a monolayer of brain endothelium. Graph shows the number of migrated monocytes that is expressed as percentage of total number of added monocytes. Freshly isolated cells (Ctrl) and vehicle-treated cells served as negative controls. Monocytes stimulated with LPS for 24h served as a positive control. Data are presented as mean ± standard error of the mean. * = P< .05 versus control cells.

No significant difference was found (Fig 5) in the number of migrated cells for SPIO-labeled monocytes (23.5±2%) as compared to vehicle-treated (21.8±0.8%, P= .33) and freshly isolated cells (Ctrl, 23.2±0.1%, P= .41). LPS stimulated monocytes showed an increased migratory capacity (30.3±2.5%, P= .003 versus ctrl).

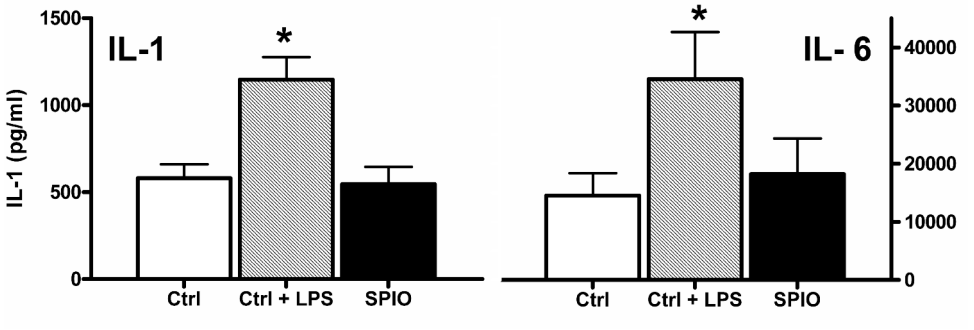

Figure 6. Graph shows IL-1 and IL-6 production of labeled monocytes 24h after incubation with SPIO at a concentration of 1mg Fe/ml. Freshly isolated monocytes (Ctrl) served as negative control. Monocytes stimulated with LPS for 24h served as positive control. Data are presented as mean ± standard error of the mean. * = P< .05 versus Ctrl.

IL-1 production (Fig 6) of labeled cells (545±100 pg/ml) was not significantly different from freshly isolated cells (Ctrl, 580±80 pg/ml, P= .77). Similarly, IL-6 levels were not significantly different for labeled cells (18200±6000 pg/ml, P= .58) compared with freshly isolated monocytes (Ctrl, 14550±3800 pg/ml). In both cases, LPS incubation increased cytokine levels by twofold (IL-1, P= .005; IL-6, P= .04 versus Ctrl). MHC class II expression on SPIO-labeled monocytes was measured and was not affected by the labeling procedure or the presence of intracellular iron (P= .83 for vehicle-treated versus Ctrl and P= .91 for SPIO-labeled versus Ctrl).

DISCUSSION

Our findings suggest that monocytes are labeled more efficiently by using SPIO instead of USPIO. The larger diameter of SPIO (150nm) as compared to that of USPIO (30nm) may result in cellular uptake by monocytes. Earlier reports confirm that phagocytotic uptake of iron oxide particles increased with particle size (Daldrup-Link et al., 2003; Matuszewski et al., 2005). Similar results were reported in a study concerning macrophage endocytosis of nanoparticles by mouse peritoneal macrophages (Raynal et al., 2004) and it is suggested that uptake of SPIO involves scavenger receptor A-mediated endocytosis. Although our study indicates that SPIO are far more suitable for in vitro labeling of primary monocytes, the long blood pool half-life of USPIO makes it the most frequently used iron oxide particle for in vivo labeling. The concept of in vivo labeling using USPIO has been studied in animals and patients in several pathologies including stroke (Rausch et al., 2001; Saleh et al., 2004) and multiple sclerosis (Dousset et al., 2001; Dousset et al., 1999; Floris et al., 2004). In humans, the blood pool half-life of USPIO is more than 24h (McLachlan et al., 1994), whereas the half-life of SPIO appears to be shorter than 6 minutes (Weissleder et al., 1989) and such a short half-life limits their possibility to label endogenous monocytes in circulation. In a recent animal study, researchers showed that with an increase in circulation time of SPIO by means of elimination of blood-borne macrophages, similar MR abnormalities may be observed as with USPIO labeling (Oweida et al., 2005).
We have shown that only a small percentage of monocytes (< 1%) is labeled by using USPIO in vitro. In most in vivo labeling studies, the iron concentration in the plasma is relatively low (34µg/ml (Metz et al., 2004)). This leads us to question the efficiency of in vivo labeling using USPIO. Although some studies have reported the presence of iron oxide particles within macrophages, hypointense areas as seen on MR images might reflect the presence of extracellular iron or other labeled phagocytic cells (Dousset et al., 1999). Thus, to ensure reliable detection of target cells in vivo, in vitro SPIO labeling of cells may be a better tool.
In our study labeling of monocytes in the presence of SPIO with a concentration of 1mg Fe/ml for 1.5h, led to an increase in the R_2 relaxation rate up to 13 s^{-1} (vehicle-treated cells; 7 s^{-1}) measured at 4.7T. We have to note that the relaxation rate of agar phantoms containing vehicle-treated cells is not different from empty agar phantoms. This finding helps to rule out the possibility of contribution to the MR signal of the beads used for monocyte isolation. For this labeling condition cell viability was not affected. This established labeling concentration is five to ten times higher than iron concentrations used for labeling other cell types in conjunction with TAs (Arbab et al., 2004; Matuszewski et al., 2005). Increasing the

iron concentration in the medium is necessary to label primary human monocytes. We have also shown that TAs in combination with SPIO and USPIO with a concentration of 1mg Fe/ml do not further increase labeling efficiency. It might be possible that longer incubation (24 – 48h) times and lower iron concentrations in combination with TAs result in comparable iron incorporation. With respect to monocyte function and application in cell tracking studies, however, a relatively short incubation time is required.

We used an exponential fit of T_2 relaxation times versus increasing numbers of SPIO-labeled monocytes in agar phantoms to calculate a detection limit of 58 labeled monocytes in 0.05µl. However, we must emphasize the fact that this is a mathematic estimation from measurements in agar phantoms at 4.7T. It is likely that, at clinical field strength of 1.5T, this detection limit will be lower due to reduced susceptibility effects of iron oxide particles. Qualitative visual detection by an actual observer will be limited. However, with the recent emergence of clinical high field scanners of 3T and higher, we believe that their detection levels may eventually be comparable with our results. When MR sequences that are more sensitive for susceptibility artifacts of iron oxide particles, such as gradient-echo-based sequences (Ericsson et al., 1991), are applied, we anticipate that the detection level could be further improved to near single-cell detection. This opens up the possibility to detect a few labeled macrophages present in an inflammatory lesion. For example, in an animal model of multiple sclerosis numerous active lesions are associated with an influx of monocyte-derived-macrophages (Bauer et al., 1995; Floris et al., 2004; Hickey, 1999). When we ignore issues like physiological noise and MR artifacts, our in vitro data suggest that SPIO labeling of monocytes is an accurate tool to monitor cell dynamics within an area of inflammation.

With a view to future in vivo tracking experiments, we used unstimulated, freshly isolated human monocytes to conduct the labeling studies. To assess the effect of iron incorporation on monocyte function, in vitro migration over brain endothelial cells and IL-1 and IL-6 production were studied. Activated monocytes (macrophages) show increased levels of cytokines IL-1 and IL-6 (Gordon, 2003). For the established SPIO concentration (1mg Fe/ml), no effect of the labeling procedure and intracellular iron on the migratory capacity and cytokine production of monocytes was found. This finding may indicate that, when in vivo tracking studies are conducted, labeled monocytes still migrate towards an area of inflammation and that the intracellular presence of iron does not activate the monocytes. In a previous study, labeled human monocytes were injected into brains of immunodeficient mice, and intracerebral migration was studied with MRI (Zelivyanskaya et al., 2003). Areas of hypointensity were detected even after day 14 post-injection; this finding suggests the possibil-

ity for monitoring monocyte/macrophage dynamics in vivo. However, it was unclear whether iron particles remained inside the target cells.
Cellular MR imaging has a unique window of opportunity to monitor cellular mechanisms underlying several diseases. For accurate imaging of target cells, efficient incorporation of contrast agents is required but not at the expense of cellular function. One of the limitations of our study was that in vitro data on cell samples in agar phantoms at 4.7T did not provide an ideal replacement for an in vivo situation; thus, further studies should therefore focus on measurements at clinical field strengths. Another limitation was that the effect of iron incorporation on cell viability was assessed directly after incubation. There might be a possibility that iron uptake is toxic after a longer period of time. Future studies should focus on cell viability at later time points. Furthermore, to elucidate the precise mechanism of preferred SPIO uptake, specific receptor binding and inhibition assays should be performed. We are currently adopting the labeling protocol for rat monocytes and exploring in vivo monocyte tracking in animal studies. Our in vitro study with human monocytes will contribute to the design of cell labeling protocols and emphasizes the need for a balance between iron incorporation and cell function.
In summary, freshly isolated human monocytes were labeled more efficiently by using SPIO at a concentration of 1mg Fe/ml. With this established iron concentration in the incubation medium, intracellular iron did not affect migratory capacity and pro-inflammatory cytokine production. Tuning into the fine balance between iron incorporation and cell function, we think that in vitro labeling of monocytes contributes to a more cell-specific and accurate way of in vivo cell tracking both in humans and animal models of neurologic disease.

ACKNOWLEDGEMENTS

The MR contrast agents were kindly provided by Guerbet, France. This work has been supported by the Dutch MS Research Foundation (MS 01-470, MS 02-489).

REFERENCES

Al-Omaishi J, Bashir R, Gendelman HE. The cellular immunology of multiple sclerosis. J Leukoc Biol 1999; 65: 444-52.

Arbab AS, Yocum GT, Wilson LB, Parwana A, Jordan EK, Kalish H, et al. Comparison of transfection agents in forming complexes with ferumoxides, cell labeling efficiency, and cellular viability. Mol Imaging 2004; 3: 24-32.

Bauer J, Huitinga I, Zhao W, Lassmann H, Hickey WF, Dijkstra CD. The role of macrophages, perivascular cells, and microglial cells in the pathogenesis of experimental autoimmune encephalomyelitis. Glia 1995; 15: 437-46.

Benderbous S, Corot C, Jacobs P, Bonnemain B. Superparamagnetic agents: physicochemical characteristics and preclinical imaging evaluation. Acad Radiol 1996; 3 Suppl 2: S292-4.

Bruck W, Sommermeier N, Bergmann M, Zettl U, Goebel HH, Kretzschmar HA, et al. Macrophages in multiple sclerosis. Immunobiology 1996; 195: 588-600.

Daldrup-Link HE, Rudelius M, Oostendorp RA, Settles M, Piontek G, Metz S, et al. Targeting of hematopoietic progenitor cells with MR contrast agents. Radiology 2003; 228: 760-7.

de Vries HE, Kuiper J, de Boer AG, Van Berkel TJ, Breimer DD. The blood-brain barrier in neuroinflammatory diseases. Pharmacol Rev 1997; 49: 143-55.

Dousset V, Brochet B, Caille JM, Petry KG. Enhancement of multiple sclerosis lesions with ultra-small particle iron oxide : phase II study. ISMRM. Glasgow, Scotland, 2001.

Dousset V, Delalande C, Ballarino L, Quesson B, Seilhan D, Coussemacq M, et al. In vivo macrophage activity imaging in the central nervous system detected by magnetic resonance. Magn Reson Med 1999; 41: 329-33.

Ericsson A, Lonnemark M, Hemmingsson A, Bach-Gansmo T. Effect of superparamagnetic particles in agarose gels. A magnetic resonance imaging study. Acta Radiol 1991; 32: 74-8.

Floris S, Blezer EL, Schreibelt G, Dopp E, van der Pol SM, Schadee-Eestermans IL, et al. Blood-brain barrier permeability and monocyte infiltration in experimental allergic encephalomyelitis: a quantitative MRI study. Brain 2004; 127: 616-27.

Floris S, Ruuls SR, Wierinckx A, van der Pol SM, Dopp E, van der Meide PH, et al. Interferon-beta directly influences monocyte infiltration into the central nervous system. J Neuroimmunol 2002; 127: 69-79.

Gordon S. Alternative activation of macrophages. Nat Rev Immunol 2003; 3: 23-35.

Hendriks JJ, Alblas J, van der Pol SM, van Tol EA, Dijkstra CD, de Vries HE. Flavonoids influence monocytic GTPase activity and are protective in experimental allergic encephalitis. J Exp Med 2004; 200: 1667-72.

Hickey WF. Leukocyte traffic in the central nervous system: the participants and their roles. Semin Immunol 1999; 11: 125-37.

Jung CW. Surface properties of superparamagnetic iron oxide MR contrast agents: ferumoxides, ferumoxtran, ferumoxsil. Magn Reson Imaging 1995; 13: 675-91.

Matuszewski L, Persigehl T, Wall A, Schwindt W, Tombach B, Fobker M, et al. Cell tagging with clinically approved iron oxides: feasibility and effect of lipofection, particle size, and surface coating on labeling efficiency. Radiology 2005; 235: 155-61.

McLachlan SJ, Morris MR, Lucas MA, Fisco RA, Eakins MN, Fowler DR, et al. Phase I clinical evaluation of a new iron oxide MR contrast agent. J Magn Reson Imaging 1994; 4: 301-7.

Metz S, Bonaterra G, Rudelius M, Settles M, Rummeny EJ, Daldrup-Link HE. Capacity of human monocytes to phagocytose approved iron oxide MR contrast agents in vitro. Eur Radiol 2004; 14: 1851-8.

Oweida A, Dunn E, Foster P. Cellular Imaging of Neuroinflammation: A novel method for Unraveling the Roles of Macrophages Populations in EAE. ISMRM. Miami beach, Florida, USA, 2005.

Rausch M, Hiestand P, Baumann D, Cannet C, Rudin M. MRI-based monitoring of inflammation and tissue damage in acute and chronic relapsing EAE. Magn Reson Med 2003; 50: 309-14.

Rausch M, Sauter A, Frohlich J, Neubacher U, Radu EW, Rudin M. Dynamic patterns of USPIO enhancement can be observed in macrophages after ischemic brain damage. Magn Reson Med 2001; 46: 1018-22.

Raynal I, Prigent P, Peyramaure S, Najid A, Rebuzzi C, Corot C. Macrophage endocytosis of superparamagnetic iron oxide nanoparticles: mechanisms and comparison of ferumoxides and ferumoxtran-10. Invest Radiol 2004; 39: 56-63.

Saleh A, Schroeter M, Jonkmanns C, Hartung HP, Modder U, Jander S. In vivo MRI of brain inflammation in human ischaemic stroke. Brain 2004; 127: 1670-7.

Sipe JC, Filippi M, Martino G, Furlan R, Rocca MA, Rovaris M, et al. Method for intracellular magnetic labeling of human mononuclear cells using approved iron contrast agents. Magn Reson Imaging 1999; 17: 1521-3.

Van der Goes A, Wouters D, Van Der Pol SM, Huizinga R, Ronken E, Adamson P, et al. Reactive oxygen species enhance the migration of monocytes across the blood-brain barrier in vitro. Faseb J 2001; 15: 1852-4.

Wang YX, Hussain SM, Krestin GP. Superparamagnetic iron oxide contrast agents: physicochemical characteristics and applications in MR imaging. Eur Radiol 2001; 11: 2319-31.

Weissleder R, Elizondo G, Wittenberg J, Rabito CA, Bengele HH, Josephson L. Ultrasmall superparamagnetic iron oxide: characterization of a new class of contrast agents for MR imaging. Radiology 1990; 175: 489-93.

Weissleder R, Stark DD, Engelstad BL, Bacon BR, Compton CC, White DL, et al. Superparamagnetic iron oxide: pharmacokinetics and toxicity. AJR Am J Roentgenol 1989; 152: 167-73.

Zelivyanskaya ML, Nelson JA, Poluektova L, Uberti M, Mellon M, Gendelman HE, et al. Tracking superparamagnetic iron oxide labeled monocytes in brain by high-field magnetic resonance imaging. J Neurosci Res 2003; 73: 284-95.

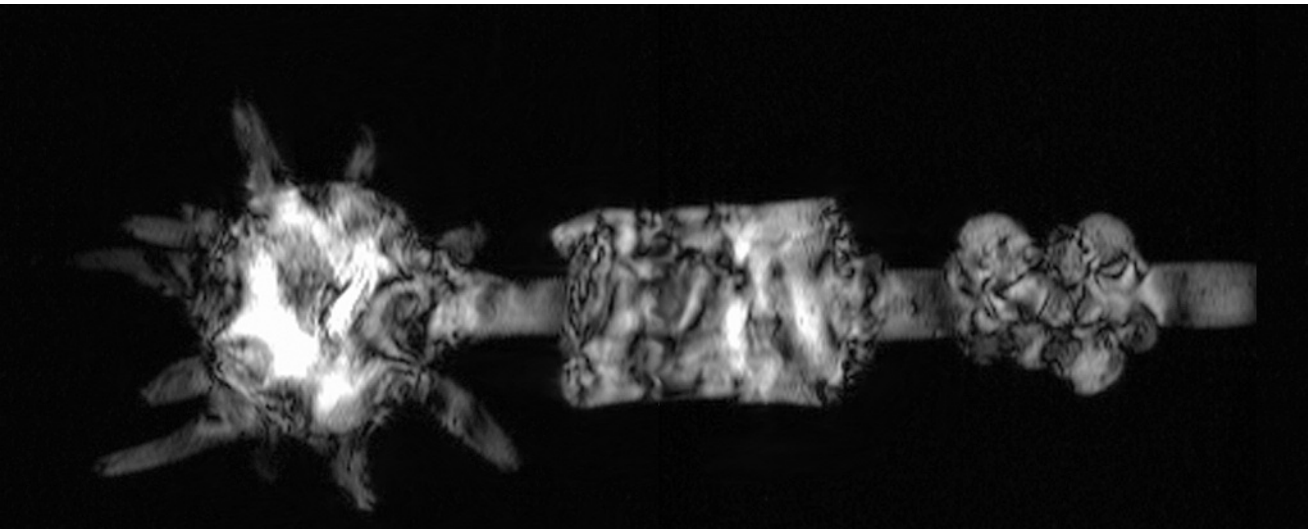

Journal of Cerebral Blood Flow & Metabolism, 2007: In press

MR Imaging of Monocyte Infiltration in an Animal Model of Neuroinflammation using SPIO-labeled Monocytes or Free USPIO

R. D. Oude Engberink[1], E.L.A. Blezer[1], E.I. Hoff[3], S.M.A. van der Pol[2], A. van der Toorn[1], R.M. Dijkhuizen[1], H.E. de Vries[2]

[1]Image Sciences Institute, University Medical Center Utrecht
[2]Molecular Cell Biology and Immunology, VU Medical Center Amsterdam
[3]Department of Neurology, University Hospital Maastricht

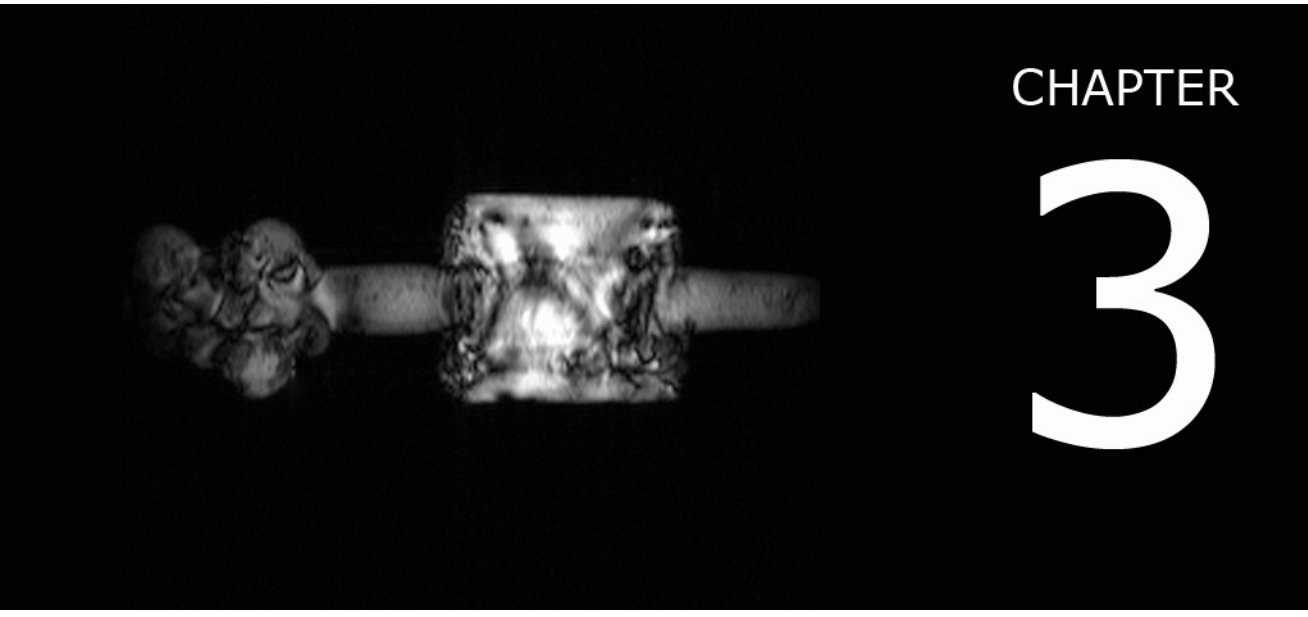

ABSTRACT

Magnetic resonance imaging (MRI) has been applied to visualize monocyte infiltration with the use of intravenously injected ultra small superparamagnetic iron oxide (USPIO). However, USPIO uptake in vivo remains elusive and the heterogeneous enhancement patterns observed by MRI point to multiple pathophysiological events. This study aimed on specific imaging of monocyte infiltration into the brain by transfusion of superparamagnetic iron oxide (SPIO)-labeled monocytes in a rat model of neuroinflammation, experimentally induced photothrombosis (PT). At day 5 after lesion induction, animals were transfused with SPIO-labeled monocytes ($5x10^6$ cells) or free USPIO (17mg Fe/kg). MRI was performed 24h, 72h and 120h later. To investigate temporal changes directly upon intravenous USPIO administration, MRI was performed repeatedly up to 8h. Relaxation time measurements demonstrated that rat monocytes were efficiently labeled in vitro using SPIO ($R_2 = 12\pm0.9s^{-1}$). Following transfusion of SPIO-labeled monocytes, a significant increase in contrast enhanced area (340±106%) in the PT lesion was observed not before 72h. Contrast enhancement following USPIO injection increased up to 407±39% at a much earlier point of time (24h) and diminished thereafter. Repetitive MRI directly after USPIO injection showed significant contrast enhancement in the lesion within 2h. Our study demonstrates that MRI enables in vivo tracking of SPIO-labeled monocytes longitudinally. More over, our data suggest that contrast enhancement after injection of free USPIO does not primarily represent signal from peripherally labeled monocytes that migrated towards the inflammatory lesion. The use of SPIO-labeled monocytes provides a better tool to specifically assess the time window of monocyte infiltration.

INTRODUCTION

Cellular infiltration in the central nervous system (CNS) is a key event during neuroinflammation and contributes to brain damage in neurological diseases like multiple sclerosis (MS) and stroke (Lassmann, 1997; Price et al., 2003; Stoll et al., 1998). CNS inflammation is characterized by increased blood-brain barrier (BBB) permeability and expression of cell adhesion molecules on brain endothelial cells which mediate cellular infiltration. It is generally believed that destruction of brain tissue and lesion development associated with inflammation is predominantly mediated by the infiltration of activated monocytes into the CNS (Dirnagl et al., 1999; Stoll et al., 1998). Previous work in animal models showed that selective depletion of the monocyte population during CNS inflammation reduced disease severity (Huitinga et al., 1995; Polfliet et al., 2002). Therefore, inhibition of monocyte infiltration is considered an attractive therapeutic strategy to limit neuroinflammation. A number of treatment studies have focused either on diminishing migratory capacity of peripheral blood mononuclear cells by immunomodulation (Corsini et al., 1997; Floris et al., 2002) or by direct blocking of cell adhesion molecules as has been shown for the alpha-4 integrin blocking molecule Natalizumab (Niino et al., 2006; Polman et al., 2006). However, continuous blocking of adhesion receptors may increase the risk of inflammation in peripheral organs. To design an effective treatment it is important to specifically intervene within the time window of monocyte infiltration into the CNS. So far, the temporal pattern of monocyte recruitment during CNS inflammation is largely unknown. There is an urgent need for non-invasive and accurate tracking tools to elucidate monocyte recruitment in the CNS longitudinally. The development of small and ultrasmall superparamagnetic iron oxides (SPIO and USPIO, respectively) extended the use of magnetic resonance imaging (MRI) to study cell dynamics in vivo (Arbab et al., 2003; Weissleder et al., 1997). Iron oxide particles shorten the transverse relaxation times T_2 and T_2^*, and clusters of cells that have taken up USPIO appear hypointense on $T_2^{(*)}$-weighted images (Yeh et al., 1993). So far, intravenous administration of USPIO has been used to study monocyte infiltration in animals models with a neuroinflammatory component like stroke (Saleh et al., 2004b; Schroeter et al., 2004) and MS (Dousset et al., 1999a; Floris et al., 2004). Recently, this methodology has been applied in clinical trials to investigate macrophage activity in stroke (Saleh et al., 2004a) and MS patients (Dousset et al., 2006). It was shown in these studies that signal changes in the brain observed 24h after USPIO administration differed from Gd-DTPA enhanced areas, which marks BBB breakdown. This difference in contrast enhancements points to distinct pathophysiological events and USPIO-enhanced MRI is suggested to pro-

vide specific information on the cellular component of neuroinflammation. Nevertheless, the exact route of USPIO uptake and distribution in vivo remains unclear, which hampers the interpretation of USPIO-related signals. USPIO enhancement in the CNS is generally believed to reflect infiltrated monocytes that have taken up USPIO in the blood circulation. However, MRI signal changes may originate from sources other than the migration of these peripherally labeled monocytes. USPIO may enter the CNS passively by leakage over a damaged BBB or by transcytosis across the brain endothelial cells (Xu et al., 1998). Moreover, it is suggested that cellular USPIO incorporation may occur outside the vasculature by activated microglia (Dousset et al., 1999a). Transfusion of monocytes that have been specifically labeled ex vivo may therefore be a better tool to exclusively address monocyte infiltration during an inflammatory response in the brain. This approach has recently been reported by Stroh et al., where they labeled spleen-derived mononuclear cells with very small superparamagnetic iron oxide (Stroh et al., 2006). Labeled cells were intravenously injected in splenectomized mice after middle cerebral artery occlusion and found to be engrafted at the lesion border zone.

The main goal in our study is to monitor exclusively brain infiltration of SPIO-labeled monocytes and compare contrast enhancement to the injection of free USPIO. We used photothrombosis (PT) (Watson et al., 1985) as a rat model for neuroinflammation. In this animal model, focal illumination of the brain after intravenous injection of a photosensitive dye induces a well-defined cortical lesion that is characterized by the presence of infiltrating monocytes (Lee et al., 1996). Previous studies using this model have demonstrated that MRI 24h after USPIO administration allows detection of the inflammatory lesion in the brain (Kleinschnitz et al., 2003; Saleh et al., 2004b). However, the USPIO uptake mechanism in vivo remains elusive, and other factors such as BBB leakage may confound the interpretation of USPIO-enhanced MRI. To address this issue, we assessed the spatiotemporal profile of USPIO enhancement in the CNS directly after intravenous administration.

MATERIAL AND METHODS

Isolation of monocytes

Rat monocytes were freshly isolated by perfusion as reported previously (Floris et al., 2002). Briefly, male adult Lewis Hannover rats were anaesthetized intraperitoneally with an overdose of pentobarbital and fixed in the supine position. The thorax was opened, 300µl heparin (5000 IE/ml) was injected in the left ventricle (apex) and two cannulae, size 16G and 20G, were inserted into the left and right ventricle, respectively.
Rats were perfused with 500ml medium (RPMI-1640), supplemented with 0.5% (w/v) Bovine Serum Albumin (BSA) and 20mM Hepes (pH 7.4), and the effluent was collected. Peripheral blood mononuclear cells (PBMC) were isolated by centrifugation on a Ficoll density gradient (Lymfoprep, 400g, 40min at room temperature) and incubated for 30min at 4ºC with alexa488-coupled monoclonal antibodies (mAb) directed against T-and B-cells (R.7.3 and OX33 respectively, 1µg/ml mAb; 1µl/10^6 target cells). Monocytes were purified from the PBMCs by negative selection using fluorescence activated cell sorting (Mo-Flo, Dakocytomation, USA). Monocyte viability was routinely checked by 7AAD (Molecular Probes, Eugene, Oregon, USA) exclusion and the purity of the isolate was 80% - 90% as determined by the number of ED8 (produced at the Department of Molecular Cell Biology and Immunology, VUMC) -positive cells using a FACScan flow cytometer (Calibur, Becton Dickinson, USA).

Labeling of monocytes with iron oxide particles

Freshly isolated monocytes were incubated in absence (vehicle-treated) or presence of USPIO (Sinerem; Guerbet, France) and SPIO (Endorem; Guerbet, France), as described previously for human monocytes (Oude Engberink et al., 2007). The optimal iron concentrations and incubation time from that study were used as a starting point to achieve efficient labeling of primary rat monocytes. Briefly, iron concentrations in culture medium (supplemented RPMI-1640) were adjusted to 1mg and 4mg Fe/ml containing 2x10^6 cells. Cells were incubated for 1.5h and viability was determined for all samples by using trypan blue exclusion.
To assess the effect of iron uptake on the migratory capacity of SPIO-labeled monocytes, their migration over a monolayer of rat brain endothelial cells was monitored as described previously (Floris et al., 2002; Hendriks et al., 2004; Van der Goes et al., 2001). Briefly, 7.5 x10^5 monocytes suspended in serum-free culture medium were allowed to migrate for 4h over a brain endothelial monolayer (established from rat brain endothelial cell line GP8/3 (Floris et al., 2002; Van der Goes et al., 2001). Monocyte migration was analyzed for labeled cells (SPIO, 4mg Fe/ml) and compared to vehicle-treated monocytes and freshly isolated monocytes. In

addition, monocytes were activated with lipopolysaccharide (LPS, 100ng/ml) for 24h. The level of migration was quantified as the percentage of migrated cells relative to the total number of monocytes present within a field of 200μm^2.

Animal procedures
All animal procedures were approved by the local ethical committee and were performed in accordance with international guidelines on handling laboratory animals.

Intracerebral injection of labeled cells
To validate the potential for in vivo MR detection of SPIO-labeled monocytes, intracerebral injections were performed. Lewis Hannover rats (n=6, 3wks of age) were anaesthetized with 2% isoflurane in a N_2O/O_2 mixture (70/30) and allowed to breath spontaneously. Animals were placed in a stereotactic frame. A hole was drilled in the cranium at 0.5mm anterior and 2.5mm lateral from bregma. Unlabeled monocytes or SPIO-labeled monocytes (ex vivo labeled in 1mg Fe/ml) were injected into the caudate putamen at a depth of 4mm from the cortical surface over a period of 5min through a 26G needle attached to a 50μl syringe (Hamilton Co., Reno, NV). A total of 2x10^6 cells in a volume of 10μl were injected. MRI was performed immediately after cell injection and animals were allowed to recover thereafter. Follow-up scans were performed 24h, 72h and 120h after cell injection.

Transfusion of SPIO-labeled monocytes and USPIO in the PT model
To study monocyte infiltration in vivo, cortical lesions were induced by photochemically initiated thrombosis (PT) (Hoff et al., 2005; Watson et al., 1985). Lewis Hannover rats (n=15, 275-300g) were anaesthetized as described above. For skull illumination, the scalp was incised and the periost was removed. The light source (2.4mm diameter) was positioned perpendicular to the skull surface at 2.7mm anterior and 2.7mm lateral to bregma for lesion induction in the frontal cortex. Each animal was intravenously injected with Erythrosin B (20mg/kg), followed by injection of 0.9% sodium chloride to a total volume of 1ml over a 2min time period. The skull was then illuminated for 2.5min (300mW/cm^2).
On day 5 after PT, animals were anaesthetized as described above. A tail vein was cannulated for intravenous administration of contrast agents. Rats either received no injection (n=4, controls), free USPIO (n=4, 17 mg Fe/kg) or SPIO-labeled monocytes (n=4, 5x10^6 cells, ex vivo labeled in 4mg Fe/ml). MRI was performed before, 24h, 72h and 120h after transfusion. At 72h, two animals per group were sacrificed for histological examination. In a subset of animals (n=3), MRI was performed repeatedly

from immediately up to 8h after intravenous USPIO administration.

Magnetic Resonance Imaging
All experiments were performed using a 4.7T horizontal bore nuclear magnetic resonance (NMR) spectrometer (Varian, Palo Alto, California, USA), equipped with a high-performance gradient insert (12cm inner diameter, maximum gradient strength 500mT/m).

In vitro MRI
To determine the efficiency of monocyte labeling with either USPIO or SPIO, we performed T_2 measurements (9x 0.5mm slices, repetition time (TR) =3200ms, 10 echoes with echo time (TE)-spacing=17.5ms, field of view (FOV) =4 x 4cm; matrix=128 x 128, receiver bandwidth=42.5kHz, number of experiments (NEX) =2) using a birdcage coil (Varian, Palo Alto, California, USA). Relaxation times were measured from agar-gel (0.4%) suspensions containing labeled monocytes ($0.5x10^6$ cells per 250µl) in 96-well plates. T_2-maps were calculated from mono-exponential fitting of MRI signal intensities as a function of TE.

In vivo MRI
Animals were anaesthetized as described above and were prepared for mechanical ventilation by endotracheal intubation. A tail vein was cannulated for injection of Gd-DTPA (Magnevist®, Schering, Berlin, Germany). Animals were immobilized in a specially designed stereotactic holder and placed in an animal cradle, which was inserted into the NMR spectrometer. During MR experiments, animals were mechanically ventilated with isoflurane (2%) in N_2O/O_2 (70/30). Expiratory CO_2 was continuously monitored and body temperature was maintained at 37 ºC using a heated water pad. An infrared sensor (Nonin Medical Inc., Plymouth, Minnesota, USA) was attached to the hind paw for monitoring heart rate and blood oxygen saturation. A homebuilt Helmholtz volume coil (Ø 85mm) and an inductively coupled surface coil (Ø 35mm) were used for radio frequency transmission and signal detection, respectively.
T_2-maps were calculated as described above from T_2 measurements (21x 1mm slices, TR=3200ms, TE-spacing=17.5ms, receiver bandwidth=54.4kHz, FOV=3.2x3.2cm; matrix=128x128, NEX=4). For animals with a PT lesion, T_2*-weighted (T_2*W) images were acquired using a gradient-echo MRI (TR=2500ms, TE=12.5 and 30ms, NEX=2). At the end of the MR session, T_1-weighted (T_1W) spin-echo images (TR=300ms; TE=11.5ms, NEX=4) were collected before and 10min after 0.5 mmol/kg Gd-DTPA injection. Pre- and post-Gd-DTPA T_1W images were subtracted for detection of Gd-DTPA enhancement. Total scanning time was 62 minutes for each animal. In a subset of animals, T_2W and T_2*W MRI was re-

peated for 16 cycles of 30min directly after intravenous USPIO administration.

Immunohistochemistry

Cell samples
Immediately after incubation with either USPIO or SPIO, cell samples were washed, centrifuged (68rpm, 5min) onto glass slides and air-dried. The presence of SPIO and USPIO was detected by Prussian blue staining of iron and cell spots were counterstained with nuclear fast red as previously described (Oude Engberink et al., 2007). Briefly, cell spots were fixed in acetone and incubated with a 1:1 mixture of 2% potassium hexacyanoferrat (II) and 2N HCL for 30 min. Glass slides were rinsed in distilled water and counterstained with nuclear fast red for 5min.

Brain sections
At 72h after lesion induction, PT animals were sacrificed for immunohistochemistry. For detection of free USPIO and SPIO-labeled monocytes, brains were rapidly removed after the final MR scans, snap-frozen in the vapor phase of liquid nitrogen and stored at -80ºC. Serial 10µm coronal cryosections (-20ºC) were cut at the level of the cortical lesion and fixed in acetone for 10min. Sections were pre-incubated in PBS with 10% Fetal Calf Serum (Biowhittaker Europe, Verviers, Belgium), followed by incubation with monoclonal antibody ED1 (1.5µg/ml; Serotec, Oxfordshire, UK) for 1h at room temperature to detect infiltrated monocytes. As secondary antibody, a rabbit -α- mouse IgG-peroxidase conjugate (1µg/ml) was used. Peroxidase activity was demonstrated by incubation with 0.5mg/ml 3.3'-diaminobenzidine-tetra-hydrochloride in Tris-HCl buffer containing 0.03% H_2O_2. Sequential sections were stained for the presence of iron as described above.

Magnetic Resonance Image analyses

In vitro MRI
For analysis of the transverse relaxation rate R_2 ($1/T_2$), regions of interest (ROI) (circular, 7.5mm in diameter) were placed in the center of a well, and special care was taken to exclude areas with air- susceptibility artifacts. R_2 values were obtained by averaging the middle five ROI of the phantom volume. These procedures generated stable relaxation time values with minimum noise levels as described previously (Oude Engberink et al., 2007).

In vivo MRI

MR images obtained from PT animals were quantitatively analyzed for the contrast-enhanced area before and after transfusion. Brains were co-registered and analyzed using the Medical Image NetCDF package (MINC; McConnell Brain Imaging Centre Montréal Neurological Institute, McGill University, Canada). Slices with a clear T_2 lesion, determined 5 days after lesion induction, were selected for further analysis. On corresponding T_2*W images, we calculated the number of hypointense voxels within the lesion defined by a signal intensity lower than the mean signal intensity minus three times the standard deviation of the signal intensity in a cortical ROI (125 voxels), placed just outside the lesion.

To assess contrast enhancement in the lesion directly following USPIO injection, a different approach was used. The lesion area was manually outlined on a pre-contrast T_2 image and the T_2 in this ROI was calculated as a function of time after USPIO injection. To determine contrast enhancement in unaffected tissue a ROI with the same dimensions was placed in the contra-lateral hemisphere.

Statistics

Data are expressed as mean ± standard error of the mean (SEM). Statistical analyses were performed using the statistical software package Sigmastat (version 3.11, 2004). Labeling efficiency and migratory capacity were analyzed using one-way analysis of variance followed by the Student-Newman-Keuls (SNK) post hoc test. In vivo MR data were evaluated by two-way repeated measures analysis of variance, followed by the SNK test. $P < .05$ was considered statistically significant.

RESULTS

Labeling of monocytes with SPIO increases R_2 without affecting migratory capacity.

In order to assess monocyte labeling efficiency using SPIO or USPIO, in vitro MRI was performed on agar phantoms containing cell suspensions (Fig 1A). Uptake of iron by freshly isolated monocytes is correlated with a decrease in T_2 relaxation time (s), that is, an increase in R_2 relaxation rate (s^{-1}). Significant increase in R_2 was found for monocytes incubated with SPIO (Fig 1B). Incubation of monocytes with 4mg Fe/ml SPIO resulted in a R_2 of $12\pm0.9s^{-1}$, which was significantly higher than values found for vehicle-treated cells or cells incubated with 1mg Fe/ml SPIO ($P< .05$). In contrast, no increase in R_2 was observed for monocytes incubated in the presence of 1mg or 4mg Fe/ml USPIO.

Prussian blue staining (Fig 1C) revealed the presence of intracellular iron clusters in cells incubated with SPIO, which were absent in cells incubated with USPIO. Semi-quantitative analysis showed that incubation for 1.5h with 4mg Fe/ml SPIO resulted in iron-positive staining in 50-70% of the cells. Incubation of monocytes in concentrations over 4mg Fe/ml SPIO resulted in the formation of large extracellular iron clusters (data not shown). Cell viability was unchanged (data not shown) and the migratory capacity of iron-labeled monocytes to cross a brain endothelial monolayer was not affected after incubation with 4mg Fe/ml SPIO, since the numbers of migrated cells were at the same levels as for freshly isolated (ctrl) monocytes (Fig 1D).

1A

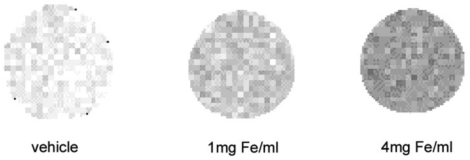

1B

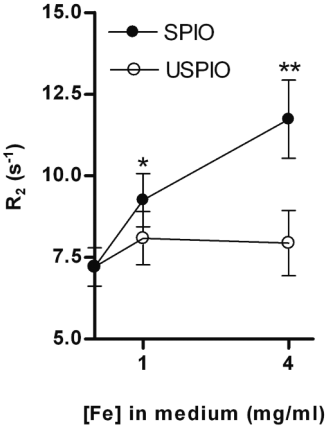

1C

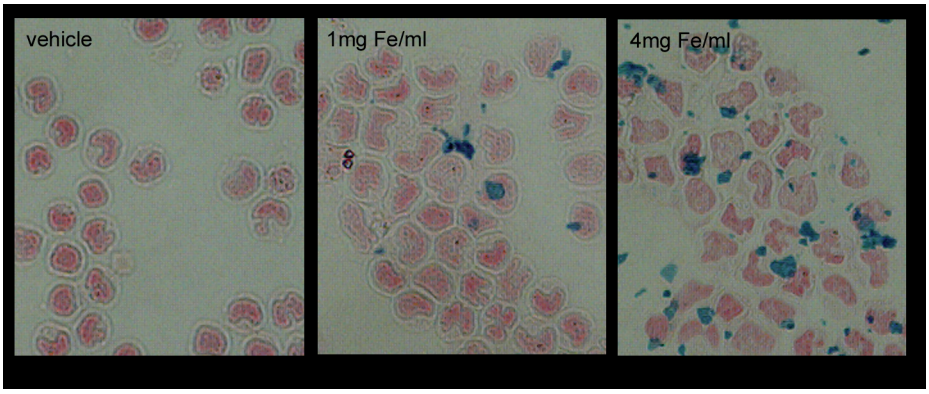

1D

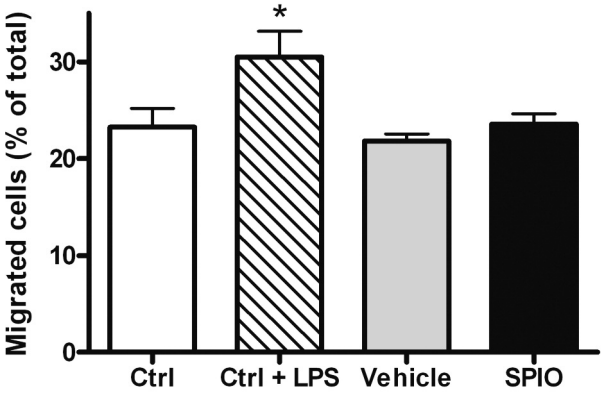

Figure 1: SPIO-labeled monocytes appear hypointense on T_2-maps and their migratory capacity to cross a monolayer of brain endothelial cells is not affected. (**A**) T_2-maps of agar phantoms containing SPIO-labeled monocytes (1 and 4mg Fe/ml). Vehicle-treated monocytes were incubated in the absence of SPIO. (**B**) Increase in R_2 ($1/T_2$) was significant after SPIO incubation (n = 3, * = P< .05 for 1mg Fe/ml versus 0mg Fe/ml and ** = P< .05 for 4mg Fe/ml versus 1mg Fe/ml). No increase is detected after USPIO incubation. (**C**) Increasing concentrations of SPIO in the incubation medium resulted in a higher number of iron-positive monocytes (iron clusters are blue, cell nuclei are red; original magnification: x40). (**D**) SPIO-labeled monocytes (4mg Fe/ml) were allowed to migrate across a monolayer of brain endothelial cells in vitro. The number of migrated monocytes (n=3 in triplicate) is expressed as percentage of the total number of added monocytes. Freshly isolated cells (Ctrl) and vehicle-treated cells served as negative controls. Monocytes stimulated with LPS for 24h showed a significant increase in migratory capacity (* = P< .05 versus Ctrl), whereas SPIO-labeled monocytes showed no increase.

Detection of SPIO-labeled monocytes after intracerebral injection

T_2W images of rat brains after injection of SPIO-labeled monocytes into the brain parenchyma revealed a hypointense area at the injection site, which was absent in animals injected with unlabeled monocytes (Fig 2). With time, the hypointense area decreased but remained detectable after 5 days.

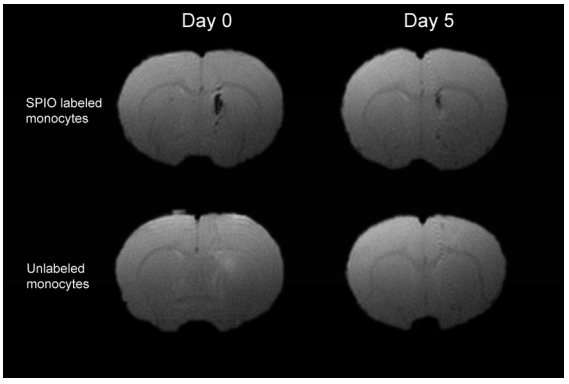

Figure 2: Intracerebral injection of SPIO-labeled monocytes resulted in strongly reduced signal intensity on T_2W images. Immediately after injection (day 0) a large hypointense area was present at the injection site in the caudate putamen. After 5 days, the hypointense area at the injection site had declined. After injection of unlabeled monocytes, a slightly hyperintense area was observed that was most likely the result of the injected fluid.

SPIO-labeled monocytes are detected in the PT lesion after transfusion and contrast enhancement differs from intravenous USPIO injection

To address monocyte infiltration upon neuroinflammation, SPIO-labeled monocytes were transfused in rats with a PT lesion. Contrast enhancement in the lesion after cell transfusion was compared to enhancement patterns in USPIO-injected rats and control rats. In the control group, lesions were induced but rats did not receive labeled cells or USPIO. Figure 3A shows coronal T_2*W images of brain sections through the center of the lesion. In rats transfused with SPIO-labeled monocytes a well-defined area of signal loss was observed after 72h but not at 24h after transfusion. In contrast, the lesion in USPIO-injected rats revealed a large hypointense area 24h after administration, which diminished after 72h. More over, contrast enhancement was present in the vasculature at 24h. In control animals, small signal voids in and around the lesion were detected at all time points.

To assess BBB damage, animals received an injection of Gd-DTPA at the end of each scan session. T_1W subtraction images at 24h showed a clear positive signal that covered the total lesion size (Fig 3B). The area of increased signal intensity was spatially similar to the area of signal loss 24h after USPIO injection.

The area of iron oxide-induced contrast enhancement was quantitatively assessed by determining the number of hypointense voxels present within the lesion (Fig 4A) and was expressed as relative increase with respect to

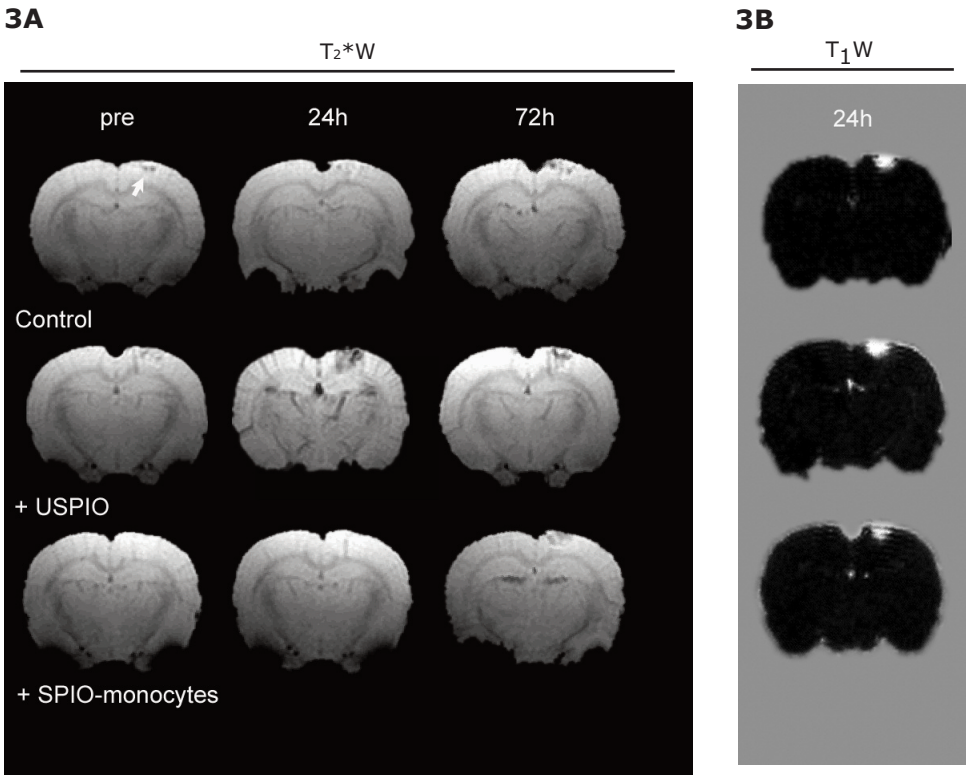

Figure 3: Transfusion of SPIO-labeled monocytes resulted in a different spatiotemporal enhancement pattern compared with injection of free USPIO. (**A**) T_2*W images of the cortical lesion (arrow) are shown for each MR time point. A control rat (top row) showed spot-like hypointensities on all images. The USPIO-injected rat (middle row) showed a large hypointense area after 24h covering the lesion, which had declined at 72h. After transfusion of SPIO-labeled monocytes a distinct area of reduced signal intensity appeared after 72h (bottom row). (**B**) Pre- minus post-Gd-DTPA T_1W images of corresponding brain sections at 24h. Note the large hyperintense area that is present for all experimental groups.

the pre-injection image (Fig 4B). Figure 4A shows a T2*W image 72h after monocyte transfusion and the area within the lesion that was defined as hypointense. The contrast-enhanced area slightly increased with time in control animals. In USPIO-injected rats the number of contrast-enhanced voxels in the lesion increased up to 400% (407 ± 39%) at 24h, which declined thereafter. In contrast, following transfusion of SPIO-labeled monocytes, there was a significant increase in the area of contrast enhancement after 72h (340 ± 106%), which remained significantly elevated up to 120h.

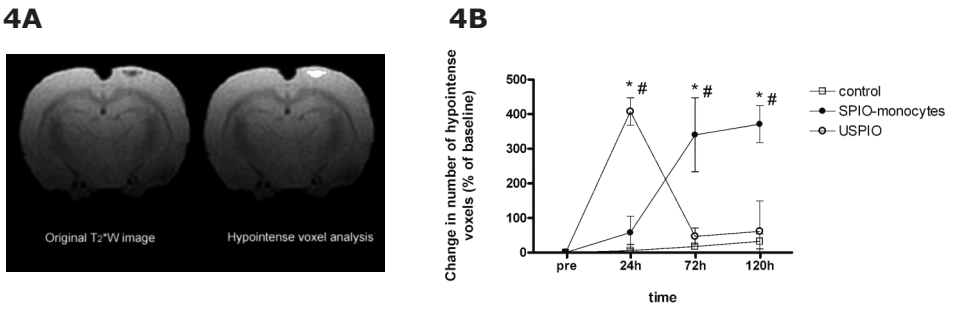

Figure 4: Temporal changes in contrast enhancement in the lesion. (**A**) Rat brain section at 72h after transfusion of SPIO-labeled monocytes without (left) and with (right) the calculated overlay of the contrast-enhanced region. (**B**) Changes in the relative number of contrast-enhanced voxels with respect to the pre-injection image for each MR time point (n=4 for pre, 24h and 72h, n=2 for 120h). In the USPIO-injected group the contrast-enhanced area showed an increase of 407±39% at 24h. (* = P< .05 versus control; # = P< .05 versus SPIO-labeled monocytes). In animals transfused with SPIO-labeled monocytes, the contrast-enhanced area was increased significantly up to 340±106% at 72h. (* = P< .05 versus control; and # = P<0 .05 versus USPIO) and remained elevated up to 120h (371±53%).

Immunohistochemical analysis shows distinct distribution of iron oxide particles in the lesion after transfusion of SPIO-labeled monocytes compared with free USPIO

Serial cryosections were analyzed to detect iron in the lesion and the presence of infiltrated monocytes (Fig 5). In all groups ED1-positive cells (monocytes) were observed throughout the lesion at 72h. In subsequent sections, Prussian blue analysis revealed small iron-positive spots inside the lesion of animals transfused with SPIO-labeled monocytes, reflecting infiltration of labeled monocytes. In contrast, in animals that received intravenous USPIO injections, Prussian blue stainings showed a large blue rim covering part of the lesion site.

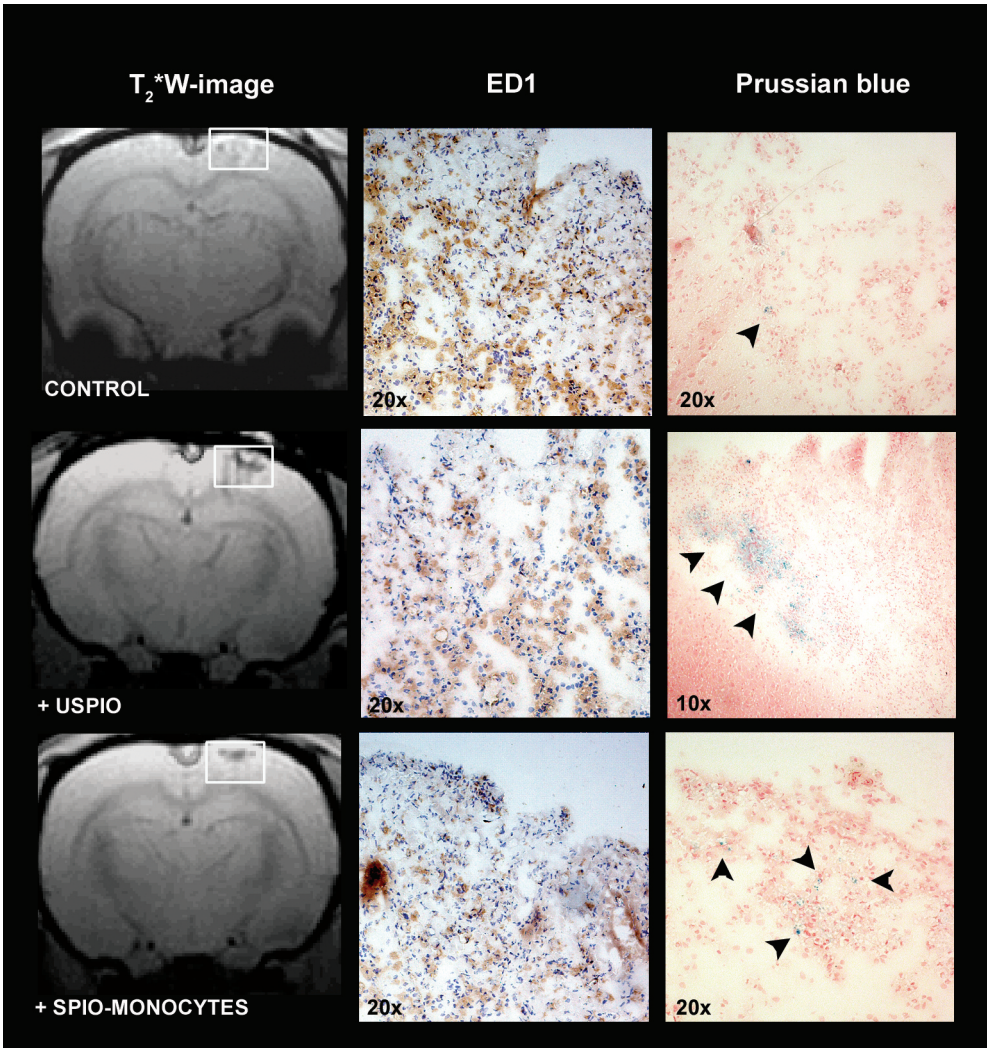

Figure 5: ED1+ cells and distinct patterns of iron accumulation are present throughout the lesion. Subsequent brain sections of animals sacrificed at 72h were stained either for infiltrated monocytes (ED1+ cells indicated by dark brown colour) or iron (Prussian blue; presence of iron (blue) is indicated by arrowheads). The presence of ED1+ cells is demonstrated for each group of animals. In USPIO-injected rats a large iron-positive rim is present in the lesion. In contrast, in animals transfused with SPIO-labeled monocytes the lesion showed a distinct pattern of iron-positive areas, reflecting the presence of infiltrated SPIO-labeled monocytes.

Time course of USPIO enhancement in PT lesion

To investigate the time course of contrast enhancement after USPIO injection in more detail, PT rats were scanned repeatedly from 0 up to 8h after USPIO injection and again after 24h. T_2-maps (Fig 6A) revealed hypointense areas in the lesion at an early stage increasing in size up to 8h.

6A

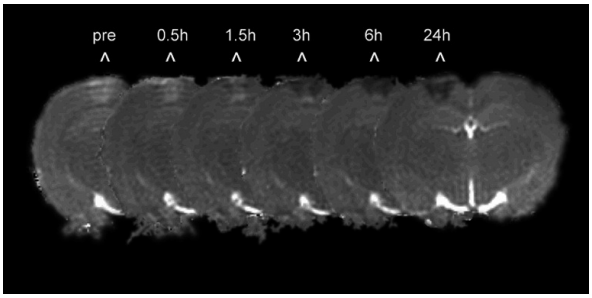

6B

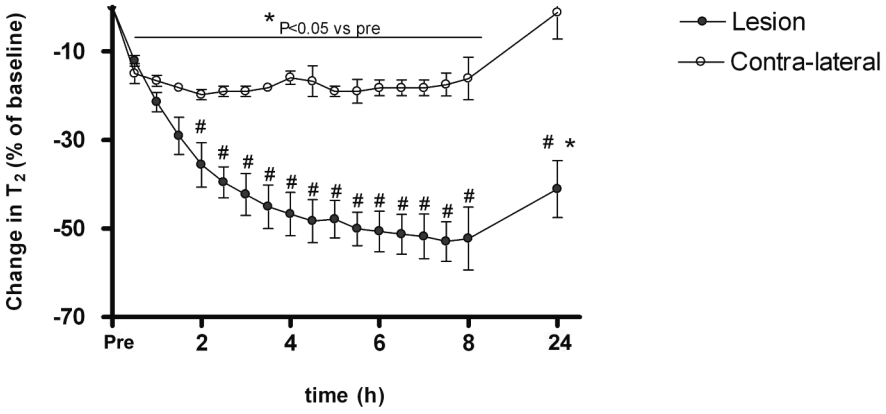

Figure 6: Contrast enhancement in the lesion differs from the contra-lateral site within 2h after USPIO injection. (**A**) T_2-maps of a rat brain section before (pre) and 0.5, 1.5, 3, 6, 24h after USPIO injection. Before USPIO injection, the lesion is characterized by a prolonged T_2. After USPIO injection, T_2 reduction was evident in the lesion after 0.5h and signal loss continued up to 8h. (**B**) Time course of T_2 reduction in the lesion and its contra-lateral counterpart following USPIO injection. Relative T_2 reduction is expressed as percentage of baseline (pre). T_2 reduction in the contra-lateral ROI stabilized at ca. 15% within 0.5h after USPIO injection, reflecting the presence of USPIO in the vasculature. T_2 was normal after 24h, indicative of USPIO washout. Relative T_2 decrease in the lesion ROI was significantly larger compared with the contra-lateral area, starting at 2h after USPIO injection (-36±5% versus -19±1% respectively). T_2 remained significantly decreased in the lesion after 24h (-41±6%). * = P< .05 versus pre and # = P< .05 versus contra-lateral.

Loss of T_2 in the lesion (Fig 6B) was significantly different from that in the contra-lateral hemisphere 2h after USPIO injection, with a maximum reduction at 6 to 8h. The T_2 in the lesion was only partially restored after 24h. The contra-lateral hemisphere showed a smaller decrease in T_2, which remained constant over 0.5 to 8h, indicating the presence of USPIO in circulation. Contra-lateral T_2 was normal again after 24h.

DISCUSSION

Our MRI study demonstrates that monocyte trafficking towards areas of neuroinflammation can be monitored longitudinally and non-invasively using monocytes that are ex vivo labeled with iron oxide particles. Importantly, in a photothrombotic cortical lesion that is accompanied by massive monocyte infiltration several days after lesion induction, the enhancement pattern in the lesion differed from MRI signal changes following intravenous administration of free USPIO. More over, USPIO enhancement was already present in the lesion within 2h after injection, while SPIO-labeled monocytes were detected after 72h. This suggests that other mechanisms such as BBB leakage or endothelial trapping contribute to early USPIO enhancement in the brain.

Monocyte infiltration is a key event in ongoing inflammation and tissue destruction in many CNS pathologies (Nilupul Perera et al., 2006; Price et al., 2003; Stoll et al., 1998). To improve the efficacy of therapeutic compounds that limit cellular infiltration, it is important to elucidate the pattern of monocyte recruitment in the CNS. Ex vivo labeling of monocytes with iron oxide particles enables MR visualization and may provide an accurate and non-invasive tracking method.

We found that freshly isolated rat monocytes can be labeled ex vivo more efficiently using SPIO than USPIO, which is in line with our previous observations on human monocytes (Oude Engberink et al., 2007). Uptake of SPIO and the labeling procedure did not affect cell viability and capacity of monocytes to cross a monolayer of brain endothelial cells. The low uptake of USPIO by monocytes compared with SPIO may be explained by the relatively small size of these particles (30nm), which excludes the endosomal pathway by receptor-mediated uptake (Raynal et al., 2004). In this study, we used USPIO rather than SPIO to investigate the effect of free iron oxide particles since the blood pool half-life of USPIO (5 to 6h in rats) is much longer compared to SPIO (less than 6min) (Weissleder et al., 1989). Earlier studies have used intravenous administration of free USPIO and performed MRI 24h later to study macrophage activity in vivo (Dousset et al., 1999a; Rausch et al., 2001; Weissleder et al., 1989). However, the pathway of free particle uptake and delivery into the brain parenchyma is not fully understood.

Therefore, we compared intravenous administration of free USPIO to transfusion of SPIO-labeled monocytes in rats with a photothrombotic lesion. Photochemically induced thrombosis elicits a strong inflammatory response resulting in a large area of monocyte infiltration, which occurs 5 to 8 days after lesion induction (Schroeter et al., 1997; Stoll et al., 1998). With MRI we detected the presence of SPIO-labeled monocytes in the lesion 72h after transfusion. Histochemical analyses demonstrated the pres-

ence of iron-positive cells in the lesion. However, MR images of control animals also showed small hypointense areas in the lesion that were present at all MR time points. These results are in line with previous studies (Saleh et al., 2004b) and may point to residues of erythrocytes accumulating in phagocytes that are clearing the lesion from debris. To overcome these confounds introduced by the PT model we quantitatively analyzed the MR images and showed that 72h after transfusion of SPIO-labeled monocytes, signal changes in the lesion were significantly increased compared with control animals. Alternatively, in future studies the introduction of a fluorescent label should be considered as this may facilitate discrimination between non-specific signal voids in the lesion from infiltrated SPIO-labeled monocytes. An earlier study has reported on MR tracking of labeled mononuclear cells in to the ischemic brain of splenectomized mice(Stroh et al., 2006). In agreement with our results, the authors reported MRI signal changes in the brain within two to four days after cell transfusion. This relatively late contrast enhancement in the lesion is different from findings from earlier studies in which free USPIO injection was applied to detect infiltration of monocytes (Dousset et al., 1999b; Saleh et al., 2004b). In these studies contrast enhancement was maximal 24h after USPIO injection. To further address this discrepancy in the time course of contrast enhancement, we directly compared enhancement patterns after injection of free or intracellular iron oxide particles.

In contrast to transfusion of SPIO-labeled monocytes, the intravenous USPIO injection resulted in strong contrast enhancement at 24h, which subsequently declined at 72h. Previous studies in this animal model reported that such USPIO enhancements in a PT lesion are in spatial agreement with ED1+ areas (Rausch et al., 2001; Saleh et al., 2004b; Schroeter et al., 2004), suggesting incorporation of USPIO in to infiltrated monocytes. The time course of contrast enhancement has been described to correspond to the time window of monocyte influx (Kleinschnitz et al., 2003). In contrast, our study showed that the spatiotemporal profile of USPIO enhancement (24h) differed from MRI signal changes following transfusion of SPIO-labeled monocytes (72h).

So far, the use of free USPIO has been suggested to specifically image macrophage infiltration. Interestingly, in an earlier study, it has been shown that after increasing the circulation time of free SPIO by elimination of blood-borne macrophages, similar contrast enhancement is observed as after free USPIO injection (Oweida et al., 2005). This supports the possibility that leakage of iron oxide particles over an impaired BBB contributes to contrast enhancement in the brain. This concept is also supported by our findings. We showed that contrast enhancement in the lesion increased significantly 2h after USPIO injection and was maximal enhanced after 6 to 8h. More over, we showed that Gd-DTPA enhance-

ment, a conventional marker for BBB breakdown, was in spatial agreement with USPIO enhancement. Within the short time frame, it is unlikely that monocytes incorporate USPIO in circulation as the labeling capacity of USPIO is very low, as discussed earlier. Intravascular trapping of iron oxide particles, due to the presence of occluded vessels, may be an alternative explanation for the observed acute enhancement in the lesion. However, intravascular trapping of USPIO has only been observed in this model upon intravenous administration of USPIO during lesion induction (Kleinschnitz et al., 2005). Previously, non-specific USPIO uptake has been reported following permanent middle cerebral artery occlusion (Rausch et al., 2001; Wiart et al., 2007). In these studies, USPIO were intravenously injected 5h after occlusion and the early signal enhancement observed in the lesion similarly supports the assumption that USPIO can penetrate a damaged brain area independent of monocyte infiltration. In our study, USPIO were injected 5 days after lesion induction reducing the possibility that USPIO are trapped in occluded vessels and most likely enter the brain parenchyma via transcytosis or passive leakage.

In conclusion, we have shown that cellular MRI can be used to specifically monitor homing of monocytes, labeled ex vivo with SPIO, towards areas of neuroinflammation in the rat brain. This strategy may provide an important tool for the evaluation of drugs that limit cellular infiltration into the CNS, thereby reducing neurological deficits. In addition, our study suggests that contrast enhancement after intravenous injection of free USPIO may not solely represent the migration of peripherally labeled cells, but may also be the result of leakage over a damaged BBB. This report may aid to elucidate the heterogeneous enhancement patterns after USPIO administration for the assessment of the inflammatory response in stroke and MS patients.

ACKNOWLEGDEMENTS

The authors thank Guerbet France for supplying the MR contrast agents. This work was supported by the Dutch MS Research Foundation (MS 01-470, MS 02-489) and the European Commission (HPRI-CT-2001-50028).

REFERENCES

Arbab AS, Bashaw LA, Miller BR, Jordan EK, Lewis BK, Kalish H, et al. Characterization of biophysical and metabolic properties of cells labeled with superparamagnetic iron oxide nanoparticles and transfection agent for cellular MR imaging. Radiology 2003; 229: 838-46.

Corsini E, Gelati M, Dufour A, Massa G, Nespolo A, Ciusani E, et al. Effects of beta-IFN-1b treatment in MS patients on adhesion between PBMNCs, HUVECs and MS-HBECs: an in vivo and in vitro study. J Neuroimmunol 1997; 79: 76-83.

Dirnagl U, Iadecola C, Moskowitz MA. Pathobiology of ischaemic stroke: an integrated view. Trends Neurosci 1999; 22: 391-7.

Dousset V, Brochet B, Deloire MS, Lagoarde L, Barroso B, Caille JM, et al. MR imaging of relapsing multiple sclerosis patients using ultra-small-particle iron oxide and compared with gadolinium. AJNR Am J Neuroradiol 2006; 27: 1000-5.

Dousset V, Delalande C, Ballarino L, Quesson B, Seilhan D, Coussemacq M, et al. In vivo macrophage activity imaging in the central nervous system detected by magnetic resonance. Magn Reson Med 1999a; 41: 329-33.

Dousset V, Gomez C, Petry KG, Delalande C, Caille JM. Dose and scanning delay using USPIO for central nervous system macrophage imaging. Magma 1999b; 8: 185-9.

Floris S, Blezer EL, Schreibelt G, Dopp E, van der Pol SM, Schadee-Eestermans IL, et al. Blood-brain barrier permeability and monocyte infiltration in experimental allergic encephalomyelitis: a quantitative MRI study. Brain 2004; 127: 616-27.

Floris S, Ruuls SR, Wierinckx A, van der Pol SM, Dopp E, van der Meide PH, et al. Interferon-beta directly influences monocyte infiltration into the central nervous system. J Neuroimmunol 2002; 127: 69-79.

Hendriks JJ, Alblas J, van der Pol SM, van Tol EA, Dijkstra CD, de Vries HE. Flavonoids influence monocytic GTPase activity and are protective in experimental allergic encephalitis. J Exp Med 2004; 200: 1667-72.

Hoff EI, oude Egbrink MG, Heijnen VV, Steinbusch HW, van Oostenbrugge RJ. In vivo visualization of vascular leakage in photochemically induced cortical infarction. J Neurosci Methods 2005; 141: 135-41.

Huitinga I, Ruuls SR, Jung S, Van Rooijen N, Hartung HP, Dijkstra CD. Macrophages in T cell line-mediated, demyelinating, and chronic relapsing experimental autoimmune encephalomyelitis in Lewis rats. Clin Exp Immunol 1995; 100: 344-51.

Kleinschnitz C, Bendszus M, Frank M, Solymosi L, Toyka KV, Stoll G. In vivo monitoring of macrophage infiltration in experimental ischemic brain lesions by magnetic resonance imaging. J Cereb Blood Flow Metab 2003; 23: 1356-61.

Kleinschnitz C, Schutz A, Nolte I, Horn T, Frank M, Solymosi L, et al. In vivo detection of developing vessel occlusion in photothrombotic ischemic brain lesions in the rat by iron particle enhanced MRI. J Cereb Blood Flow Metab 2005.

Lassmann H. Basic mechanisms of brain inflammation. J Neural Transm Suppl 1997; 50: 183-90.

Lee VM, Burdett NG, Carpenter A, Hall LD, Pambakian PS, Patel S, et al. Evolution of photochemically induced focal cerebral ischemia in the rat. Magnetic resonance imaging and histology. Stroke 1996; 27: 2110-8; discussion 2118-9.

Niino M, Bodner C, Simard ML, Alatab S, Gano D, Kim HJ, et al. Natalizumab effects on immune cell responses in multiple sclerosis. Ann Neurol 2006; 59: 748-54.

Nilupul Perera M, Ma HK, Arakawa S, Howells DW, Markus R, Rowe CC, et al. Inflammation following stroke. J Clin Neurosci 2006; 13: 1-8.

Oude Engberink RD, van der Pol SM, Dopp EA, de Vries HE, Blezer EL. Comparison of SPIO and USPIO for in vitro labeling of human monocytes: MR detection and cell function. Radiology 2007; 243: 467-74.

Oweida A, Dunn E, Foster P. Cellular Imaging of Neuroinflammation: A novel method for Unraveling the Roles of Macrophages Populations in EAE. ISMRM. Miami beach, Florida, USA, 2005.

Polfliet MM, van de Veerdonk F, Dopp EA, van Kesteren-Hendrikx EM, van Rooijen N, Dijkstra CD, et al. The role of perivascular and meningeal macrophages in experimental allergic encephalomyelitis. J Neuroimmunol 2002; 122: 1-8.

Polman CH, O'Connor PW, Havrdova E, Hutchinson M, Kappos L, Miller DH, et al. A randomized, placebo-controlled trial of natalizumab for relapsing multiple sclerosis. N Engl J Med 2006; 354: 899-910.

Price CJ, Warburton EA, Menon DK. Human cellular inflammation in the pathology of acute cerebral ischaemia. J Neurol Neurosurg Psychiatry 2003; 74: 1476-84.

Rausch M, Sauter A, Frohlich J, Neubacher U, Radu EW, Rudin M. Dynamic patterns of USPIO enhancement can be observed in macrophages after ischemic brain damage. Magn Reson Med 2001; 46: 1018-22.

Raynal I, Prigent P, Peyramaure S, Najid A, Rebuzzi C, Corot C. Macrophage endocytosis of superparamagnetic iron oxide nanoparticles: mechanisms and comparison of ferumoxides and ferumoxtran-10. Invest Radiol 2004; 39: 56-63.

Saleh A, Schroeter M, Jonkmanns C, Hartung HP, Modder U, Jander S. In vivo MRI of brain inflammation in human ischaemic stroke. Brain 2004a; 127: 1670-7.

Saleh A, Wiedermann D, Schroeter M, Jonkmanns C, Jander S, Hoehn M. Central nervous system inflammatory response after cerebral infarction as detected by magnetic resonance imaging. NMR Biomed 2004b; 17: 163-9.

Schroeter M, Jander S, Huitinga I, Witte OW, Stoll G. Phagocytic response in photochemically induced infarction of rat cerebral cortex. The role of resident microglia. Stroke 1997; 28: 382-6.

Schroeter M, Saleh A, Wiedermann D, Hoehn M, Jander S. Histochemical detection of ultrasmall superparamagnetic iron oxide (USPIO) contrast medium uptake in experimental brain ischemia. Magn Reson Med 2004; 52: 403-6.

Stoll G, Jander S, Schroeter M. Inflammation and glial responses in ischemic brain lesions. Prog Neurobiol 1998; 56: 149-71.

Stroh A, Zimmer C, Werner N, Gertz K, Weir K, Kronenberg G, et al. Tracking of systemically administered mononuclear cells in the ischemic brain by high-field magnetic resonance imaging. Neuroimage 2006.

Van der Goes A, Wouters D, Van Der Pol SM, Huizinga R, Ronken E, Adamson P, et al. Reactive oxygen species enhance the migration of monocytes across the blood-brain barrier in vitro. Faseb J 2001; 15: 1852-4.

Watson BD, Dietrich WD, Busto R, Wachtel MS, Ginsberg MD. Induction of reproducible brain infarction by photochemically initiated thrombosis. Ann Neurol 1985; 17: 497-504.

Weissleder R, Cheng HC, Bogdanova A, Bogdanov A, Jr. Magnetically labeled cells can be detected by MR imaging. J Magn Reson Imaging 1997; 7: 258-63.

Weissleder R, Stark DD, Engelstad BL, Bacon BR, Compton CC, White DL, et al. Superparamagnetic iron oxide: pharmacokinetics and toxicity. AJR Am J Roentgenol 1989; 152: 167-73.

Wiart M, Davoust N, Pialat JB, Desestret V, Moucharaffie S, Cho TH, et al. MRI monitoring of neuroinflammation in mouse focal ischemia. Stroke 2007; 38: 131-7.

Xu S, Jordan EK, Brocke S, Bulte JW, Quigley L, Tresser N, et al. Study of relapsing remitting experimental allergic encephalomyelitis SJL mouse model using MION-46L enhanced in vivo MRI: early histopathological correlation. J Neurosci Res 1998; 52: 549-58.

Yeh TC, Zhang W, Ildstad ST, Ho C. Intracellular labeling of T-cells with superparamagnetic contrast agents. Magn Reson Med 1993; 30: 617-25.

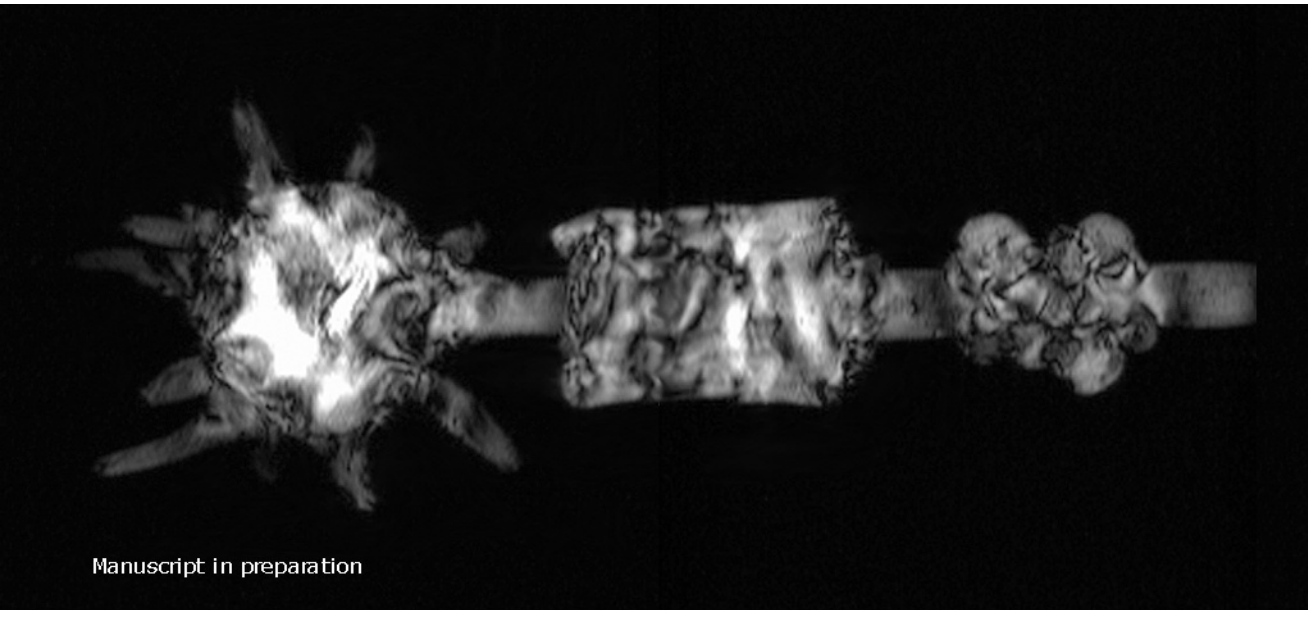

Manuscript in preparation

Magnetic Resonance Imaging of Monocytes Labeled with USPIO using Magneto Electroporation in an Animal Model of Multiple Sclerosis

R.D. Oude Engberink[1], H.E. de Vries[2], S.M.A. van der Pol[2], P. Walczak[3,5], J.W.M. Bulte[3,4,5], A. van der Toorn[1], M.A. Viergever[1], C.D. Dijkstra[2], E.L.A. Blezer[1]

[1]Image Sciences Institute, University Medical Center Utrecht
[2]Molecular Cell Biology and Immunology, VU Medical Center Amsterdam
[3]Russell H. Morgan Department of Radiology and Radiological Science, Division of MR Research, [4]Department of Chemical and Biomolecular Engineering, and [5]Cellular Imaging Section, Institute for Cell Engineering, The Johns Hopkins University School of Medicine, Baltimore, Maryland, USA

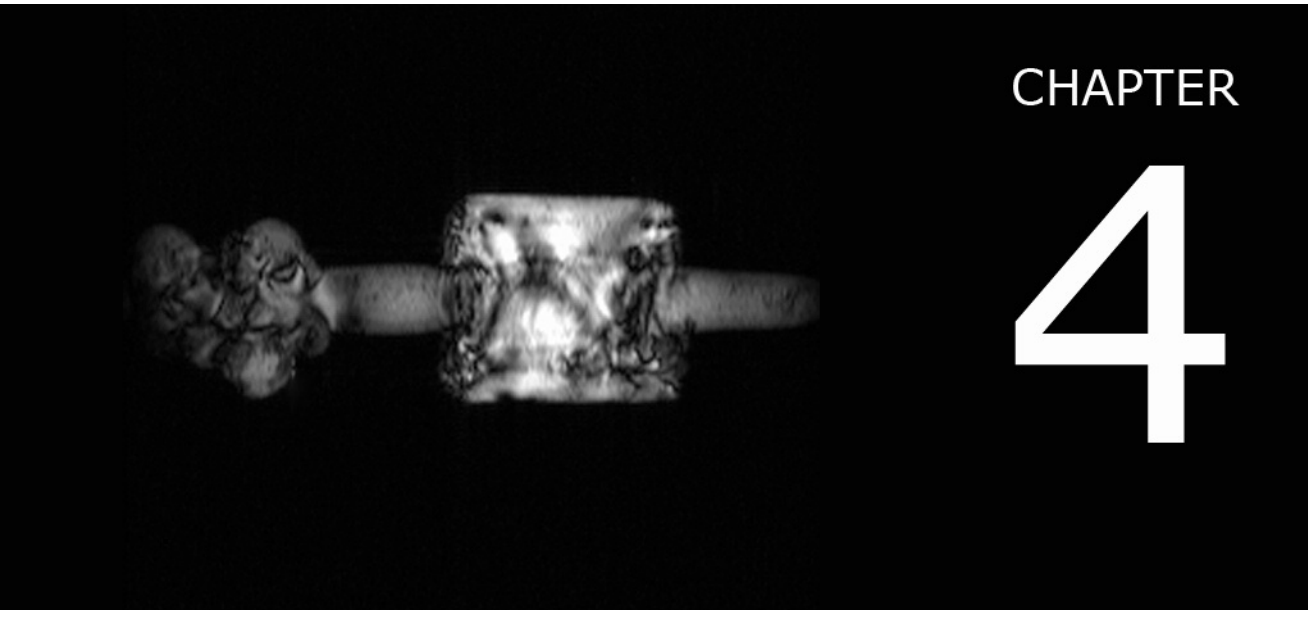

ABSTRACT

Monocyte infiltration in the central nervous system (CNS) plays a crucial role in lesion development and progression in multiple sclerosis (MS). Sensitive methods to monitor their infiltration kinetics are lacking. Labeling monocytes with superparamagnetic particles of iron oxide (SPIO) and tracking by magnetic resonance imaging (MRI) may be a powerful approach to specifically address monocyte recruitment to multiple inflammatory lesions in the CNS.

Here we used magneto-electroporation (MEP) to label rat monocytes with clinical grade iron oxide particles (Sinerem, Endorem and Supravist). Best labeling results were obtained with the smaller sized and charged Supravist and labeled monocytes were intravenously injected in animals with experimental autoimmune encephalomyelitis. Imaging at 4.7T revealed multiple foci of decreased signal intensity in the CNS 24h and 72h later. Ex vivo high resolution MRI (9.4T) showed that these hypointensities were predominantly located in the white matter of the cerebellum.

Our findings demonstrate that MEP highly improves visualization of labeled monocytes migrating towards multiple lesions in the CNS. This technique allows fast and effective labeling and re-injection of monocytes and may be developed as diagnostic and evaluation tool in MS patients in the near future.

INTRODUCTION

In recent years, magnetic resonance imaging (MRI) has become one of the most widely used imaging modalities to visualize pathological processes in a non-invasive manner. In neuroinflammatory diseases like multiple sclerosis (MS), stroke and Alzheimer's disease, MRI is used as diagnostic tool and as a measure for disease progression (Gebarski et al. 1985; Kertesz, Black et al. 1987; Drayer 1988). Recently, the development of superparamagnetic particles of iron oxide (SPIO) has made it possible to study the underlying cellular pathology (Corot et al. 2004). SPIO consist of an iron oxide core that distorts the magnetic field causing a rapid loss of signal and clusters of SPIO-loaded cells appear hypointense on a T_2-weighted image (Bulte and Kraitchman 2004).

The success of cellular MRI relies on specific and efficient labeling of cells with SPIO without interfering with cell function. Ideally, cells of interest should be isolated from the subject, labeled ex vivo with MR contrast agents and re-injected in a short period of time. To visualize neuroinflammatory processes using intravenous injections of ex vivo labeled monocytes, we and others have shown that cellular MRI is capable of tracking mononuclear cells that are recruited towards large ischemic lesions in the central nervous system (CNS) (Stroh et al. 2006; Oude Engberink et al. 2007).

However, imaging of monocyte infiltration in CNS pathologies with multiple small lesions, as in the case of MS, is still a major challenge related to smaller-sized lesions and consequently an accumulation of a low number of labeled monocytes. So far, no successful strategy to track monocytes in experimental autoimmune encephalomyelitis (EAE), using monocytes labeled with SPIO has been described. EAE, widely used as animal model of MS, mimics the important pathologic events during MS, i.e. increased permeability of the blood-brain barrier (BBB) and the formation of cellular infiltrates in the CNS (de Vries et al. 1997; Al-Omaishi et al. 1999). These infiltrates are present throughout the brain and spinal cord and mainly consist of monocyte-derived macrophages which are key players in the process of myelin degradation and tissue damage (Bruck et al. 1996). Therefore, selective inhibition of monocyte infiltration is considered an attractive therapeutic strategy to limit inflammatory tissue damage. To design an effective treatment it is desired to specifically intervene at the moment of monocyte entry, a crucial event yet largely unknown.
Cellular MRI applied to tracking monocytes in EAE may be able to elucidate the spatio-temporal pattern of monocyte infiltration during the course of the disease. To increase the MR detection limit for individual monocytes

that infiltrate the CNS, a high load of contrast agent per cell is crucial. In addition, to avoid cell activation and cell death during prolonged incubation or culture, the labeling strategy must be fast and performed prior to cell transfusion. Here, we describe the use of a novel labeling technique, magneto-electroporation (MEP) that efficiently labels monocytes within a few milliseconds (Walczak et al. 2005) and demonstrate that it is a promising method for labeling and tracking monocytes by MRI into multiple CNS lesions.

MATERIALS AND METHODS

All procedures described in this study were approved by the local ethical committee and were performed in accordance with international guidelines on handling laboratory animals.

Labeling of monocytes by magneto-electroporation

Rat monocytes were freshly isolated by perfusion as reported previously (Floris et al. 2002). Monocytes were suspended in phosphate-buffered saline (PBS) at a density of 5 to $10x10^6$ cells/ml in gene pulser® cuvettes (0.4cm, Bio-Rad Laboratories, USA). To test the uptake of different iron oxide particles with respect to size and surface charge, we used three different contrast agents; Sinerem (30nm, Guerbet, France), Endorem (150nm, Guerbet, France) and Supravist (26nm, Schering AG, Germany). Contrast agents were mixed with cell suspensions at a concentration of 1 and 3mg Fe/ml and cooled on ice for 5min and subsequently placed in the electroporator machine (BTX electroporation system; Harvard Apparatus ECM830, Holliston, USA). Electroporation parameters were adjusted to a pulse strength of 100V using 5 pulses of 5ms with an interpulse delay of 100ms. These pulse parameters have been optimized in a pilot experiment to efficiently label freshly isolated rat monocytes without affecting cell viability. After electroporation, cell samples were put on ice for 5 min, washed three times in PBS and re-suspended at a density of $2x10^7$ cells/ml for cell transfusion.

Assessment of monocyte viability, metabolic activity and iron oxide particle incorporation

Cell viability was determined by using a trypan blue exclusion assay. Dead cells were counted with a microscope in a total area of $25mm^2$ (approximately 150 cells) using a calibrated counting chamber.

The metabolic activity of labeled monocytes was determined as previously described (Walczak et al. 2006) using a MTS assay (CellTiter 96 Aqueous one assay, Promega, Madison, USA). In a 96-well plate, monocytes were incubated with 20µl of MTS solution at 37°C for 4h. The absorbance at 492nm was measured using a microplate reader (Beckman Coulter AD200, Fullerton, USA).

To determine intracellular iron uptake histochemically, cytospin samples were stained with Prussian blue (PB). Cells were fixed in acetone and incubated with a 1:1 mixture of 2% potassium hexacyanoferrat (II) and 2N HCL for 30 min, rinsed in distilled water and counterstained with nuclear fast red for 5min. For intracellular iron quantification, samples containing $1x10^6$ labeled monocytes were acid-digested using a Ferrozin-based spectrophotometric assay as previously described (Bulte et al. 2001).

In vitro MRI of labeled monocytes

T_2-relaxation time measurements were performed using a 4.7T horizontal bore NMR spectrometer (Varian, Palo Alto, USA) with the following parameters: 9x 0.5mm slices, repetition time (TR) =3200ms, 10 echoes with echo time (TE)-spacing=17.5ms, field of view (FOV) =4 x 4cm; matrix=128 x 128, number of experiments (NEX) =2. T_2-relaxation times were measured from agar-gel (0.4%) suspensions containing a series of samples of labeled monocytes (0.02 – 0.5 $x10^6$ cells per 250µl) in 96-well plates. Monocytes were electroporated with Supravist at a concentration of 2mg Fe/ml. T_2-maps were calculated from mono-exponential fitting of MRI signal intensities as a function of TE.

Induction of acute EAE and intravenous injection of labeled monocytes

Acute EAE (n=10) was induced in male Lewis Hannover rats (210 – 240g, Harlan, Zeist, The Netherlands) as previously described (Schreibelt et al. 2006). For EAE induction, rats were injected at day 0 subcutaneously in one hind footpad with 20µg of guinea pig myelin basic protein (MBP) in PBS mixed with complete Freund's adjuvant (Difco Laboratories, Detroit, USA) while anaesthetized with 2% isoflurane in a N_2O/O_2 mixture (70/30). Clinical symptoms were scored daily and graded from 1 to 5: 0, no clinical signs; 0.5, partial loss of tail tonus; 1, complete loss of tail tonus; 2, unsteady gait; 2.5, partial hind limb paralysis; 3, complete hind limb paralysis; 4, paralysis of the complete lower part of the body up to the diaphragm; 5, death due to EAE. At day 10 after immunization, clinical symptoms start to develop and this day is marked as disease onset. At day 13, clinical scores are maximal and it represents the peak of the disease. Freshly prepared monocytes were electroporated (2mg Fe/ml Supravist) and directly injected (1.0-1.2$x10^7$ labeled monocytes per animal) in the tail vein of recipient rats at day 10 (n=4) and day 13 (n=4). EAE rats without cell injection (n=2) served as negative control.

In vivo MRI following intravenous injection of labeled monocytes

Animals were imaged just before, and 24h and 72h after monocyte injection using a 4.7T horizontal bore NMR spectrometer (Varian, Palo Alto, USA). Prior to MRI, rats were initially anaesthetized as described for EAE induction followed by endotracheal intubation for mechanical ventilation with isoflurane (2%) in N_2O/O_2 (70/30). Slice positions were determined on a transversal scout image and the central slice was positioned directly caudal of the cerebellum. The slices covered the upper part of the spinal cord, the cerebellum and caudal part of the cerebrum. T_2-relaxation time MRI was performed with the following parameters: 21x 1mm slices, TR=3200ms, 9 echoes with TE-spacing=17.5ms, FOV=32 x 32mm; ma-

trix=128 x 128, NEX=4. T_2*-weighted (T_2*W) images were acquired using a gradient-echo sequence: TR=2500ms, TE=12.5, NEX=2. To reduce intrinsic T_2* effects caused by paramagnetic deoxyhemoglobin in erythrocytes, the percentage O_2 in the anesthesia gas mix was changed to 100% O_2 during T_2*W measurements.

Ex vivo MRI and histology

Directly after the 72h scan, rats were sacrificed by intraperitoneal injection of pentobarbital (euthesate®) and perfused transcardially with saline followed by 4% paraformaldehyde in 0.1M phosphate buffer. Brain and spinal cord were dissected and post-fixed in formaldehyde.

Ex vivo MRI experiments were performed using a 9.4T horizontal bore NMR spectrometer (Varian, Palo Alto, USA) with a quadrature surface coil (RAPID, Biomedical, Rimpar, Germany). Brain and spinal cords were immersed in Fomblin (perfluorinated polyether, Solvay Solexis, Weesp, The Netherlands) to prevent air-tissue artifacts. T_2*W images were acquired using a 3D gradient-echo sequence with the following parameters for brains: TR=2500ms, TE=12.5ms, FOV=25x25x25mm, matrix size=256x256x256, NEX=8, giving a final isotropic resolution of 98µm. For spinal cords, we used a field of view of 100x30x30 and a matrix size of 512x256x256.

Following ex vivo MRI, brains were processed for the detection of infiltrated monocytes (ED1) and the presence of iron oxide particles (Prussian blue) as described elsewhere (Oude Engberink et al. 2007).

Quantitative analysis of hypointensities

To quantify regions of low signal intensity as a result of labeled monocyte recruitment, 10 consecutive slices were selected and analyzed by two blinded observers. The slices covered the upper spinal cord, brain stem and cerebellum. This area was chosen because CNS lesions are likely to develop here and signal changes can be readily identified. For the two time points, 24h and 72h after cell injection, the images were compared to the pre-injection images and each slice was analyzed for the presence of regions with low signal intensity. The percentage of slices with abnormal hypointensities was calculated.

Statistical analysis

Data are expressed as mean ± standard error of the mean (SEM). Statistical analysis was performed using the statistical software package Sigmastat (version 3.11, 2004). Data were evaluated by two-way repeated measures analysis of variance, followed by the Student-Newman-Keuls post hoc test. $P < .05$ was considered statistically significant.

RESULTS

Labeling efficiency after magneto-electroporation is dependent on the type of iron oxide particle

Monocyte function was assessed after electroporation with three different iron oxide particles. Cell viability was not changed by the electroporation procedure compared with freshly isolated monocytes (Fig 1A). Metabolic

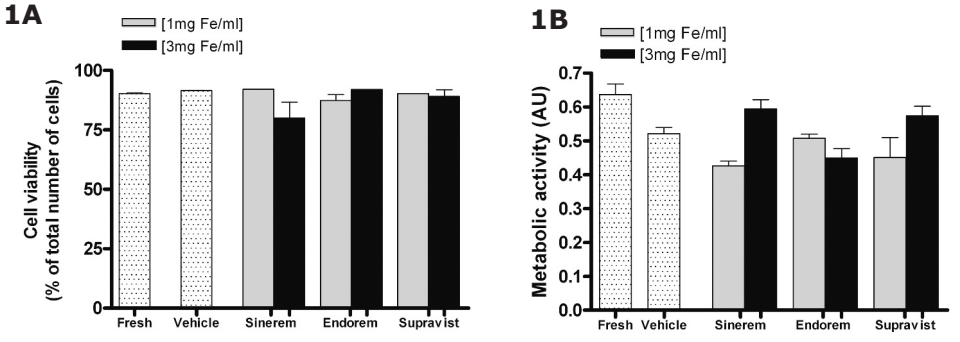

Figure 1: (A) Cell viability measured by trypan blue exclusion after MEP in absence (vehicle) or presence of iron oxide particles. Cell viability has not changed compared with non-electroporated monocytes (fresh). **(B)** Monocyte metabolic activity decreased after MEP in absence (vehicle) and in the presence of iron oxide particles compared with non-electroprated monocytes (fresh).

activity was slightly decreased, independent of the presence or absence of iron oxide particles (Fig 1B). To quantitatively assess particle incorporation by monocytes, the iron content in the cell samples was determined. No increase in intracellular iron content was detected after electroporation with Sinerem (4pg Fe/cell) compared with monocytes electroporated without contrast agents (Fig 2A). Electroporation with Endorem and Supravist resulted in elevated iron levels. Increasing the Endorem concentration did not improve labeling efficiency, whereas an increase in Supravist concentration to 3mg Fe/ml resulted in an intracellular iron content of 25pg per monocyte.

Prussian blue staining of cytospin samples (Fig 2B) confirmed these findings. No iron-positive cells were detected for electroporated monocytes with Sinerem, whereas following MEP with Supravist (1mg Fe/ml), we observed labeled monocytes containing multiple iron-positive clusters (blue color) distributed throughout the cytoplasm. After electroporation with 3mg Fe/ml Supravist, an increase in iron oxide particle accumulation was observed.

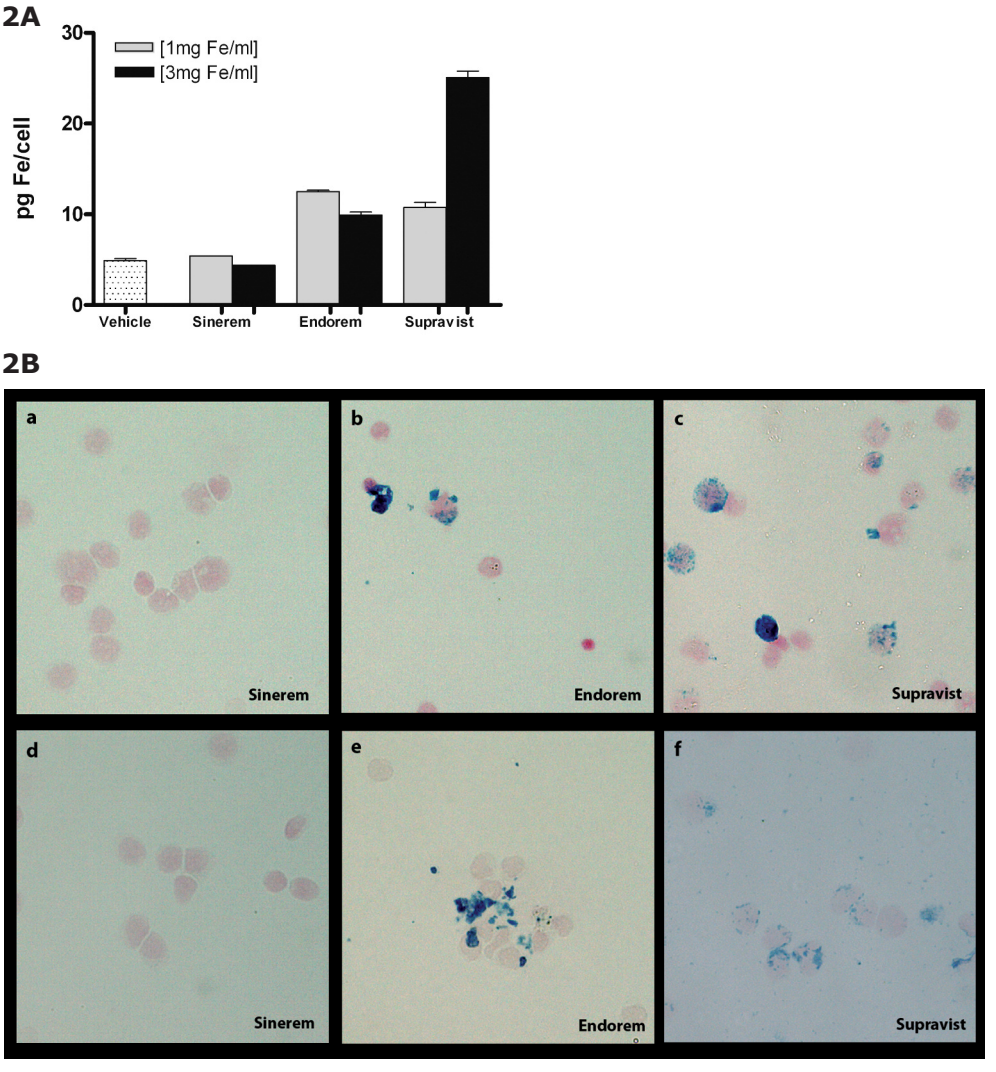

Figure 2: (A) Iron incorporation as quantified by a ferrozin assay. No increase in intracellular iron was detected following electroporation with Sinerem. MEP with Supravist at a concentration of 3mg Fe/ml resulted in an intracellular iron concentration of 25pg per cell. **(B)** Prussian blue staining of cytospin samples showed the presence of intracellular iron (blue) exclusively for monocytes labeled with Endorem and Supravist. Panels a, b and c show monocytes labeled at 1mg Fe/ml and panels d, e and f show labeling at 3mg Fe/ml.

Monocytes labeled by magneto-electroporation decrease T_2-relaxation time in vitro

Based upon labeling and viability assessments, Supravist at 2mg Fe/ml was selected to efficiently label rat monocytes by MEP for future studies. To determine the change in T_2-relaxation time, agar phantoms containing monocytes labeled with Supravist were imaged. Loss of signal is observed

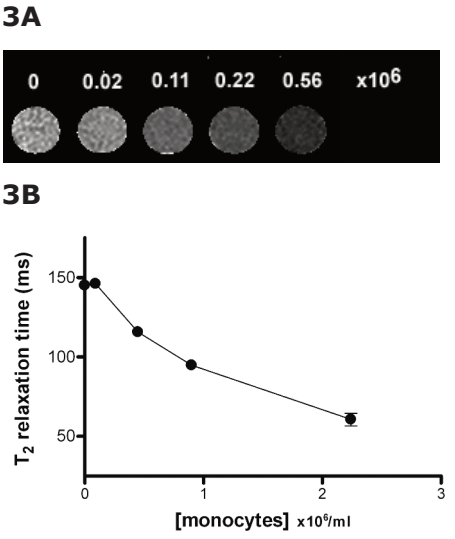

Figure 3: (A) Typical example of a T_2-relaxation time image of agar phantoms containing increasing numbers of monocytes labeled by MEP with Supravist (2mg Fe/ml). A strong decrease in signal intensity is observed for increasing concentrations of labeled monocytes **(B)** Corresponding T_2-relaxation times of labeled monocytes. At a concentration of $2x10^6$/ml, monocytes labeled by MEP cause a nearly 60% reduction in signal intensity.

with increasing cell concentrations. Quantification of T_2-relaxation times for the different monocyte concentration shows a 60% decrease in signal for $2x10^6$ labeled monocytes per ml (Fig 3).

Injection of labeled monocytes in EAE rats results in focal hypointensities in the CNS

Rat monocytes were electroporated with Supravist (2mg Fe/ml) and immediately injected ($1.0\text{-}1.2x10^7$ labeled monocytes per animal) at day 10 when EAE rats started to lose tail tonus (disease onset, mean clinical score 0.1±0.19) and day 13 when all animals are clinically ill (peak of the disease, mean clinical score 2.7±1.23) (Fig 4A).

Imaging was performed just prior to monocyte injection (pre), and after monocyte injection (24h and 72h). Small areas of decreased signal intensity were detected in the cervical cord, brainstem and cerebellum (Fig 4B) indicating infiltration of labeled monocytes.

To quantify hypointensities in the CNS of EAE rats following monocyte injection, the percentage of slices that contained changes in signal intensity compared with the pre-injection images was determined (Fig 4C). Injection of labeled monocytes at disease onset resulted in hypointense regions in approximately 30% of the slices (31±2.4% in 24h scan and 29±5.5% in 72h scan). Monocyte injection at disease peak resulted in low signal intensities in 51±2.4% of the slices in the 24h scan which was significantly higher compared with disease onset ($P < .05$). The percentage of slices containing hypointensities had declined at 72h (44±6.6%, $P > .05$ versus disease onset).

4A

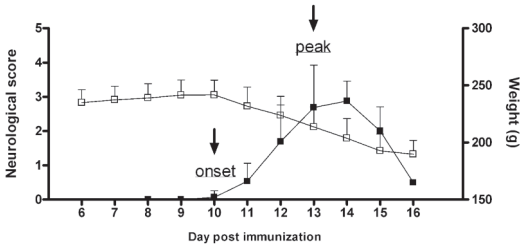

4B

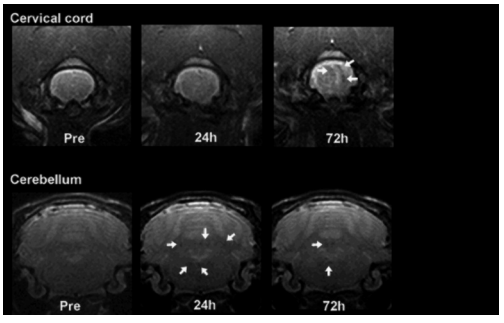

4C

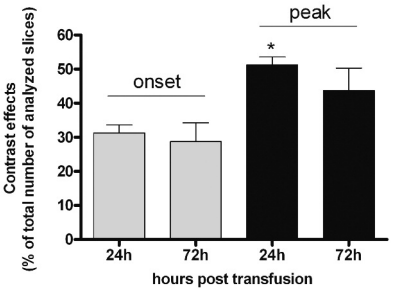

Figure 4: (A) Time course of (■) neurological scores and (□) body weight of acute experimental autoimmune encephalomyelitis in rats. Animals were immunized with MBP emulsified in CFA at day 0 (n=10). Neurological symptoms were scored daily. The black arrows indicate the injection of MEP-labeled monocytes at day 10 and day 13 after immunization. **(B)** Typical example of T_2*W images of EAE rats injected at disease onset. Hypointensities (arrows) after injection of labeled monocytes are detected in the 24h scan and the 72h scan, predominantly in cerebellum and cervical cord. **(C)** To quantify the loss of signal intensity, the percentage of slices that contained abnormal hypointensities is plotted for each time point. Injection of labeled monocytes resulted in an increase of slices with abnormal hypointensities for all time points. At disease peak this increase was significantly higher 24h after injection compared with disease onset ($P < .05$ versus 24h-onset and 72h-onset).

High resolution MRI reveals focal hypointensities predominantly in white matter

Ex vivo imaging of brains at high field strength (9.4T) resulted in a three dimensional data-set in which detailed anatomical structures could be visualized (Fig 5). In EAE rats without monocyte injections (control), no abnormalities were detected in the CNS (Fig 5A). In contrast, focal areas of signal decrease were detected in the white matter area of EAE rats that were injected with labeled monocytes. In two out of eight EAE animals, a relatively large hypointensity was detected in the lumbar part of the spinal cord (Fig 5B) pointing to the diffuse pattern of monocyte infiltration in the CNS of EAE rats.

5A

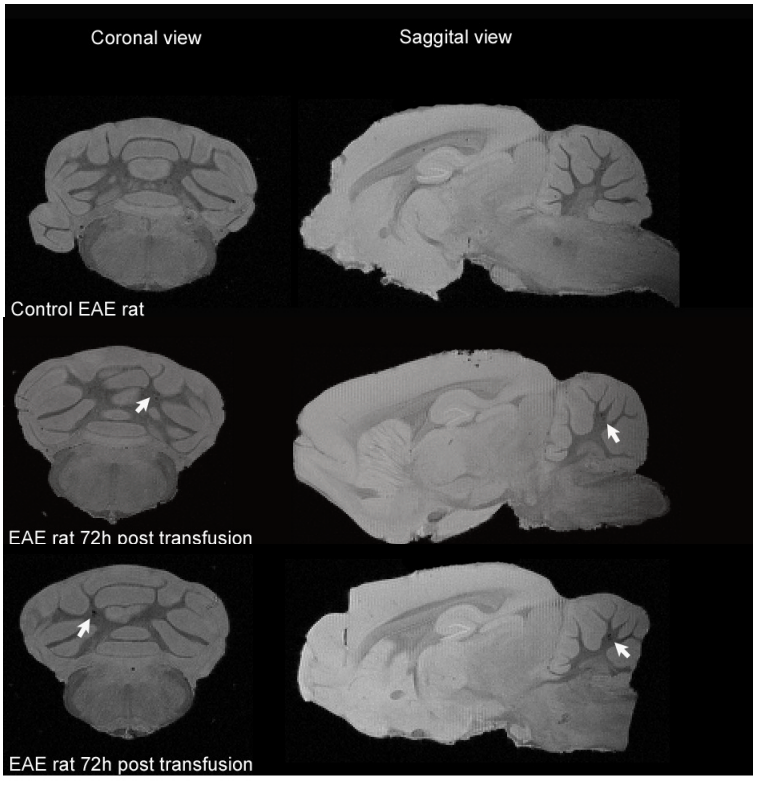

5B

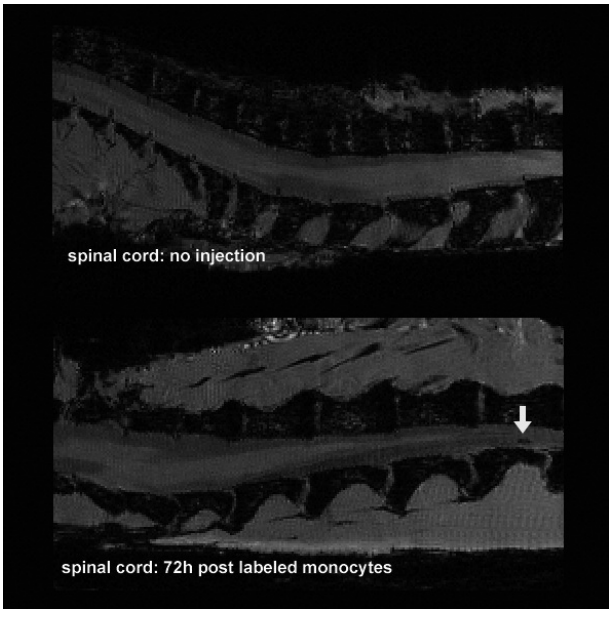

Figure 5: (A) Ex vivo high resolution T_2*W images of EAE brains showing infiltrated labeled monocytes. No hypointense areas are detected in control EAE brains (upper panel). In animals that were administered labeled monocytes, focal areas of signal loss were detected in the white matter (arrows in middle and lower panel). **(B)** Ex vivo T_2*W images of EAE spinal cord in sagittal orientation. In two out of eight rats that received labeled monocytes, hypointense regions were detected (arrow, lower panel) in the lumbar cord.

Iron-positive cells are detected in ED1+ infiltrates

To validate the source of the hypointense areas, corresponding sections of the cerebellum (72h after injection of labeled monocytes) were stained for infiltrating monocytes (ED1) and the presence of iron (PB). Typically, in the area of focal hypointensities on ex vivo MR images (Fig 6A), a number of ED1+ (brown) cell infiltrates were found (Fig 6B).

Magnification of these infiltrates in the brainstem revealed the presence of iron-positive cells indicating the infiltration of labeled monocytes. Some iron-positive cells were found attached to the luminal side of a vessel possibly penetrating the BBB (Fig 6C). Others were detected in the parenchyma in close proximity to a vessel (Fig 6D).

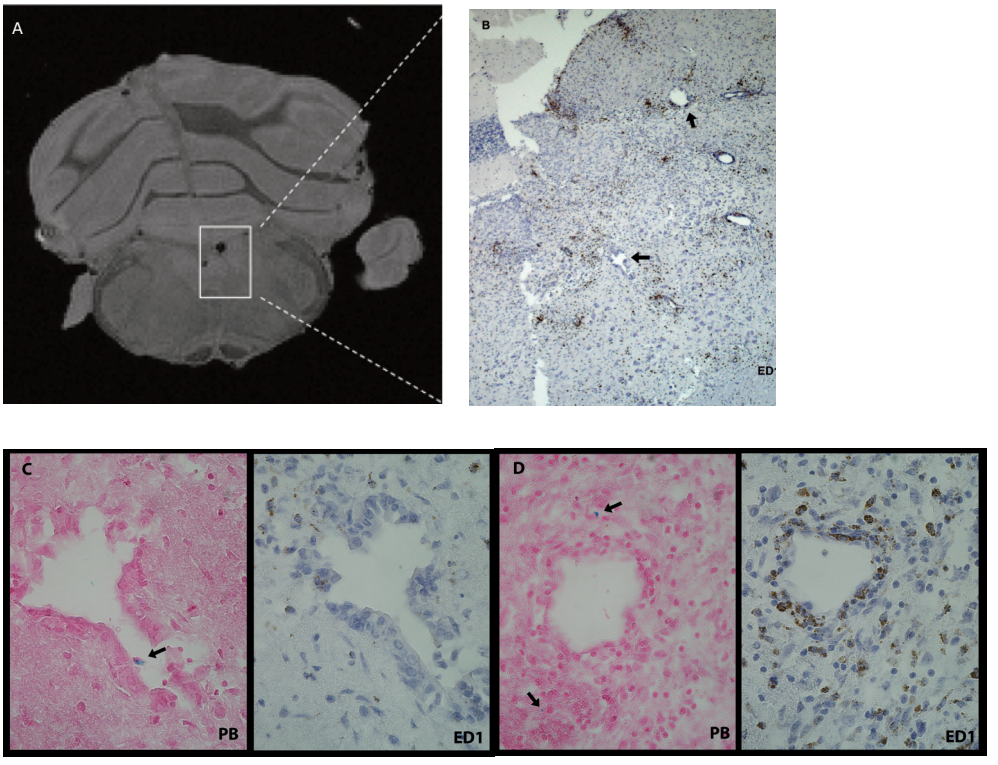

Figure 6: Histological analysis for the presence of iron (Prussian blue) and the presence of infiltrated monocytes (ED1+ cells) in the brain of EAE rats 72h after injection of labeled monocytes. **(A)** Ex vivo T_2*W image of the cerebellum containing focal hypointensities (box). **(B)** In the corresponding area several ED1+ infiltrates are detected (arrows). (C-D) ED1+ infiltrates are magnified (left image) and the sequential section stained for the presence of iron oxide particles (right image). Iron-positive monocytes (arrows) are attached to **(C)** or in close proximity to the vessel wall **(D)**.

DISCUSSION

In this study, we have demonstrated efficient labeling of rat monocytes with iron oxide particles using MEP and report on successful implementation for in vivo monocyte tracking in rats with EAE.

Cellular MRI requires high amounts of contrast agent per cell without affecting cell function. We showed that electroporation of cells meets both of these requirements. More over, we found that labeling efficiency using MEP depended on the choice of iron oxide particle. Iron staining and quantification revealed that the larger-sized Endorem was preferred over smaller-sized Sinerem indicating the importance of the size of the particle. However, best results were obtained with Supravist that emphasizes the advantage of an ionic surface charge. Previous studies using other procedures similarly showed that cell labeling efficiency is depends on size (Raynal et al. 2004; Matuszewski et al. 2005; Oude Engberink et al. 2007) and charge of the iron oxide particle (Metz et al. 2004). In contrast to cell labeling by straight forward incubation, MEP is a voltage based method causing a temporarily loss of cell membrane integrity which drives the uptake of contrast agents present in the medium (Walczak et al. 2006). Here, we provide MR evidence for the labeling efficiency using MEP and report on T_2-relaxation times determined for rat monocytes labeled with Supravist. Importantly, we obtained better results using MEP than previously achieved for rat monocytes using an optimized incubation protocol (Oude Engberink et al. 2007). An improved labeling strategy will benefit the detection of small amounts of labeled monocytes in vivo.

To test the improved detection level of monocytes, we injected monocytes labeled with Supravist in EAE rats at onset and peak of the disease. Upon monocyte injection we showed that abnormal hypointensities could be detected in vivo, which were predominantly located in the cervical cord and cerebellum. Previous studies have also reported on hypointense regions in these areas after intravenous injections of free ultra small SPIO (USPIO) (Dousset et al. 1999; Floris et al. 2004) and it was suggested that USPIO-related signal changes reflect the presence of monocyte infiltrates. However, we previously showed that monocyte labeling efficiency by incubation with Sinerem in vitro was low (Oude Engberink et al. 2007) and in a recent study it was shown that Sinerem was not incorporated in leukocytes in the circulation (Wu et al. 2007) of rats. Clearly, multiple pathways exist for the uptake of USPIO in vivo, like BBB leakage and trancytosis by endothelial cells (Xu et al. 1998). To monitor and intervene in an inflammatory response it is crucial to discriminate between leakage and monocyte infiltration. Therefore, tracking of ex vivo labeled monocytes is the pre-

ferred tool. Here, we report that ex vivo labeling of monocytes by MEP significantly improved their visualization by MRI and allowed to monitor the migration process at multiple inflammatory sites. More over, our approach was able to discriminate between disease onset and peak in this model and showed that monocyte migration into the CNS was increased at disease peak.

To facilitate the detection of small infiltrates containing a few labeled monocytes, we also obtained high resolution images ex vivo at a high magnetic field strength. Here, we show that rat EAE brains scanned at 9.4T (isotropic resolution of 98µm) clearly outlined the areas of signal loss predominantly located in white matter myelin, the primary target of infiltrated monocytes in MS (Bruck et al. 1996).
Recently, SPIO-labeled T-cells, that were adoptively transferred to induce EAE in a mouse model, were detected by MRI in the lumbar cord at disease onset (Anderson et al. 2004). It is suggested that T-cell entry precedes the infiltration of monocytes. Interestingly in our study we detected in a few rats hypointense areas in similar areas of the spinal cord, reflecting the infiltration of labeled monocytes. These results suggest that the lumbar cord is a vulnerable area in EAE and sensitive to cellular infiltration. The use of high field MRI provides excellent tissue characterization and thereby a better localization of small clusters of iron oxide-loaded cells in CNS pathologies.
Histological analysis demonstrated the presence of iron-positive cells in the vicinity of small ED1+ infiltrates corresponding to the areas of low signal intensity on the ex vivo T_2*W images. So far, this has only been described in animal models with large brain lesions (Strohr et al. 2006; Oude Engberink et al. 2007) using incubation procedures to label monocytes. Our histological data underlines the strength of MEP to label monocytes efficiently which highly improves their visualization with MRI.

In conclusion, our study demonstrates that MEP is a potent labeling strategy and provides the opportunity to specifically visualize the migration process of monocytes in vivo. A key feature of MEP is the high iron load per cell which brings single cell visualization within reach. Therefore, MEP contributes to a better understanding of their infiltration kinetics and indirectly to an accurate design and evaluation of therapies aimed to limit monocyte entry into the CNS. Since MEP is an easily implemented labeling strategy, successful with clinical grade contrast agents and ultra-fast, bench to bedside translation may be of interest in the near future.

ACKNOWLEDGEMENTS

The authors thank Guerbet, France for kindly providing the contrast agent Sinerem and Endorem. The contrast agent Supravist was kindly provided by Bayer Schering Pharma, Germany. This work has been supported by the Dutch MS Research Foundation (MS 01-470, MS 02-489 and W06-02), the Netherlands Organization for Scientific Research (NWO) and by the Du Pré Grant of Multiple Sclerosis International Federation (MSIF).

REFERENCES

Al-Omaishi J, Bashir R, Gendelman HE. The cellular immunology of multiple sclerosis. J Leukoc Biol 1999; 65: 444-52.

Anderson SA, Shukaliak-Quandt J, Jordan EK, Arbab AS, Martin R, McFarland H, et al. Magnetic resonance imaging of labeled T-cells in a mouse model of multiple sclerosis. Ann Neurol 2004; 55: 654-9.

Bruck W, Sommermeier N, Bergmann M, Zettl U, Goebel HH, Kretzschmar HA, et al. Macrophages in multiple sclerosis. Immunobiology 1996; 195: 588-600.

Bulte JW, Douglas T, Witwer B, Zhang SC, Strable E, Lewis BK, et al. Magnetodendrimers allow endosomal magnetic labeling and in vivo tracking of stem cells. Nat Biotechnol 2001; 19: 1141-7.

Bulte JW, Kraitchman DL. Iron oxide MR contrast agents for molecular and cellular imaging. NMR Biomed 2004; 17: 484-99.

Corot C, Petry KG, Trivedi R, Saleh A, Jonkmanns C, Le Bas JF, et al. Macrophage imaging in central nervous system and in carotid atherosclerotic plaque using ultrasmall superparamagnetic iron oxide in magnetic resonance imaging. Invest Radiol 2004; 39: 619-25.

de Vries HE, Kuiper J, de Boer AG, Van Berkel TJ, Breimer DD. The blood-brain barrier in neuroinflammatory diseases. Pharmacol Rev 1997; 49: 143-55.

Dousset V, Delalande C, Ballarino L, Quesson B, Seilhan D, Coussemacq M, et al. In vivo macrophage activity imaging in the central nervous system detected by magnetic resonance. Magn Reson Med 1999; 41: 329-33.

Drayer BP. Imaging of the aging brain. Part II. Pathologic conditions. Radiology 1988; 166: 797-806.

Engberink RD, Blezer EL, Hoff EI, van der Pol SM, van der Toorn A, Dijkhuizen RM, et al. MRI of monocyte infiltration in an animal model of neuroinflammation using SPIO-labeled monocytes or free USPIO. J Cereb Blood Flow Metab 2007.

Floris S, Blezer EL, Schreibelt G, Dopp E, van der Pol SM, Schadee-Eestermans IL, et al. Blood-brain barrier permeability and monocyte infiltration in experimental allergic encephalomyelitis: a quantitative MRI study. Brain 2004; 127: 616-27.

Floris S, Ruuls SR, Wierinckx A, van der Pol SM, Dopp E, van der Meide PH, et al. Interferon-beta directly influences monocyte infiltration into the central nervous system. J Neuroimmunol 2002; 127: 69-79.

Gebarski SS, Gabrielsen TO, Gilman S, Knake JE, Latack JT, Aisen AM. The initial diagnosis of multiple sclerosis: clinical impact of magnetic resonance imaging. Ann Neurol 1985; 17: 469-74.

Kertesz A, Black SE, Nicholson L, Carr T. The sensitivity and specificity of MRI in stroke. Neurology 1987; 37: 1580-5.

Matuszewski L, Persigehl T, Wall A, Schwindt W, Tombach B, Fobker M, et al. Cell tagging with clinically approved iron oxides: feasibility and effect of lipofection, particle size, and surface coating on labeling efficiency. Radiology 2005; 235: 155-61.

Metz S, Bonaterra G, Rudelius M, Settles M, Rummeny EJ, Daldrup-Link HE. Capacity of human monocytes to phagocytose approved iron oxide MR contrast agents in vitro. Eur Radiol 2004; 14: 1851-8.

Oude Engberink RD, van der Pol SM, Dopp EA, de Vries HE, Blezer EL. Comparison of SPIO and USPIO for in vitro labeling of human monocytes: MR detection and cell function. Radiology 2007; 243: 467-74.

Raynal I, Prigent P, Peyramaure S, Najid A, Rebuzzi C, Corot C. Macrophage endocytosis of superparamagnetic iron oxide nanoparticles: mechanisms and comparison of ferumoxides and ferumoxtran-10. Invest Radiol 2004; 39: 56-63.

Schreibelt G, Musters RJ, Reijerkerk A, de Groot LR, van der Pol SM, Hendrikx EM, et al. Lipoic acid affects cellular migration into the central nervous system and stabilizes blood-brain barrier integrity. J Immunol 2006; 177: 2630-7.

Stroh A, Zimmer C, Werner N, Gertz K, Weir K, Kronenberg G, et al. Tracking of systemically administered mononuclear cells in the ischemic brain by high-field magnetic resonance imaging. Neuroimage 2006.

Walczak P, Kedziorek DA, Gilad AA, Lin S, Bulte JW. Instant MR labeling of stem cells using magnetoelectroporation. Magn Reson Med 2005; 54: 769-74.

Walczak P, Ruiz-Cabello J, Kedziorek DA, Gilad AA, Lin S, Barnett B, et al. Magnetoelectroporation: improved labeling of neural stem cells and leukocytes for cellular magnetic resonance imaging using a single FDA-approved agent. Nanomedicine 2006; 2: 89-94.

Wu YJ, Muldoon LL, Varallyay C, Markwardt S, Jones RE, Neuwelt EA. In vivo leukocyte labeling with intravenous ferumoxides/protamine sulfate complex and in vitro characterization for cellular magnetic resonance imaging. Am J Physiol Cell Physiol 2007; 293: C1698-708.

Xu S, Jordan EK, Brocke S, Bulte JW, Quigley L, Tresser N, et al. Study of relapsing remitting experimental allergic encephalomyelitis SJL mouse model using MION-46L enhanced in vivo MRI: early histopathological correlation. J Neurosci Res 1998; 52: 549-58.

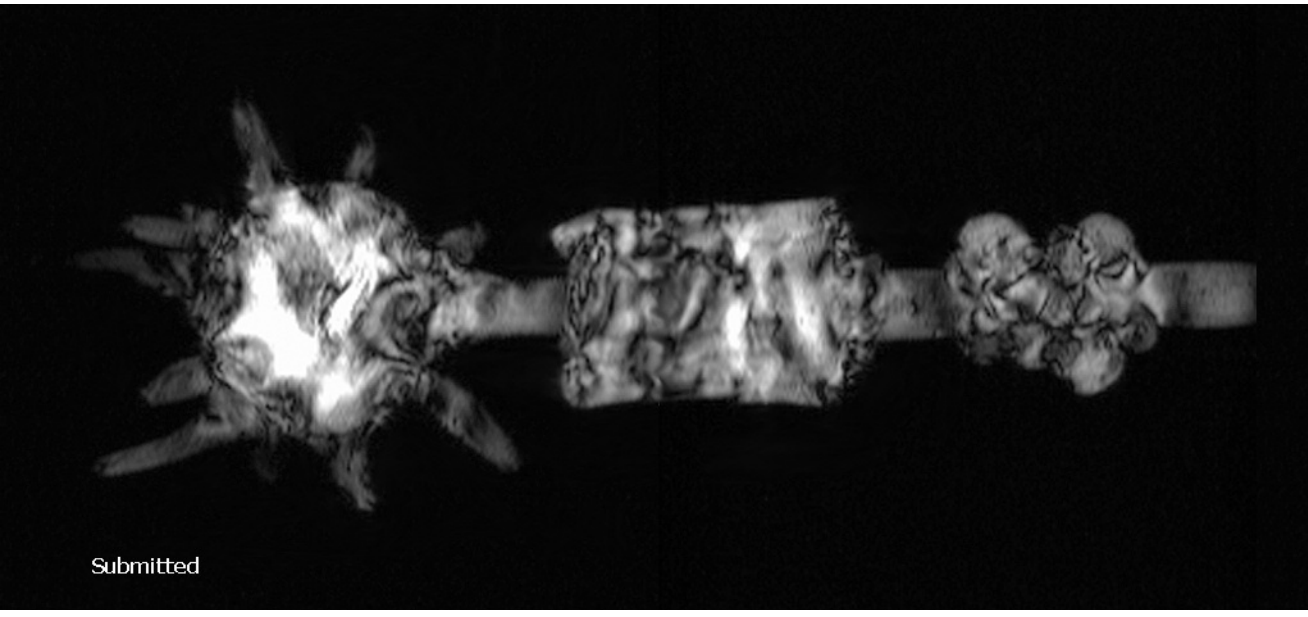

Submitted

Dynamics and Fate of USPIO in the Central Nervous System in Experimental Autoimmune Encephalomyelitis

R.D. Oude Engberink[1], E.L.A. Blezer[1], C.D. Dijkstra[2], S.M.A. van der Pol[2], A. van der Toorn[1], H.E. de Vries[2]

[1]Image Sciences Institute, University Medical Center Utrecht
[2]Molecular Cell Biology and Immunology, VU Medical Center Amsterdam

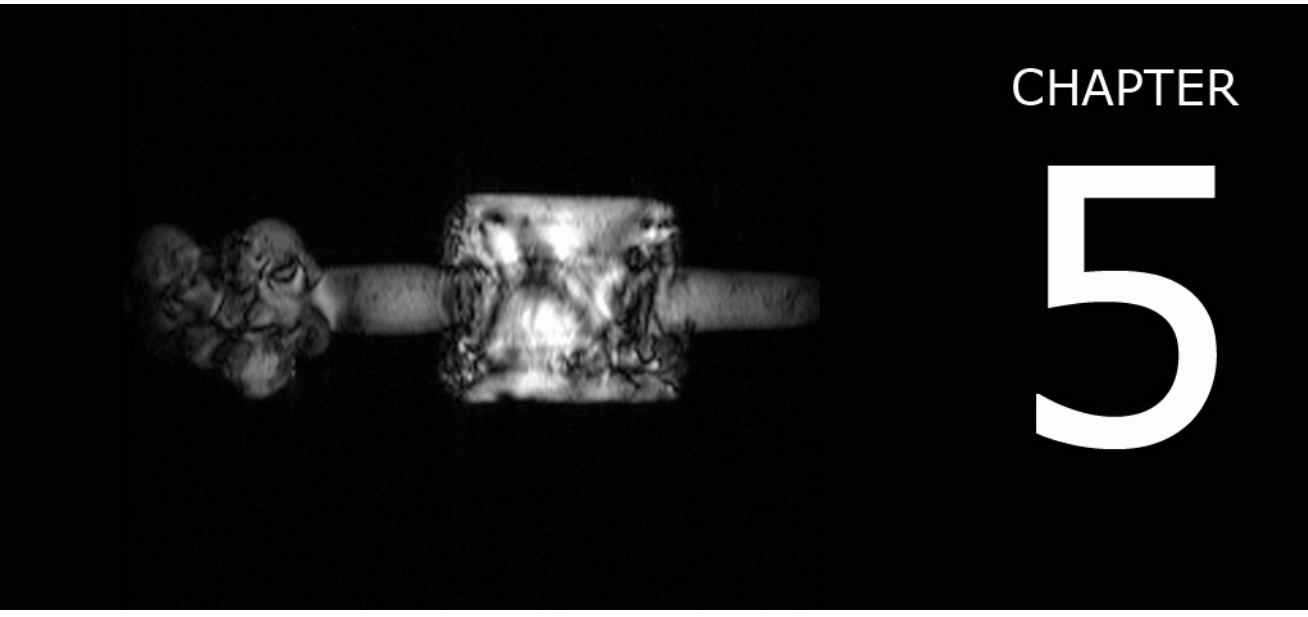

ABSTRACT

Contrast effects observed after magnetic resonance imaging (MRI) of the central nervous system (CNS) following intravenous administration of ultra small superparamagnetic particles of iron oxide (USPIO) have been correlated with immune cell activity in lesions. To date, the mechanism of USPIO uptake in vivo is unknown. USPIO may enter the CNS after incorporation by immune cells which traffic to inflammatory sites or USPIO may leak over an impaired blood-brain barrier (BBB).
The purpose of this study was to monitor USPIO enhancement longitudinally and determine their fate after injection in experimental autoimmune encephalomyelitis (EAE), an animal model of multiple sclerosis. Insight in USPIO dynamics will contribute to correct interpretation of post-USPIO MR images and possibly lead to new applications of this contrast agent.

Acute EAE was induced in Lewis Hannover rats and USPIO (Sinerem®, 300µmol Fe/kg) were intravenously injected at onset of the disease (day 10 after immunization) and at the peak of the disease (day 13 after immunization). To monitor USPIO presence in brain, spinal cord and cervical lymph nodes (CLN), repetitive MRI was performed before and directly after USPIO injection every 30 minutes up to 6h. A group of animals was scanned 24h and 72h later. Tissue sections were processed for histology to detect the presence of USPIO, infiltrated monocytes and damage to the BBB.

USPIO were detected in the CNS within 1h after injection and corresponding histological analysis revealed extracellular iron clusters around the lesions distinct from ED1+ cell infiltrates. MRI performed 24h later revealed more contrast effects in the CNS after injections at disease peak. USPIO-related changes in signal intensity were no longer apparent 72h post injection, independent of disease course. MR images of CLN showed USPIO accumulation up to 72h at disease onset of EAE. In contrast, injection at disease peak resulted in signal loss in CLN that was maximal after 24h. CLN histology demonstrated USPIO accumulation predominantly in the medulla and subcapsular sinus macrophages.

The current study demonstrates that USPIO enter the CNS directly after administration that predominantly contributes to the signal loss observed after 24h. Moreover, longitudinal MRI analysis suggested that a possible mechanism for particle efflux from the inflammatory CNS is via drainage by CLN. These data shed a new light on the use of USPIO in neuroinflammatory diseases, identifying USPIO as a marker for both cellular infiltration and BBB damage.

INTRODUCTION

Multiple Sclerosis (MS) is a chronic inflammatory disease of the central nervous system (CNS) and is characterized by increased permeability of the blood-brain barrier (BBB) and cellular infiltrates in brain and spinal cord (Al-Omaishi et al., 1999; de Vries et al., 1997; Ewing and Bernard, 1998). Infiltrated monocytes are thought to play a key role in ongoing inflammation, demyelination and axonal damage (Bruck et al., 1996; Hendriks et al., 2005). However, the time window of monocyte infiltration during disease development is largely unknown. Increased knowledge by non-invasive imaging studies may lead to improvement of therapies specifically aimed at the inhibition of cellular infiltration.

Contrast-enhanced magnetic resonance imaging (MRI) using ultra small superparamagnetic particles of iron oxide (USPIO) has been described to visualize areas of neuroinflammation at the cellular level (Kaim et al., 2002; Saleh et al., 2004b). The presence of iron oxide particles results in local magnetic field disturbances causing loss of MR signal and hence, clusters of cells that have taken up these particles will appear hypointense on T_2-weighted MR images (Schoepf et al., 1998; Weissleder et al., 1997). Monocyte imaging with USPIO has recently been performed in rats and mice with experimental autoimmune encephalomyelitis (EAE), the animal model for MS. Studies have demonstrated that cellular infiltrates can be visualized by MRI 24h after intravenous injection of USPIO (Dousset et al., 1999; Floris et al., 2004). An early event in the EAE model preceding clinical symptoms is an increased permeability of the BBB, as can be visualized by Gd-DTPA-enhanced MRI (Floris et al., 2004; Hawkins et al., 1990; Karlik et al., 1993; Namer et al., 1992). Since the BBB is compromised during inflammation, intravenously injected USPIO may have various ways of entering the CNS. USPIO may either be taken up by circulating monocytes, captured by endothelial cells (Xu et al., 1998) of the BBB or diffuse through the disrupted BBB followed by uptake and accumulation in infiltrated macrophages and activated microglia in the brain. As a result of these diverse mechanisms of USPIO entrance into the brain parenchyma, it is therefore unclear what pathological events are visualized by USPIO. In previous studies in EAE animals (Dousset et al., 1999; Floris et al., 2004), MRI is commonly performed 18 - 24h after USPIO injection, but data on USPIO enhancement directly upon administration are lacking. We hypothesized that USPIO can enter the CNS rapidly through an impaired BBB and that this early USPIO accumulation contributes to MR abnormalities detected at later stages.

Also, little is known on the fate of USPIO in the CNS of EAE rats at later time frames than 24h post injection. USPIO persistence in or drainage from the brain may provide additional information on disease progression. Previously, it was shown in healthy rats that iron oxide particles injected into the brain parenchyma are transported to the cervical lymph nodes (CLN) (Muldoon et al., 2004). In EAE it is suggested that the CLN play a pivotal role as a site for antigen drainage and the priming of T-cells (Phillips et al., 1997). We hypothesized that one of the mechanisms by which USPIO leave the EAE brain is through drainage to the CLN, as observed for myelin antigens (de Vos et al., 2002), which can be visualized by MRI.

In this report, we perform repetitive MRI and describe USPIO dynamics in the CNS of EAE rats after a single injection of USPIO both at disease onset and disease peak. More over, USPIO accumulation in the CLN is monitored with time and may provide a novel tool to non-invasively study drainage of antigens in the inflammatory brain.

MATERIALS AND METHODS

Induction of acute EAE

All animal procedures were approved by the local ethical committee and were performed in accordance with international guidelines on handling laboratory animals. Acute EAE was induced in male Lewis Hannover rats (n=11, 210 – 240g, Harlan, The Netherlands) according to Schreibelt (Schreibelt et al., 2006). Animals were kept under standard laboratory conditions with water and food ad libitum. At day 0, rats were injected subcutaneously in one hind footpad with 20µg of guinea pig myelin basic protein in phosphate-buffered saline (PBS) mixed with complete Freund's adjuvant (CFA; Difco Laboratories, Detroit, USA). For EAE induction, animals were anaesthetized with 2% isoflurane in a N_2O/O_2 mixture (70/30) and allowed to breathe spontaneously. Clinical symptoms were scored daily and graded from 1 to 5: 0, no clinical signs; 0.5, partial loss of tail tonus; 1, complete loss of tail tonus; 2, unsteady gait; 2.5, partial hind limb paralysis; 3, complete hind limb paralysis; 4, paralysis of the complete lower part of the body up to the diaphragm; 5, death due to EAE. At day 10 after immunization, clinical symptoms start to develop and this day is marked as disease onset. At day 13, clinical scores are maximal and this day is marked as peak of the disease.

Injection of contrast agent

USPIO (Sinerem®, Guerbet, France) was used as contrast agent and consists of dextran-coated particles with a crystalline core of iron oxide with a mean hydrodynamic diameter of 20-30nm (Benderbous et al., 1996; Jung, 1995). The contrast agent is provided as lyophilized powder and right before use reconstituted with sterile 0.9% saline to yield a final concentration of 200µmol Fe/ml. At disease onset (day 10, n=4) and disease peak (day 13, n=3), animals were anaesthetized as described above. A tail vein was cannulated and the contrast agent was intravenously injected at a dose of 300µmol Fe/kg rat. Animals were allowed to recover thereafter and MRI was performed 24h and 72h later. After the 72h-scan, animals were sacrificed for histological validation. In a group of animals (day10 and 13, n=2), injection of contrast agent was performed inside the scanner after a pre-injection scan, and subsequently repetitive MRI was performed up to 6h. Animals were sacrificed thereafter. Control rats (n=4) received similar USPIO injections.

Magnetic Resonance Imaging

All experiments were performed using a 4.7T horizontal bore NMR spectrometer (Varian, Palo Alto, California, USA), equipped with a high-performance gradient insert (12cm inner diameter, maximum gradient

strength 500mT/m). Animals were initially anaesthetized as described above and prepared for mechanical ventilation by endotracheal intubation. A tail vein was cannulated for injection of gadopentetate dimeglubine (Gd-DTPA; Magnevist®, Schering, Berlin, Germany). In the scanner, animals were immobilized in a specially designed stereotactic holder and placed in an animal cradle. Animals were mechanically ventilated with isoflurane (2%) in a mixture of N_2O/O_2 (70/30). Expiratory CO_2 was continuously monitored and body temperature was maintained at 37 ºC using a heated water pad. An infrared sensor (Nonin Medical Inc., Plymouth, Minnesota, USA) was attached to the hind paw for monitoring heart rate and blood oxygen saturation. A homebuilt Helmholtz volume coil (Ø 85mm) and an inductively coupled surface coil (Ø 35mm) were used for radio frequency transmission and signal detection, respectively.
Slice positions were determined on a transversal scout image and the central slice was positioned directly caudal of the cerebellum. The slices covered the upper part of the spinal cord, the cerebellum and caudal part of the cerebrum. We performed T_2 measurements (21x 1mm slices, repetition time (TR) =3200ms, 9 echoes with echo time (TE)-spacing=17.5ms, field of view (FOV) =3.2 x 3.2cm; matrix=128 x 128, number of experiments (NEX) =4). T_2-maps were calculated from mono-exponential fitting of MRI signal intensities as a function of TE. At the end of each MR session, T_1-weighted (T_1W) spin-echo images (TR=300ms; TE=11.5ms, NEX=4) were collected before and 10min after 0.5mmol/kg Gd-DTPA injection. Post- and pre-Gd-DTPA T_1W images were subtracted for detection of Gd-DTPA enhancement. In the repetitive MRI experiment, T_2W-MRI was repeated for 12 cycles of 30min directly after intravenous USPIO administration.

Immunohistochemistry
Brains and cervical lymph nodes were rapidly removed, snap-frozen in the vapor phase of liquid nitrogen and stored at -80ºC. Serial 10µm coronal cryosections (-20ºC) were cut and fixed in acetone for 10min. Sections were pre-incubated in PBS with 10% Fetal Calf Serum (Biowhittaker Europe, Verviers, Belgium). To detect infiltrated monocytes or phagocytic microglia, monoclonal antibody ED1 (1.5µg/ml; Serotec, Oxfordshire, UK) was used for 1h at room temperature. To assess damage to the BBB, sequential sections were stained with rabbit-a-rat IgG (DAKO, 1:300). As secondary antibody, biotinylated rabbit -α- mouse immunoglobulin F(ab)2 fragments (DAKO, 1:300) were used and biotinylated swine anti-rabbit immunoglobulins F(ab)2 fragments (DAKO, 1:800), respectively. Finally, sections were incubated at room temperature with avidin-biotin-peroxidase complexes (StrepABComplex HRP, DAKO, 1:200). Peroxidase activity was demonstrated by 10min incubation with 0.5mg/ml 3.3'-di-

aminobenzidine-tetra-hydrochloride in Tris-HCl buffer containing 0.03% H_2O_2
To detect the presence of USPIO, sequential sections were stained by Prussian blue and counterstained with nuclear fast red (NFR) as previously described (Oude Engberink et al., 2007). Briefly, tissue sections were fixed in acetone and incubated with a 1:1 mixture of 2% potassium hexacyanoferrat (II) and 2N HCL for 30 min. Glass slides were rinsed in distilled water and counterstained with NFR for 5min.

Blood samples were collected via the tail vein 6h, 24h and 72h after USPIO injection and analyzed for the presence of USPIO in circulation. Blood samples were re-suspended in 1ml PBS, centrifuged (1500 rpm, 5min) and 1ml of distilled water was added to the pellet for 15s to discard the erythrocytes. Cell samples were reconstituted with 1ml 1.8% saline to restore the physiological status and cytospots of the white blood cells were prepared and processed for histochemical staining as described above. Cytospots of the blood samples were only stained for the presence of USPIO.

MRI data analysis
T_2W images (17.5ms, 1st echo of the multi-echo sequence) of rat brains were qualitatively analyzed for the presence of low signal intensities following USPIO injection and compared with the pre-injection image. For quantitative analysis of the area of low signal intensity in the cervical lymph nodes the Medical Image Processing, Analysis and Visualization (MIPAV, version 2.7.101, 2006) program was used. Regions of interest (ROI) with abnormally decreased signal intensities were automatically outlined in 8 consecutive slices using the level-set method of MIPAV. The slices covered the cerebellum and the upper part of the spinal cord. The ROI enclosed the position of the CLN around the bifurcation of the carotid arteries. The volumes of the ROI were calculated.

Statistics
Data are expressed as mean ± standard error of the mean (SEM where appropriate). Statistical analyses were performed using the statistical software package Sigmastat (version 3.11, 2004). Data were evaluated by two-way repeated measures analysis of variance, followed by the Student-Newman-Keuls post hoc test. $P < .05$ was considered statistically significant.

RESULTS

Clinical course of acute EAE

Acute EAE in rats is characterized by a monophasic disease course (Fig 1). Loss of weight is accompanied by the first clinical signs at day 10 after immunization, when animals start to lose tail tonus (disease onset, mean clinical score 0.2±0.12). At days 13 to 14 all animals were clinically ill (peak of the disease, mean clinical score 3.3±0.37) followed by a period of recovery.

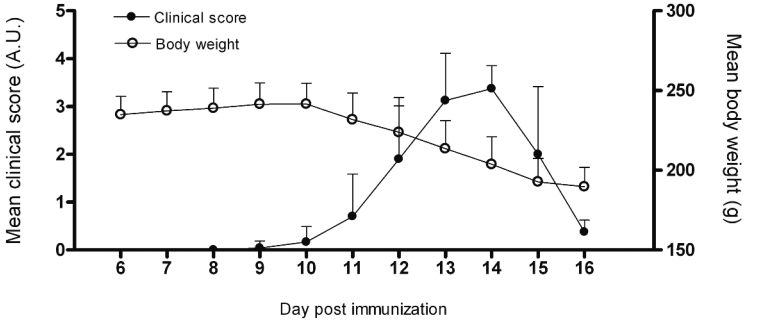

Figure 1: Time course of clinical scores (●) and body weight (o) of acute experimental autoimmune encephalomyelitis. Animals were immunized with MBP emulsified in CFA at day 0 (n=12). Neurological symptoms were scored daily.

USPIO detection in the CNS after intravenous injection

At disease onset (day 10) contrast effects as a result of USPIO in the lesion were detected on T_2W images within 1h after intravenous injection (Fig 2A). The pre-injection image showed a hyperintense lesion (white arrow) in the cerebellum which turned hypointense in the studied time period; 0 to 6h. After injection of Gd-DTPA, an increase in signal intensity was observed in the corresponding area, indicating BBB leakage.
USPIO injection at disease peak (Fig 2B) resulted in multiple areas of decreased signal intensity in the cerebellum. However, these contrast effects were less intense compared with USPIO injections at disease onset. T_1W subtraction images showed a diffuse pattern of Gd-DTPA enhancement.

2A **2B**

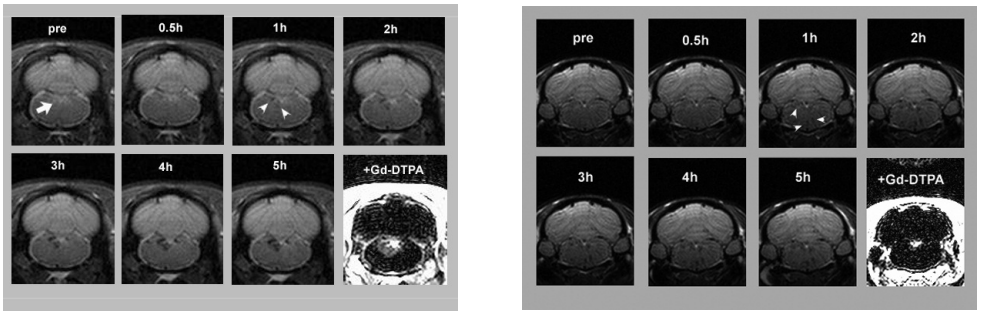

Figure 2: Typical examples of T_2W images displaying the time course of signal loss in the EAE brain directly after an USPIO injection. (A) Animal injected at disease onset (day 10). The pre-injection image shows a hyperintense lesion in the cerebellum (white arrow). Within 1h after injection, hypointense spots (white arrowheads) appear in the lesion center and around the lesion which gradually increase in size. (B) Animal injected at disease peak (day 13). Multiple small hypointense foci are detected after 1h (white arrowheads). Gd-DTPA-T_1W subtraction images at 6h show the increase in T_1W signal intensity as a measure of BBB damage.

Decreased signal intensities in the CNS are not detected 72h later

To monitor the fate of USPIO in EAE lesions in the course of time, MRI was performed 24h and 72h after USPIO injection. A few hypointense areas were detected at 24h in the upper spinal cord and in the cerebellum of animals injected at day 10 (Fig 3A). Loss of signal intensity at 24h was detected in the same brain regions, compared with MR images obtained after 6h. However, loss of signal was less pronounced. In all MR images, con-

3A

3B

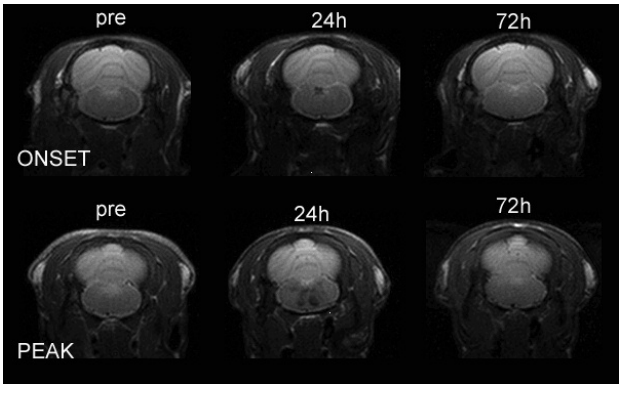

Figure 3: USPIO enhancement at later stages following intravenous administration. (A) Typical example of an animal injected at disease onset. On the T_2W images a small hypointense area is detected at 24h which is absent at 72h. (B) In an animal injected at disease peak a higher number of hypointense areas is detected at 24h in the medulla which are no longer detected at 72h.

trast effects were no longer apparent after 72h, indicating breakdown of USPIO or efflux from the CNS.
After injection at day 13 (peak of the disease; Fig 3B), contrast effects in the 24h-scan had increased as compared to the 24h-images following USPIO injections at day 10. These areas of decreased signal intensity were detected at multiple areas in spinal cord, cerebellum and midbrain. Interestingly, in comparison to the MR images obtained after 6h, the signal intensity in these regions had further decreased after 24h (compare Fig 3B with Fig 2B). Loss of signal intensity was no longer detected in scans performed 72h after USPIO injection.

USPIO accumulation in cervical lymph nodes differs between onset and peak of the disease

The absence of contrast effects in the 72h-scans of the inflammatory brain pointed to a mechanism of USPIO efflux. Therefore, the CLN were imaged and the area of signal changes in the CLN was analyzed. Typically, animals injected at disease onset showed a decrease in signal intensity at 24h in the CLN that further decreased at 72h (Fig 4A). Following USPIO injections at the disease peak, signal loss was detected in similar regions after 24h and 72h.
Quantitative analysis of the area of signal changes in the CLN (Fig 4B) showed that USPIO injections at disease onset resulted at 24h in an increase of 121±41% (P< .05 versus 24h-control) in hypointense area compared with the pre-injection image. In the 72h-scan, this area had increased up to 238±47% (P< .05 versus 24h-onset and 72h-control). USPIO injections at the disease peak resulted in an equal increase in size of the hypointense area at 24h (137±15%; P< .05 versus 24h-control). However, the size of this area was not changed 72h after injection (147±36%), suggesting that there was no further accumulation of USPIO

4A

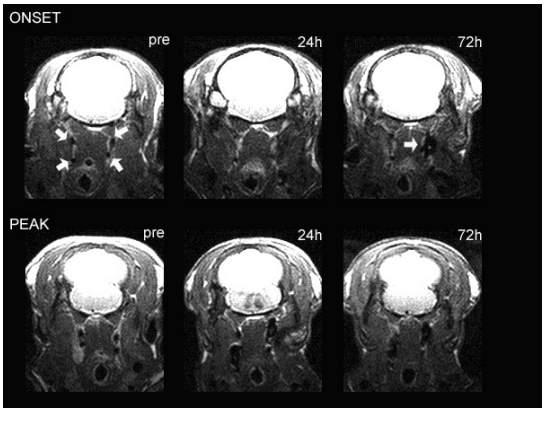

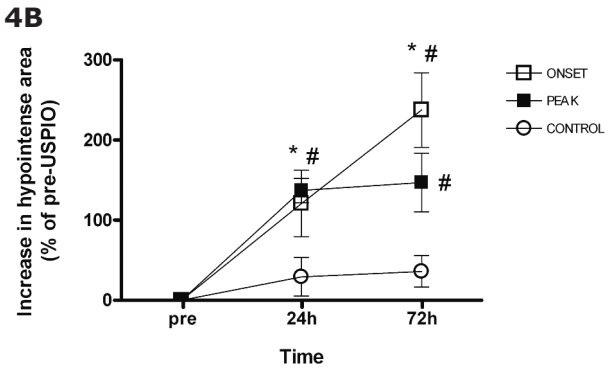

Figure 4: USPIO accumulation is detected in cervical lymph nodes of EAE animals and quantification marks onset and peak of the disease. (A) CLN itself are not detectable on T_2W images but are located around the carotid arteries (white arrows in onset pre-image) at the level of the posterior part of the cerebellum. After USPIO injection, hypointense areas are detected around the carotid arteries at 24h, indicative for USPIO accumulation in CLN. Note the large area of signal loss (white arrow) present at 72h for the animal injected at disease onset. (B) Quantification of the size of hypointense areas with time, plotted as increase (in %) in relation to the area before USPIO injection. Note the increase at 72h for animals injected at day 10, whereas no further increase is detected at 72h for animals injected at day 13. * = P< .05 versus previous time point and # = P< .05 versus control.

at this stage of the disease. USPIO injections in healthy animals (control) showed in a similar time frame little changes in signal intensity in the CLN.

USPIO in circulation after intravenous injection

Blood samples depleted from erythrocytes were analyzed for the presence of iron to study USPIO in circulation of EAE rats. In cell spots prepared 6h after USPIO injection and stained with PB, blue iron clusters were observed which were not cell associated (Fig 5A). Analysis of cell spots prepared 24h and 72h after injection of USPIO revealed a few iron-positive cells (Fig 5B-C).

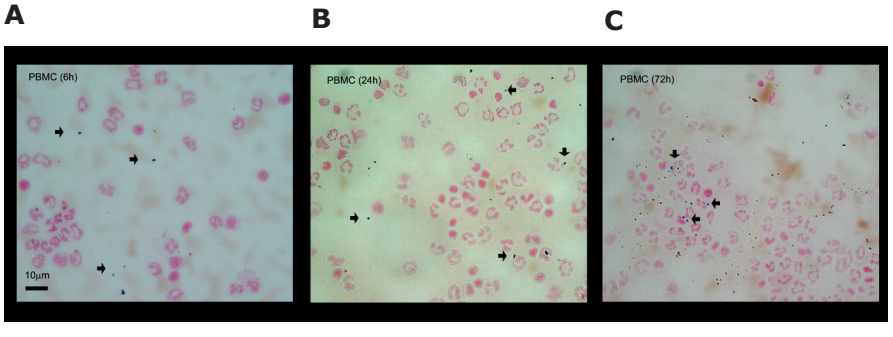

Figure 5: Presence of iron clusters in circulation after USPIO injection in EAE rats at disease onset. (A) Prussian blue staining of peripheral blood mononuclear cells (PBMC) 6h after USPIO injection showed extracellular iron (blue spots marked by arrows) in between the cells. PBMC are counterstained with nuclear fast red (pink color). After 24h (B) and 72h (C) iron particles are still detected in the blood samples and appear to be clustered and cell-associated. Scale bar = 10µm.

USPIO are histologically detected in damaged brain areas

To investigate cellular localization of USPIO in the brain parenchyma, cryosections of the cerebellum and spinal cord were analyzed for the presence of infiltrated monocytes (ED1+ cells), iron (PB stain) and BBB damage (IgG leakage). In tissue sections prepared 6h after injection at disease onset (day 10), several ED1-positive infiltrates were detected (Fig 6A-C). In the vicinity of the infiltrates, USPIO were detected as small blue spots of which a number co-localized with ED1+ cells and others showed to be extracellular iron deposits. Immunohistochemical analysis of IgG (as a

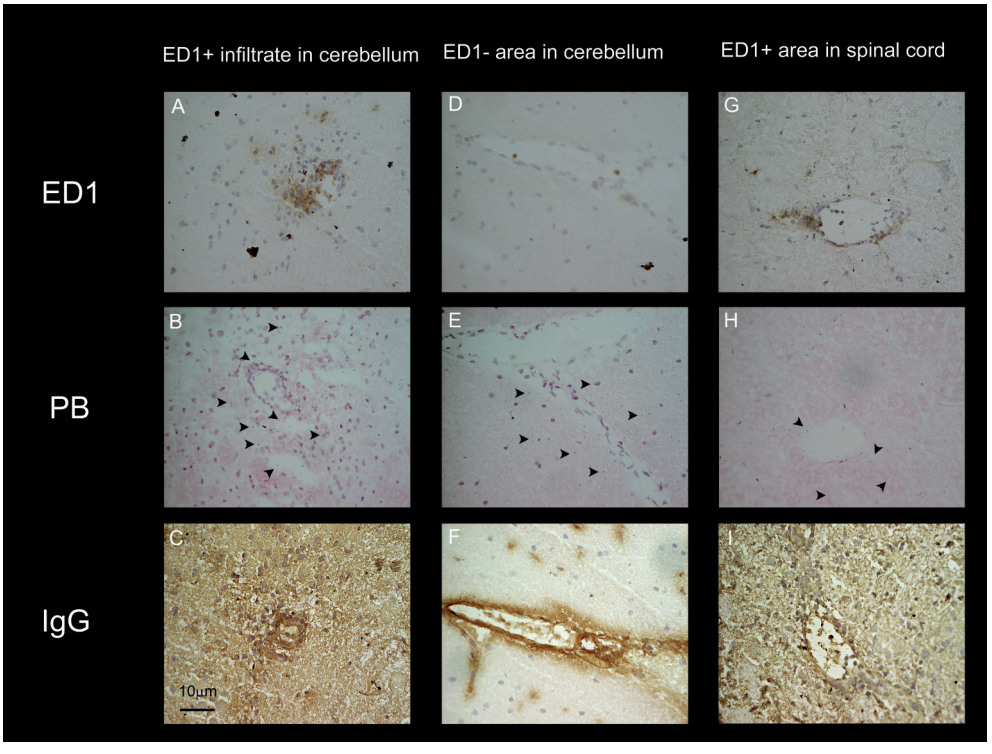

Figure 6: Iron clusters are detected predominantly extracellular in the vicinity of ED1+ infiltrates, 6h after USPIO injection at disease onset. **(A)** ED1+ cells (brown) detected in the cerebellum with **(B)** multiple iron clusters (blue) present in close proximity. Note that the iron clusters (black arrowheads) do not overlap with the ED1+ cells and are localized in the area of **(C)** IgG leakage (brown). **(D-E)** Extracellular iron clusters located around a vessel wall without ED1+ cells (ED-). **(F)** IgG staining shows a small rim of leakage expanding from the corresponding vessel wall. **(G-I)** Small ED1+ infiltrate located in the spinal cord, similarly shows extracellular iron clusters in the spinal cord parenchyma in close proximity to the vessel. Scale bar = 20µm.

marker for BBB damage) in corresponding sections, showed a large area of BBB impairment in which the intra- and extracellular iron clusters were located. Interestingly, we also found extracellular USPIO deposits in close

proximity to vessels without ED1+ infiltrate (ED-) in the cerebellum (Fig 6D-F). IgG detection in the corresponding section showed a thick rim lining the vessel wall, indicative for BBB impairment. Additionally, in the spinal cord (Fig 6G-I), a few ED1+ infiltrates were detected with extracellular iron clusters present in close proximity to the vasculature.

USPIO accumulation in the CLN was observed on MR images 24h and 72h after USPIO injection. Histological analysis of cryosections prepared from the CLN 72h after injection at day 10, showed ED1+ cells predominantly in the medulla of the CLN (Fig 7). In the corresponding section, USPIO-positivity was detected in a similar pattern in the medulla. Also, small iron clusters (arrowheads) were present in the outer rim possibly co-localizing with the macrophages in the subcapsular sinuses. A magnification of this border area reveals intracellular clusters of USPIO.

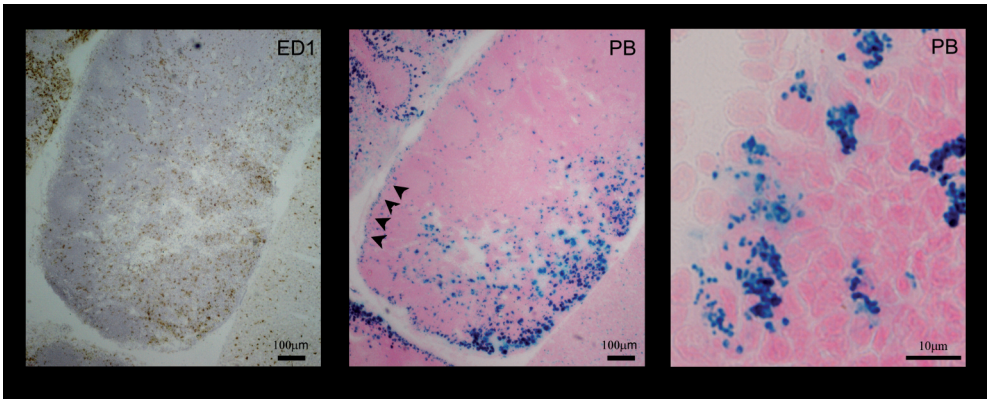

Figure 7: USPIO clusters are present in the cervical lymph nodes of EAE animals 72h after USPIO injection. ED1+ cells (left image, brown) are predominantly detected in the medulla of the lymph node. In the corresponding region (center image) iron clusters (blue) are located. Arrowheads point to the rim of iron clusters present near the subcapsular sinuses. A magnification of a small part of this border demonstrates intra-cellular iron clusters (right image). Scale bar = 100 en 10µm.

DISCUSSION

In this study we investigated MR contrast effects in the CNS of EAE rats after a single injection of USPIO with time at various disease stages. USPIO presence in the brain of EAE animals was monitored repeatedly and directly after injection up to 6h and 24h and 72h later. In vivo MRI of brain, upper spinal cord and CLN was performed and results were compared with histopathological findings.

Here, we show for the first time that areas of decreased signal intensity, reflecting the presence of USPIO, appear in the CNS of EAE rats within 1h after USPIO injection. The presence of USPIO in the brain parenchyma in this time frame may point to cell independent transport over an impaired BBB. This assumption is further supported by our data from simultaneous Gd-DTPA injections, a much smaller contrast agent, which showed enhancement at similar locations in the cerebellum. Previously, Xu et al. reported on changes in signal intensity detected in the brain after 6h using the iron oxide particle MION-46L in a chronic EAE model, demonstrating USPIO presence in CNS lesions (Xu et al., 1998). To investigate USPIO presence at different stages of EAE, we administered USPIO at the onset of clinical symptoms and at full blown EAE.

Interestingly, injection at disease onset resulted in a strong loss of signal intensity that was confined to the border between medulla and cerebellum. In contrast, repetitive MRI following USPIO injection at the disease peak resulted in a different hypointense pattern compared with disease onset. Areas of signal loss were more abundant in the medulla, reflecting the presence of multiple inflammatory lesions. However, loss of signal was less intense compared with injections at disease onset. Results suggest a change in BBB permeability for nano-sized particles during the course of the disease. Maximal increase in BBB permeability at onset of EAE has been reported previously (Koh et al., 1993; Pan et al., 1996). Changes in BBB permeability also include changes in specific transport systems during the disease course (Pan et al., 1996) that may explain the differences in USPIO accumulation directly upon administration.

So far, USPIO-enhanced areas during neuroinflammatory conditions have been put forward as an in vivo marker for macrophage activity, because in most cases hypointense patterns as observed on MR images correspond to ED1+ areas in histological sections (Kaim et al., 2002; Kleinschnitz et al., 2003). Recently, USPIO have been administered in humans suffering from stroke and MS and results suggested that USPIO can reveal the presence of inflammatory lesions (Dousset et al., 2006; Saleh et al., 2004a).

With this increase in clinical applications comes an emerging need to understand USPIO incorporation and kinetics in inflammatory tissue. However, knowledge on the mechanism responsible for their presence in the brain parenchyma is limited. In this study, extracellular iron deposits in the brain parenchyma were detected in animals sacrificed 6h after USPIO injection. Our findings suggest that BBB leakage is one of the most important physiological mechanisms responsible for USPIO entrance in the inflammatory CNS. This is further supported by our previous results which show that USPIO are not incorporated by human monocytes in vitro within 6h (Oude Engberink et al., 2007). The relatively small size of the particles limits effective incorporation by Kupffer cells which increases half-life in circulation (Weissleder et al., 1990). Similarly, the small size decreases the labeling efficiency of monocytes in circulation. Taken together, data from our study strongly suggest that USPIO, monitored directly after intravenous administration, can be used as a marker for BBB damage. In line with our results, cell independent USPIO uptake in the brain parenchyma has been reported previously following permanent middle cerebral artery occlusion (Rausch et al., 2001; Wiart et al., 2007). In these studies, USPIO were intravenously injected 5h after occlusion and the early signal changes observed in the lesion similarly supports the assumption that USPIO can penetrate a damaged brain area independent of monocyte infiltration. In contrast to BBB opening and tissue damage by ischemia, our study investigated immune induced BBB damage.

Imaging 24h after USPIO injection revealed that contrast effects in EAE rats, injected at disease peak, were more pronounced than in animals injected at disease onset. Our results provide evidence for the potential of USPIO injections as a marker for disease progression and are in line with previous reports on USPIO enhancement in the CNS after 24h, which show a correlation between the presence of USPIO and clinical status of EAE rats (Dousset et al., 2002; Floris et al., 2004). It is generally believed that 24h after USPIO injection, USPIO have accumulated in phagocytic cells (Corot et al., 2004). However, the fate of free or incorporated USPIO in the CNS at later time points has not yet been investigated.
In the present study, MR imaging was performed longitudinally and results showed that areas of signal loss, detected at 24h in the CNS, were absent 72h after USPIO injection independent of the disease course. It is known that USPIO are biodegradable and in vivo the dextran-coating can be cleaved off and the iron oxide core will be degraded into iron ions (Corot et al., 2004), resulting in loss of its superparamagnetic properties. However, we have shown previously that signal loss following an intracerebral injection of iron oxide labeled cells in healthy rats remained detectable up to 5 days (Oude Engberink et al., 2007). Therefore, other processes may

play a role in the loss of USPIO detection at inflammatory areas.

An alternative explanation is that USPIO are drained from the CNS in EAE rats and transported away from the lesion site. In our study, we imaged the CLN longitudinally to investigate USPIO accumulation during the disease course in EAE rats. Quantitative analysis revealed a significant USPIO-enhanced area in the CLN 24h after injection. Interestingly, in EAE rats injected at disease onset the area of signal loss had further increased up to 250% at 72h, which is the peak of the disease for these animals. In animals injected at disease peak, the size of the USPIO-enhanced area had not further increased after 72h. Earlier, it was shown that iron oxide particles directly injected in the brain parenchyma of healthy rats could be detected later in the CLN (Muldoon et al., 2004). Additionally, they reported no loss of signal intensity in the CLN of animals that received USPIO intravenously, indicating that USPIO do not enter the CLN via extravasation from the blood. In our study, we injected a higher amount of USPIO intravenously and observed small contrast effects in healthy animals. However, contrast effects observed in our EAE animals were significantly larger. Staining of CLN sections of EAE animals with Prussian blue showed the presence of USPIO predominantly in the medulla of the nodes, suggesting that USPIO that enter the CNS of EAE rats can be drained to the CLN. The region of USPIO detection corresponded to the presence of ED1+ cells in the medulla. Moreover, clusters of USPIO were detected as a rim lining the subcapsular sinuses, suggesting incorporation by macrophages of the subcapsular sinus. Recently, these macrophages in mice have been identified to capture lymph-borne viruses and translocate viral particles for presentation to follicular B-cells (Junt et al., 2007). Interestingly, in the light of potential causal factors in MS, the Epstein-Barr virus and infected B-cells have been associated with the incidence of MS (Pender and Greer, 2007; Serafini et al., 2007).
Antigen translocation and presentation in lymphoid organs may play an important role in MS pathology. Previously in a primate EAE model, the presence of myelin antigens in the brain draining CLN was demonstrated, originating from ongoing demyelination in the CNS (de Vos et al., 2002). Moreover, myelin proteins have been detected in the CLN of MS patients (Fabriek et al., 2005) and non-invasive imaging of this transport process may contribute to a better understanding of immune regulation in MS. A possible mechanism for translocation of antigen (loaded cells) out of the CNS has been suggested involving a fiber-like network of basal membrane molecules underlying the inflammatory foci in MS patients (van Horssen et al., 2005). Our data suggest that USPIO particles at inflammatory sites are partly drained by the CLN and that this process can be monitored non-invasively.

In conclusion, this report shows USPIO entrance in the CNS of EAE rats in a short time frame suggesting a cell independent mechanism. This mechanism may be partly responsible for the frequently reported contrast effects at 24h in the inflammatory brain. Furthermore, MR monitoring of the CLN suggests a potential role in USPIO drainage at later time points. With a view to the increasing clinical applications of USPIO, these data will contribute to a better interpretation of USPIO enhancement in CNS pathology.

ACKNOWLEDGEMENTS

The MR contrast agents were kindly provided by Guerbet, France. This work has been supported by the Dutch MS Research Foundation (MS 01-470, MS 02-489).

REFERENCES

Al-Omaishi J, Bashir R, Gendelman HE. The cellular immunology of multiple sclerosis. J Leukoc Biol 1999; 65: 444-52.

Benderbous S, Corot C, Jacobs P, Bonnemain B. Superparamagnetic agents: physicochemical characteristics and preclinical imaging evaluation. Acad Radiol 1996; 3 Suppl 2: S292-4.

Bruck W, Sommermeier N, Bergmann M, Zettl U, Goebel HH, Kretzschmar HA, et al. Macrophages in multiple sclerosis. Immunobiology 1996; 195: 588-600.

Corot C, Petry KG, Trivedi R, Saleh A, Jonkmanns C, Le Bas JF, et al. Macrophage imaging in central nervous system and in carotid atherosclerotic plaque using ultrasmall superparamagnetic iron oxide in magnetic resonance imaging. Invest Radiol 2004; 39: 619-25.

de Vos AF, van Meurs M, Brok HP, Boven LA, Hintzen RQ, van der Valk P, et al. Transfer of central nervous system autoantigens and presentation in secondary lymphoid organs. J Immunol 2002; 169: 5415-23.

de Vries HE, Kuiper J, de Boer AG, Van Berkel TJ, Breimer DD. The blood-brain barrier in neuroinflammatory diseases. Pharmacol Rev 1997; 49: 143-55.

Dousset V, Brochet B, Deloire MS, Lagoarde L, Barroso B, Caille JM, et al. MR imaging of relapsing multiple sclerosis patients using ultra-small-particle iron oxide and compared with gadolinium. AJNR Am J Neuroradiol 2006; 27: 1000-5.

Dousset V, Delalande C, Ballarino L, Quesson B, Seilhan D, Coussemacq M, et al. In vivo macrophage activity imaging in the central nervous system detected by magnetic resonance. Magn Reson Med 1999; 41: 329-33.

Dousset V, Doche B, Petry KG, Brochet B, Delalande C, Caille JM. Correlation between clinical status and macrophage activity imaging in the central nervous system of rats. Acad Radiol 2002; 9 Suppl 1: S156-9.

Ewing C, Bernard CC. Insights into the aetiology and pathogenesis of multiple sclerosis. Immunol Cell Biol 1998; 76: 47-54.

Fabriek BO, Zwemmer JN, Teunissen CE, Dijkstra CD, Polman CH, Laman JD, et al. In vivo detection of myelin proteins in cervical lymph nodes of MS patients using ultrasound-guided fine-needle aspiration cytology. J Neuroimmunol 2005; 161: 190-4.

Floris S, Blezer EL, Schreibelt G, Dopp E, van der Pol SM, Schadee-Eestermans IL, et al. Blood-brain barrier permeability and monocyte infiltration in experimental allergic encephalomyelitis: a quantitative MRI study. Brain 2004; 127: 616-27.

Hawkins CP, Munro PM, MacKenzie F, Kesselring J, Tofts PS, du Boulay EP, et al. Duration and selectivity of blood-brain barrier breakdown in chronic relapsing experimental allergic encephalomyelitis studied by gadolinium-DTPA and protein markers. Brain 1990; 113 (Pt 2): 365-78.

Hendriks JJ, Teunissen CE, de Vries HE, Dijkstra CD. Macrophages and neurodegeneration. Brain Res Brain Res Rev 2005; 48: 185-95.

Jung CW. Surface properties of superparamagnetic iron oxide MR contrast agents: ferumoxides, ferumoxtran, ferumoxsil. Magn Reson Imaging 1995; 13: 675-91.

Junt T, Moseman EA, Iannacone M, Massberg S, Lang PA, Boes M, et al. Subcapsular sinus macrophages in lymph nodes clear lymph-borne viruses and present them to antiviral B cells. Nature 2007; 450: 110-4.

Kaim AH, Wischer T, O'Reilly T, Jundt G, Frohlich J, von Schulthess GK, et al. MR imaging with ultrasmall superparamagnetic iron oxide particles in experimental soft-tissue infections in rats. Radiology 2002; 225: 808-14.

Karlik SJ, Grant EA, Lee D, Noseworthy JH. Gadolinium enhancement in acute and chronic-progressive experimental allergic encephalomyelitis in the guinea pig. Magn Reson Med 1993; 30: 326-31.

Kleinschnitz C, Bendszus M, Frank M, Solymosi L, Toyka KV, Stoll G. In vivo monitoring of macrophage infiltration in experimental ischemic brain lesions by magnetic resonance imaging. J Cereb Blood Flow Metab 2003; 23: 1356-61.

Koh CS, Gausas J, Paterson PY. Neurovascular permeability and fibrin deposition in the central neuraxis of Lewis rats with cell-transferred experimental allergic encephalomyelitis in relationship to clinical and histopathological features of the disease. J Neuroimmunol 1993; 47: 141-5.

Muldoon LL, Varallyay P, Kraemer DF, Kiwic G, Pinkston K, Walker-Rosenfeld SL, et al. Trafficking of superparamagnetic iron oxide particles (Combidex) from brain to lymph nodes in the rat. Neuropathol Appl Neurobiol 2004; 30: 70-9.

Namer IJ, Steibel J, Poulet P, Armspach JP, Mauss Y, Chambron J. In vivo dynamic MR imaging of MBP-induced acute experimental allergic encephalomyelitis in Lewis rat. Magn Reson Med 1992; 24: 325-34.

Oude Engberink RD, van der Pol SM, Dopp EA, de Vries HE, Blezer EL. Comparison of SPIO and USPIO for in vitro labeling of human monocytes: MR detection and cell function. Radiology 2007; 243: 467-74.

Pan W, Banks WA, Kennedy MK, Gutierrez EG, Kastin AJ. Differential permeability of the BBB in acute EAE: enhanced transport of TNT-alpha. Am J Physiol 1996; 271: E636-42.

Pender MP, Greer JM. Immunology of multiple sclerosis. Curr Allergy Asthma Rep 2007; 7: 285-92.

Phillips MJ, Needham M, Weller RO. Role of cervical lymph nodes in autoimmune encephalomyelitis in the Lewis rat. J Pathol 1997; 182: 457-64.

Rausch M, Sauter A, Frohlich J, Neubacher U, Radu EW, Rudin M. Dynamic patterns of USPIO enhancement can be observed in macrophages after ischemic brain damage. Magn Reson Med 2001; 46: 1018-22.

Saleh A, Schroeter M, Jonkmanns C, Hartung HP, Modder U, Jander S. In vivo MRI of brain inflammation in human ischaemic stroke. Brain 2004a; 127: 1670-7.

Saleh A, Wiedermann D, Schroeter M, Jonkmanns C, Jander S, Hoehn M. Central nervous system inflammatory response after cerebral infarction as detected by magnetic resonance imaging. NMR Biomed 2004b; 17: 163-9.

Schoepf U, Marecos EM, Melder RJ, Jain RK, Weissleder R. Intracellular magnetic labeling of lymphocytes for in vivo trafficking studies. Biotechniques 1998; 24: 642-6, 648-51.

Schreibelt G, Musters RJ, Reijerkerk A, de Groot LR, van der Pol SM, Hendrikx EM, et al. Lipoic acid affects cellular migration into the central nervous system and stabilizes blood-brain barrier integrity. J Immunol 2006; 177: 2630-7.

Serafini B, Rosicarelli B, Franciotta D, Magliozzi R, Reynolds R, Cinque P, et al. Dysregulated Epstein-Barr virus infection in the multiple sclerosis brain. J Exp Med 2007; 204: 2899-912.

van Horssen J, Bo L, Vos CM, Virtanen I, de Vries HE. Basement membrane proteins in multiple sclerosis-associated inflammatory cuffs: potential role in influx and transport of leukocytes. J Neuropathol Exp Neurol 2005; 64: 722-9.

Weissleder R, Cheng HC, Bogdanova A, Bogdanov A, Jr. Magnetically labeled cells can be detected by MR imaging. J Magn Reson Imaging 1997; 7: 258-63.

Weissleder R, Elizondo G, Wittenberg J, Rabito CA, Bengele HH, Josephson L. Ultrasmall superparamagnetic iron oxide: characterization of a new class of contrast agents for MR imaging. Radiology 1990; 175: 489-93.

Wiart M, Davoust N, Pialat JB, Desestret V, Moucharaffie S, Cho TH, et al. MRI monitoring of neuroinflammation in mouse focal ischemia. Stroke 2007; 38: 131-7.

Xu S, Jordan EK, Brocke S, Bulte JW, Quigley L, Tresser N, et al. Study of relapsing remitting experimental allergic encephalomyelitis SJL mouse model using MION-46L enhanced in vivo MRI: early histopathological correlation. J Neurosci Res 1998; 52: 549-58.

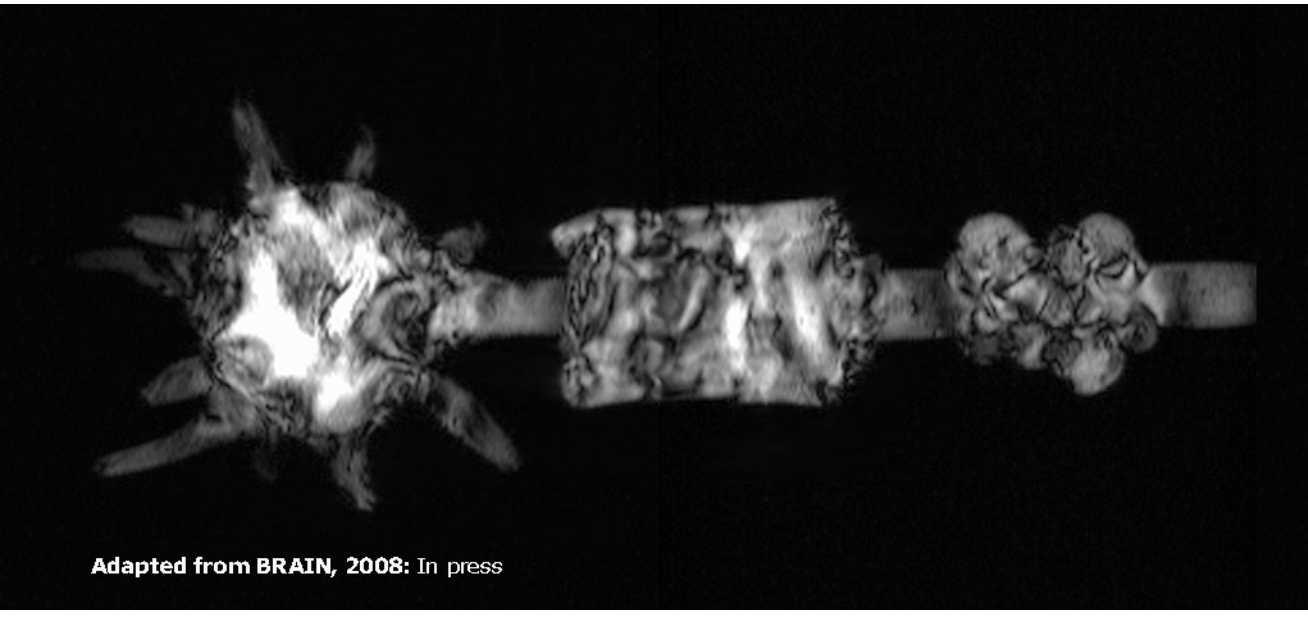

Adapted from BRAIN, 2008: In press

Pluriformity of inflammation in multiple sclerosis shown by ultra small iron oxide particle enhancement

M.M. Vellinga[1], R.D. Oude Engberink[7], A. Seewann[1], P.J.W. Pouwels[3], M.P. Wattjes[5], S.M.A. van der Pol[2], C. Pering[4], C.H. Polman[1], H.E. de Vries[2], J.J.G. Geurts[5, 6], F. Barkhof[5]

MS Centre Amsterdam[1,2,5], VU University medical center, Amsterdam, the Netherlands, Depts. of Neurology [1], Cell Biology and Immunology[2], Radiology[5], Pathology[6], Physics and Medical Technology[3], Bayer Schering Pharma, Berlin, Germany, Dept. of Diagnostic Imaging[4], Image Sciences Institute, University Medical Center Utrecht, The Netherlands [7]

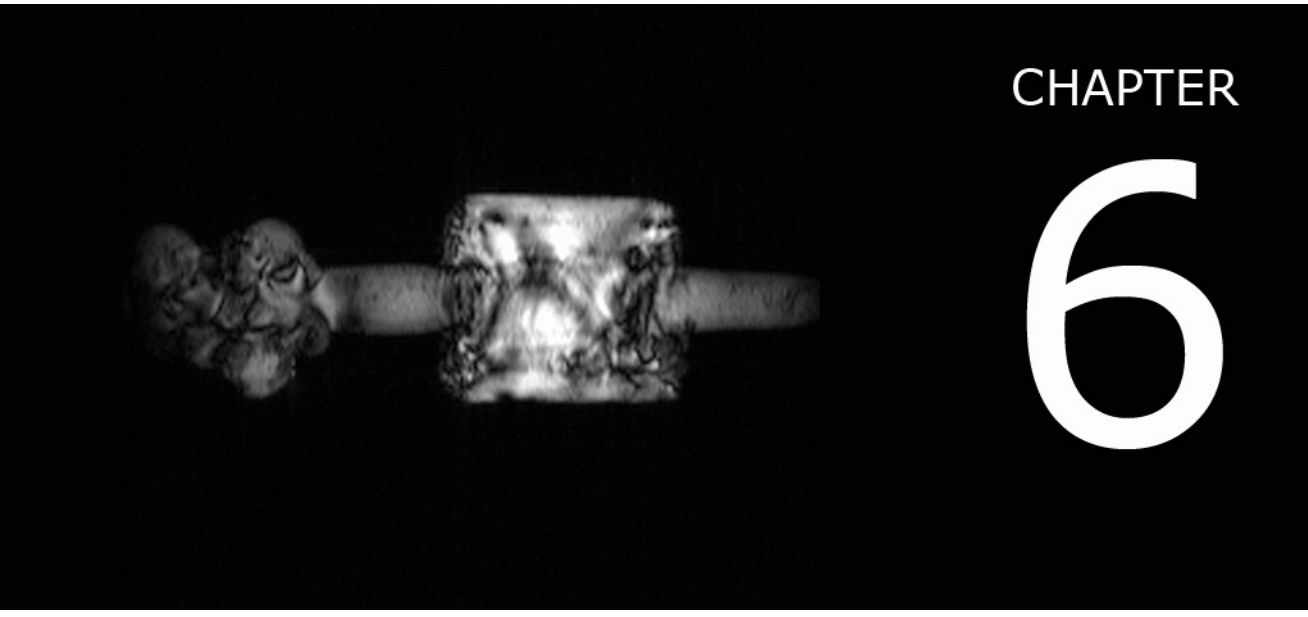

ABSTRACT

Gadolinium-DTPA (Gd-DTPA) is routinely used as a marker for inflammation in magnetic resonance imaging (MRI) to visualize breakdown of the blood-brain barrier (BBB) in multiple sclerosis (MS). Recent data suggest that ultra small superparamagnetic particles of iron oxide (USPIO) can be used to visualise cellular infiltration, another aspect of inflammation. This project aimed to compare the novel USPIO particle SHU 555 C to the longitudinal pattern of Gd-DTPA enhancement in MS.

Nineteen relapsing-remitting MS patients were screened monthly using Gd-DTPA-enhanced MRI. In case of new enhancing lesions, USPIO were injected and 24h later, MRI was performed and blood was collected to confirm USPIO loading of circulating monocytes. Lesion development was monitored by 3 monthly Gd-DTPA-enhanced scans and a final scan 7-11 months after injection. Additionally, in vitro MRI of monocyte samples containing intra- and extracellular USPIO in different concentrations was performed to explore the effect of concentration and compartmentalization on signal intensity in T_1-weighted (T_1W) and T_2*-weighted (T_2*W) images. USPIO enhancement was observed as hyperintensity on T_1W images, whereas no signal changes were observed on T_2*W images. Judged by the in vitro data, this corresponds with a relatively low number of labeled monocytes. In 14 patients with disease activity, 188 USPIO-positive lesions were seen, 144 of which were Gd-negative. By contrast, there were a total of 59 Gd-positive lesions, 15 of which were USPIO negative. Three patterns of USPIO enhancement were seen: 1. focal enhancement, 2. ring-like enhancement, and 3. return to isointensity of a previously hypointense lesion. The latter was most frequently observed for lesions that turned out to be transiently hypointense on follow-up scans, and ring-enhancing lesions were less likely to evolve into black holes at follow-up than lesions without ring-like USPIO enhancement; we speculate this to be associated with remyelination. In 4% of the USPIO-positive/Gd-negative lesions, USPIO enhancement preceded Gd enhancement by 1 month. USPIO enhancement remained visible for up to 3 months in 1.5% of all USPIO-positive lesions. In 29% of the lesions enhancing with both contrast agents, USPIO enhancement persisted whereas Gd enhancement had already resolved.

In conclusion, the new nano-particle SHU 555 C provides complementary information to Gd-enhanced MRI, probably related to monocyte infiltration. The use of USPIO-enhanced MRI is likely to lead to more insight in the pluriformity of inflammation in MS.

INTRODUCTION

Multiple Sclerosis (MS) is a multifocal disease of the central nervous system (CNS), characterized by inflammation, demyelination and axonal loss. Although magnetic resonance imaging (MRI) is highly sensitive in detecting MS lesions, it lacks histopathological specificity. The current MRI marker for inflammation in MS lesions is gadolinium-diethylene-triamine pentaacetic-acid (Gd-DTPA), which visualizes blood-brain barrier (BBB) leakage (Grossman et al*.,* 1988), occurring as a result of inflammation, but not inflammation in itself. Correlation between Gd-DTPA enhancement and clinical disability in MS is poor (Kappos et al*.,* 1999).

A new class of contrast agents based on ultra small superparamagnetic particles of iron oxide (USPIO) has recently been developed for clinical MRI. Their superparamagnetic iron oxide core decreases T_1- and T_2-relaxation times of the surrounding water molecules, resulting in a signal increase on T_1W images. Moreover, the susceptibility effect causes a signal reduction on T_2-weighted gradient-echo (T_2*W) images (Corot et al*.,* 2006). Phagocytosis of USPIO by cells of the monocyte-macrophage system enables MRI to visualise macrophage activity in inflammatory diseases (Corot et al*.,* 2006). Thus, USPIO enhancement, reflecting cellular infiltration, may complement Gd-DTPA enhancement in visualising cellular aspects of inflammation in MS.

So far, most animal and human studies exploring USPIO in inflammatory CNS diseases were performed with ferumoxtran-10, a 30nm USPIO particle (Dousset et al*.,* 1999b; Rausch et al*.,* 2004; Floris et al*.,* 2004; Brochet et al*.,* 2006), although other compounds were previously studied (Xu et al., 1998). In experimental autoimmune encephalomyelitis (EAE), USPIO enhancement was hypointense on T_2*W images. Immunohistochemical analysis revealed USPIO in infiltrated monocytes in inflammatory lesions (Floris et al*.,* 2004) (Dousset et al*.,* 1999a). USPIO enhancement patterns differed from Gd enhancement in time, demonstrating that BBB leakage, as shown by Gd enhancement, and cellular infiltration as shown by USPIO enhancement are two separate mechanisms that can be distinguished in vivo (Rausch et al*.,* 2003; Rausch et al*.,* 2004; Floris et al*.,* 2004; Bendszus et al*.,* 2005; Dousset et al*.,* 2006). The clinical relevance of this distinction is emphasized by data showing that USPIO enhancement correlated with disability, axonal loss and response to therapy (Rausch et al*.,* 2004; Floris et al*.,* 2004; Brochet et al*.,* 2006).

In humans, ferumoxtran-10 demonstrated the presence of phagocytic cells in the CNS in MS (Dousset et al*.,* 2006) (Manninger et al*.,* 2005), stroke (Saleh et al*.,* 2004; Nighoghossian et al*.,* 2007) and intracranial tumors (Neuwelt et al*.,* 2004). USPIO enhancement was hyperintense on T_1W images, matching with the expected distribution of macrophages, but not al-

ways with Gd enhancement. This may suggest that USPIO are more specific for cellular infiltration. Immunohistochemical staining of USPIO-enhancing brain tumors demonstrated USPIO particles in macrophages and astrocytes (Neuwelt et al., 2004).
The present study aimed at visualizing cellular infiltration in MS lesions, using a novel USPIO particle, SHU 555C, which is smaller than ferumoxtran-10 (25 versus 30nm), has a shorter plasma half-life time (6-8h versus 24–30h), and is negatively charged which has shown to enhance uptake by activated monocytes in vitro (Metz et al., 2004). USPIO enhancement of MS lesions was compared to Gd enhancement both in space and in time, and labeling of monocytes was confirmed in blood samples. In vitro samples of intra- and extracellular USPIO were imaged to explore the impact of concentration and compartmentalization on signal intensity changes on T_1W and T_2*W images.

MATERIALS AND METHODS

Patient recruitment

In this clinical phase II study, 19 MS patients were included, 14 of whom eventually underwent USPIO-enhanced MRI. The protocol was approved by the local ethical review board; all subjects gave informed consent. Inclusion criteria were: relapsing-remitting MS; age 18 years or older, adequate hepatic and kidney functions, and at least one Gd-enhancing MS lesion on a historic brain MRI. Patients were excluded if they had a predisposition to allergic disease.

Study design

Patients underwent monthly Gd-enhanced brain MRI screening for Gd-enhancing MS lesions. If present, USPIO were injected within 24 – 48h, followed by another MRI 24h after USPIO injection. Blood was then withdrawn to evaluate liver and kidney functions, monocyte activity and labeling. Follow-up consisted of 3 monthly Gd-enhanced MRI scans and 1 long-term follow-up scan performed 7-11 months after USPIO injection. Treatment status, relapses and adverse events were registered, and disability was measured at inclusion using the Expanded Disability Status Scale (EDSS, possible range: 1 to 10, wither a higher score indicating a higher degree of disability) (Kurtzke 1983).

MR image acquisition and contrast agents

Imaging was performed on a 1.5T MR scanner (Siemens Vision; Erlangen, Germany), using a standard circularly polarized transmit-receive headcoil. For every scan, the same protocol was used: axial T_1W spin-echo (TR=830ms; TE=15ms; 2 acquisitions), dual-echo T_2W spin-echo (TR=3837ms; TE=16 and 98ms; 1 acquisition), and T_2 gradient-echo (T_2W) (TR=615ms; TE=27ms; 1 acquisition). In-plane resolution was 1x1 mm^2 and the slice thickness 4mm. For follow-up images the repositioning was performed according to internal anatomical landmarks

T_1W images were obtained before and after Gd-DTPA administration (Magnevist®, Schering, Berlin, Germany; 0.2ml/kg BW). For the scan 24h after USPIO administration (SH U555C, Schering, Berlin (Germany), diameter: 25nm, $T_{1/2}$ 6-8h, 40 µmol Fe/kg BW at 5 ml/s) no Gd-DTPA was administered.

Image analysis

USPIO enhancement was marked in consensus on post-USPIO T_1W images, using pre-USPIO T_2- and proton density (PD)-images for lesion identification, and pre-Gd T_1W images for comparison, blinded to post-Gd images. Then, Gd enhancement of lesions was marked on post-Gd T_1W

images, again using pre-Gd T_1W, T_2- and PD-images as references, and blinded to post-USPIO images. T_1 hypointensity of lesions was determined as described (van Walderveen et al*.,* 1995) on historic, baseline and long-term follow-up scans blinded to post-USPIO images. According to longitudinal appearance, black holes were classified as follows: 'chronic black holes' were already hypointense on historical MRI and remained so throughout the study period. 'Acute and persistent black holes' were hypointense at USPIO-injection and follow-up. 'Transiently T_1-hypointense lesions' were hypointense around USPIO-injection, but neither on historical nor on long-term follow-up MRI. USPIO-enhanced return to isointensity of a T_1-hypointense lesion was defined by two criteria: firstly, post-USPIO signal intensity was in the range of signal intensity of the surrounding white matter, secondly, signal intensity of the lesion had changed at least 2 standard deviations more than signal intensity of the surrounding white matter, compared to pre-USPIO images. To determine associations between ring-like USPIO enhancement and longitudinal T_1 patterns of lesions, a control group of USPIO-negative (USPIO-) T_2 lesions was created blinded for hypointensity status, after which their T_1 pattern was analysed.

Cell assays and iron staining

To collect peripheral blood mononuclear cells (PBMC) from patients 24h after USPIO injection, whole blood samples were layered on lymphocyte separation medium (Lymphoprep™, Fresenius Kabi Norge) and centrifuged (25min, 800g, 18°C). Mononuclear interphase cells were isolated and washed with phosphate-buffered saline in 10% of serum collected from the top layer of the gradient. Production of reactive oxygen species (ROS) by isolated monocytes was measured as a marker for cell activation using dihydrorhodamine as described (Schreibelt et al*.,* 2006). Cell viability was routinely checked by 7-aminoactinomycin D (7AAD, Molecular Probes, Eugene, Oregon, USA) exclusion and the percentage of monocytes was determined by the number of CD14 (BD Pharmingen) -positive cells using a FACScan flow cytometer (Calibur, Becton Dickinson, Mountain view, CA, USA). Cell spots were prepared from PBMC to detect the presence of intracellular USPIO by Prussian blue staining as described (Oude Engberink et al*.,* 2007).

Preparation of cell samples for in vitro MRI

To assess the MR signal intensity of intra- and extracellular iron oxide particles, phantoms were prepared using human monocytes isolated from buffycoats of healthy donors (Sanquin blood bank, the Netherlands) as described previously (Oude Engberink et al*.,* 2007). To create phantoms of intracellular USPIO, freshly isolated monocytes were incubated for 6h in

the presence of 1mg Fe/ml USPIO. Agar-gel (2ml, 0.4%) suspensions were prepared in 2ml vials containing 0.1, 0.5, 1.0, 2.5, 5.0 and $10.0x10^6$ labeled monocytes. Extracellular iron phantoms were prepared by adding a standard concentration USPIO (25pg/cell (Metz et al*.,* 2004)) to the monocytes followed by immediate fixation in agar-gel. The vials, containing a range of concentrations of labeled cells, matched to the same range of concentration of unlabeled cells mixed with a fixed dose of free iron oxide particles per cell, were put in a brain slice holder and T_1W and T_2*W images were collected using the same MRI protocol as described in the MR acquisition paragraph, planning a single slice of 4mm thickness, through the samples. For analysis of signal intensity, regions of interest (ROI; circular, 5mm in diameter) were placed in the center of the phantoms.

RESULTS

Patients

Five patients displayed no Gd-DTPA enhancing lesions within 5 months after inclusion, and did not receive USPIO injection. Of the 14 patients receiving SHU555C (five males, nine females, median EDSS at inclusion: 3.0 [range 1.5 – 5.0]), the mean disease duration at USPIO injection was 4.2 years [range 0.3 – 16] and the mean time from most recent relapse to USPIO injection was 16 months [range 0 – 84]). Nine patients were on immunomodulatory treatment. No patients developed any adverse events.

Three patterns of USPIO enhancement

USPIO enhancement was hyperintense on T_1W images. On T_2W and T_2*W images, no signal changes were observed in any of the lesions, but blood vessels appeared slightly hypointense. In the 14 patients given USPIO, there were 59 Gd+ lesions and 188 USPIO+ lesions. 144 (77%) out of these 188 USPIO+ lesions were Gd- (Table 1). In total, 15 (25%) of the

Table 1

Cross-sectional USPIO and Gd-enhancement of MS lesions: numbers of lesions in different enhancement patterns.

USPIO-enhancement	Gd-enhancement		Total
	yes	no	
Yes	44	144	188
Focal	24	55	79
Ring-like	6	64	70
Return to isointensity	14	25	39
No	15	NA	15
Total	59	144	203

Gd+ lesions were USPIO-. USPIO enhancement occurred in 3 different patterns (Figs 1 and 2): focal enhancement (42%), ring-like enhancement (37%), mostly around pre-existing T_2-hyperintense lesions), and return to isointensity of lesions that were hypointense on pre-contrast T_1W images (21%). Focal and ring-like USPIO+ lesions could be either Gd+ or

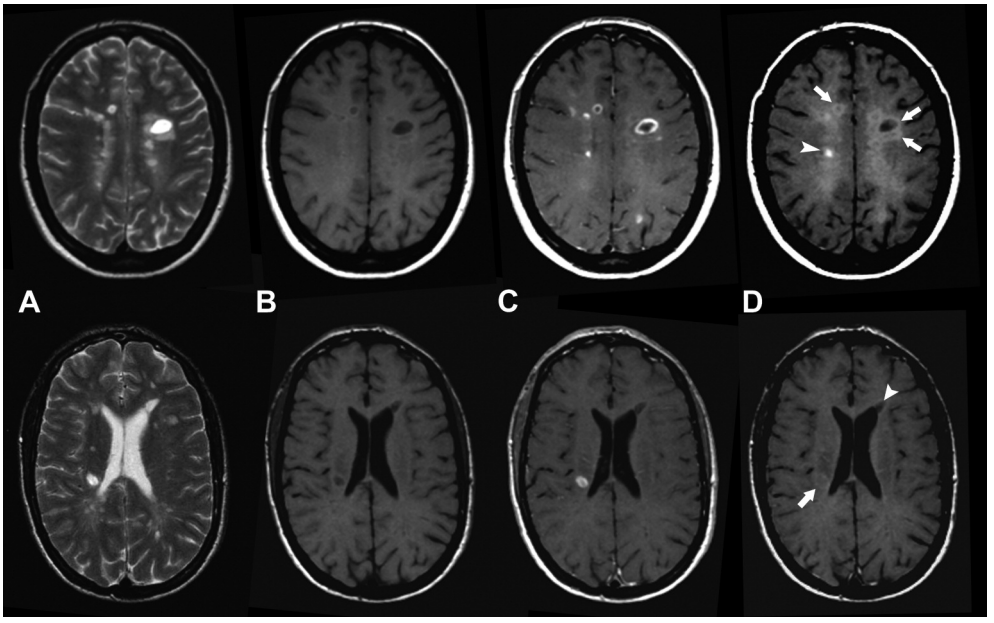

Figure 1: Cross-sectional patterns of lesion enhancement. (A) Pre-Gd T_2 SE images showing multiple periventricular MS lesions. (A) Pre-Gd T_1W images showing hypointensity of some lesions. (C) Post-Gd T_1W images show that several MS lesions enhance with Gd in focal and ring-like patterns. (D) Post-USPIO T_1W images show different patterns of USPIO enhancement: arrowhead upper row: focal USPIO enhancement; arrows upper row: ring-like USPIO enhancement; arrow bottom row: change to isointensity of a previously hypointense lesion as seen on pre-contrast T_1W images (see B); arrowhead bottom row: a hypointense lesion that remains hypointense on post-USPIO images.

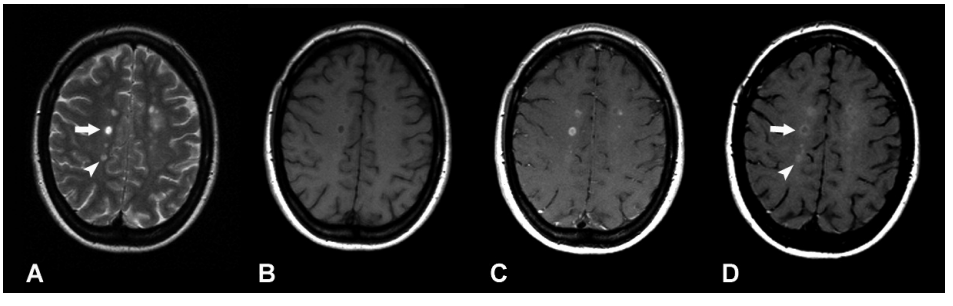

Figure 2: Cross-sectional patterns of lesion enhancement: (A) Pre-Gd T_2 SE images showing multiple MS lesions. (B) Pre-Gd T_1W images showing hypointensity of some of the MS lesions. (C) Some lesions are Gd-DTPA-positive. (D) Post-USPIO images show a Gd-DTPA-positive, USPIO ring-enhancing lesion (arrow) and a Gd-DTPA-negative, focally USPIO-positive lesion (arrowhead).

Gd-. Incidentally, subtle diffuse enhancement of normal-appearing white matter was observed in some patients. Use of immunomodulatory treatment did appear to relate to the different patterns of enhancement.

'Return to isointensity' was mostly detected in transiently T_1-hypointense lesions

In total, 200 T_1-hypointense lesions were observed around the time of USPIO injection, which on follow-up could be classified as either chronic, or acute and persistent, or transient (Table 2). Only 8 (6%) of the 127

Table 2

Longitudinal T_1 patterns (rows) of the 200 identified hypointense lesions around USPIO injection, related to patterns of USPIO-enhancement (columns) of these lesions.

T_1 pattern	Pattern of USPIO-enhancement				
	Return to isointensity	Focal	Ringlike	No USPIO-enhancement	Total
Chronic	8	0	8	111	127
Acute and persistent	4	0	1	27	32
Transient	27	0	1	13	41
Total	39	0	10	151	200

chronic black holes showed a return to isointensity USPIO enhancement pattern. 4 (13%) of the 32 acute and persistent black holes showed a return to isointensity. In contrast, 27 (66%) of the 41 transiently T_1-hypointense lesions appeared isointense on post-USPIO images. 69% of all black holes appearing isointense on post-USPIO images, were transient. When hypointense lesions showed enhancement with both contrast agents, they were mainly transiently hypointense (Table 3), whereas non-enhancing black holes were mostly chronic.

Ring-like USPIO enhancement was mostly detected in lesions not developing into chronic black holes

Of all lesions showing ring-like USPIO enhancement (n=70), 31% was hypointense around the time of USPIO imaging, compared to 33% of the control-group (n=76) of USPIO-negative T_2 lesions. However, at long-term follow-up, 13% of the ring-enhancing lesions had evolved into chronic black holes, compared to 28% of the control lesions.

Table 3

Longitudinal T_1 patterns (rows) of the 200 identified hypointense lesions around USPIO injection, related to crosssectional USPIO- and Gd-DTPA enhancement status (columns) of these lesions.

T_1 pattern	USPIO/Gd-DTPA enhancement status				
	USPIO+/Gd-	USPIO+/Gd+	USPIO-/Gd+	USPIO-/Gd-	Total
Chronic	15	1	0	111	127
Acute and persistent	4	1	0	27	32
Transient	16	12	0	13	41
Total	35	14	0	151	200

USPIO enhancement remained visible for up to 3 months after injection

At 1 month follow-up, 85% of the originally USPIO+/Gd- lesions showed no enhancement with either contrast agent. 11% of the lesions were still USPIO+/Gd-, and 4% of the lesions had become Gd+ (Fig 3). Of the 15 USPIO-/Gd+ lesions, 3 (20%) were still Gd+ at 1 month follow-up, the remaining 80% showing no enhancement. For the 44 USPIO+/Gd+ lesions, 45% showed no enhancement with either contrast agent after 1 month, but 12% still enhanced with both agents. 29% enhanced with USPIO only, and 14% showed only Gd enhancement. After 2 months, 92% of the 188 originally USPIO+ and /or Gd+ lesions did not enhance anymore, and after 3 months, only 1.5% of these lesions still appeared USPIO+. In these cases, USPIO enhancement had completely resolved at the long-term follow-up scan performed 7-11 months after injection.

USPIO are taken up by monocytes in the bloodstream

Qualitative analysis of the Prussian blue staining on patient PBMC obtained 24h after USPIO injection revealed several iron-positive cells, providing evidence of cellular incorporation of USPIO in monocytes in the circulation (Fig 4). The monocyte fraction in patient PBMC 24h after USPIO injection showed no elevated levels of ROS, indicating that USPIO uptake does not activate monocytes (data not shown).

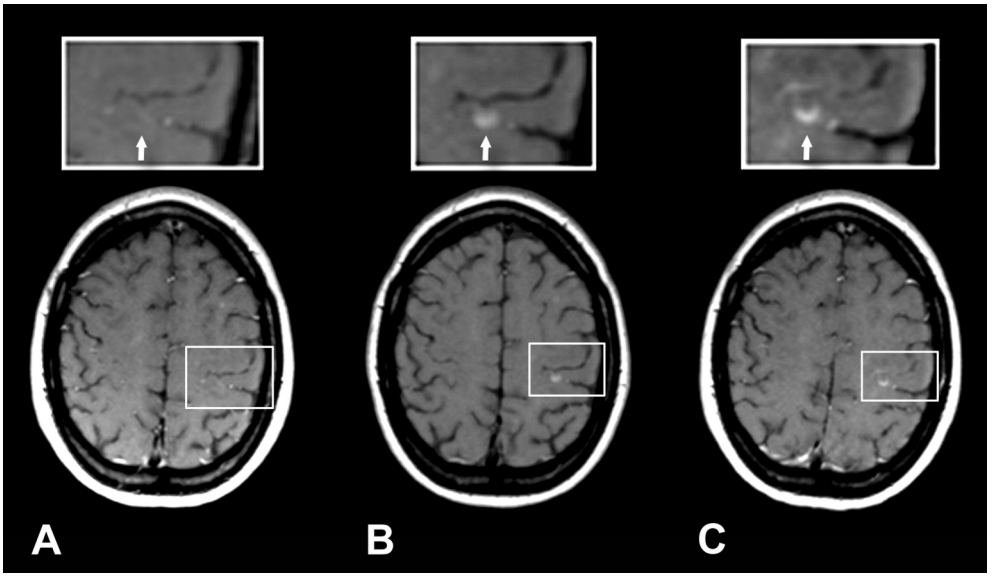

Figure 3: An USPIO+/Gd- lesion becoming Gd+ at 1 month follow-up. (A) Post-Gd image at time point around USPIO injection showing no lesion enhancement (a lesion was present on the T_2 SE image at that time point). (B) Post-USPIO image showing focal USPIO enhancement. (C) Post-Gd image 1 month after USPIO injection showing Gd enhancement. (data not shown: on the pre-Gd T_1W image at that time point, no focal enhancement was visible, meaning that this focal hyperintense enhancement is Gd enhancement, instead of remaining USPIO enhancement.)

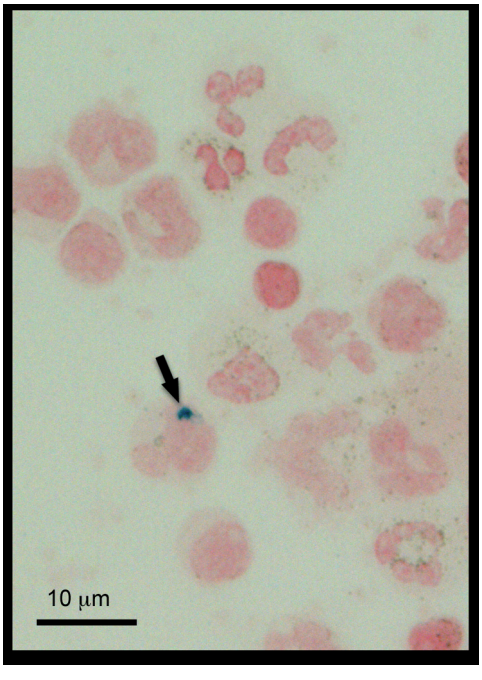

Figure 4: Microscopy image: Iron-positive cells (arrow) were detected in patient PBMC 24h after USPIO injection, though at low numbers.

USPIO enhancement depends on concentration and intracellular incorporation

Figure 5 shows T_1W and T_2*W signal intensities as a function of cell concentration in vials containing intra- and extracellular USPIO particles. For extracellular particles (Fig 5A), a strong increase in signal intensity on T_1W images was observed for phantoms containing low concentrations of cells. This effect on signal intensity was counterbalanced at higher concentrations, by a strong decay of T_2* due to the susceptibility effect at higher monocyte concentrations (corresponding with a higher amount of iron). T_1W signal intensity for intracellular USPIO (Fig 5B) showed an initial increase at low concentrations of labeled monocytes, which remained constant because of a lack of a strong T_2* effect.

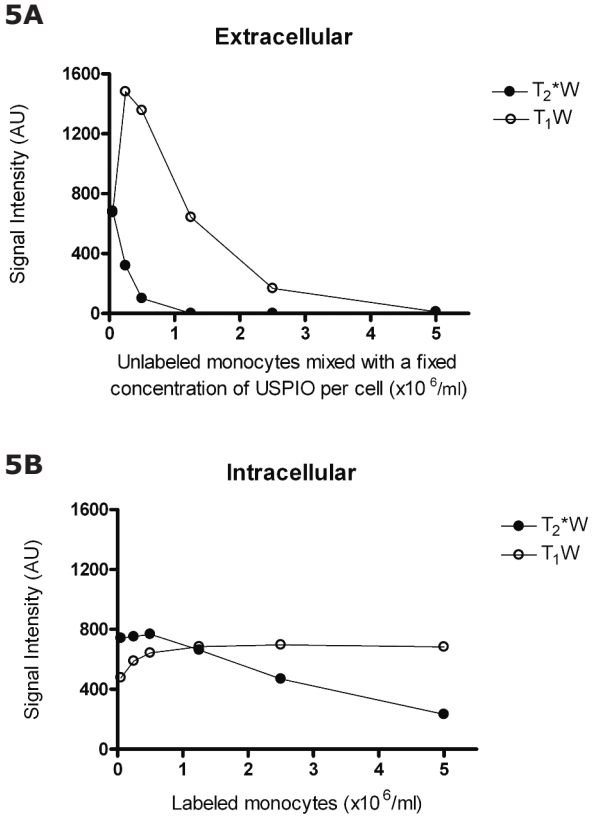

Figure 5: In vitro MRI shows distinct effects of USPIO concentration and compartmentalization on T_1W and T_2*W signal intensities. (A) Extracellular USPIO mixed with monocytes (25pg Fe per cell) result in a large effect on signal intensity both in T_1W and T_2*W images in a range of monocyte concentrations. (B) Intracellular USPIO (approximately 25pg per cell) showed an initial increase in T_1W signal intensity, whereas in low concentrations of labeled monocytes, no change was detected in T_2*W signal intensity.

DISCUSSION

This is the first study to describe SHU555C lesion enhancement in MS patients. USPIO enhancement occurred more than Gd-DTPA enhancement, remained visible for a longer period than Gd-DTPA enhancement and, in some cases, preceded Gd-DTPA enhancement. Lesions enhancing with both contrast agents at baseline were more prone to continue enhancing after one and two months, compared to lesions enhancing with only one of the two contrast agents. USPIO enhancement occurred in three patterns: focal enhancement (with or without Gd-DTPA enhancement), ring-like enhancement (around pre-existing T_2-hyperintense lesions) and return to isointensity of (mainly transient) T_1-hypointense lesions. Taken together, this indicates that USPIO enhancement provides relevant information over Gd-DTPA enhancement, and illustrates the pluriformity of inflammation in MS.

We have good reasons to assume that USPIO enhancement directly reflects entrance of monocytes into the CNS. Blood samples, collected 24h after USPIO administration, revealed incorporation of USPIO particles into PBMC in the bloodstream. In vitro MRI of intra- and extracellular USPIO samples demonstrated concentration- and compartment-dependent T_1W and T_2*W signal intensities. Low concentrations of labeled cells resulted in signal increase on T_1W images without signal decrease on T_2*W images. The ability of USPIO to visualize macrophage infiltration on MRI has been shown previously (Kooi et al*.,* 2003; Neuwelt et al*.,* 2004; Dousset et al*.,* 2006; Brochet et al*.,* 2006; Corot et al*.,* 2006; Jander et al*.,* 2007). The major challenge in validating USPIO enhanced MRI as a marker for cellular infiltration in MS lesions lies in excluding the possibility that USPIO may reach the brain parenchyma in ways not specifically related to monocyte infiltration. Leakage of non-incorporated USPIO over a damaged BBB might play a role. However, as in the current study 77% of USPIO+ lesions were found in areas with an intact BBB (as marked by absence of Gd enhancement), and 25% of the lesions showing BBB leakage were USPIO-, our data suggest that USPIO enhancement is subject to a different, probably cell-specific mechanism. On the other hand, Gd enhancement may not be fully sensitive to BBB damage. For example, it is known that sensitivity depends on dosage (Silver et al*.,* 2001), and subtle BBB changes that do not enhance with Gd may occur in normal-appearing white matter (Vos et al*.,* 2005).

Spatial and temporal discrepancies between BBB leakage as demonstrated by Gd enhancement, and cellular infiltration as demonstrated by USPIO enhancement have been reported previously in studies using ferumoxtran-10 (Sinerem®) (Manninger et al*.,* 2005; Dousset et al*.,* 2006). These discrepancies were smaller than in the current study, where SHU555C was

used. SHU555C differs from Sinerem in size, plasma half-life and ionic charge. In vitro, the smaller, negatively charged SHU555C particle was incorporated more efficiently by monocytes than Sinerem (Metz et al., 2004), but its shorter plasma half-life time may counteract this advantage in vivo. The differences between our results, and previous results using Sinerem may also be explained by patient characteristics. Comparative in vivo studies are needed to further explore the possible differences between SHU555C and Sinerem.

It is tempting to speculate about the three patterns of USPIO enhancement found in this study. When lesions were both USPIO+ and Gd+, enhancement usually occurred in a similar focal pattern; this may implicate the co-occurrence of active and passive BBB leakage. Return to isointensity of a previously hypointense lesion was not noticed before as a type of contrast enhancement. This 'change to isointensity' of black holes on post-USPIO images may selectively indicate the presence of USPIO in macrophages within these lesions. Interestingly, this pattern of enhancement was seen especially in temporarily hypointense T_1 lesions compared to chronic, persistent black holes. While the latter are associated with matrix destruction and axonal loss, the temporarily T_1-hypointense lesions may reflect remyelination (van Waesberghe et al., 1998; Rovira et al., 1999; Barkhof et al., 2003). If so, USPIO enhancement may be associated with a beneficial aspect of inflammation, possibly associated with repair mechanisms (Hohlfeld 2007). Of course this hypothesis has to be validated in future studies, but it may also explain our finding that T_2 lesions showing ring-like USPIO enhancement were less prone to evolving into chronic black holes compared to USPIO-negative T_2 lesions.

Considering all USPIO+ lesions longitudinally, we found that in 85% of these lesions, USPIO enhancement had resolved after 1 month (USPIO were injected only once), but some lesions (1.5 %) remained USPIO+ for up to 3 months. USPIO enhancement remained visible after Gd enhancement had resolved, and USPIO+/Gd+ lesions were more prone to keep enhancing after 1 month than lesions that enhanced with only one contrast agents. In a fraction (4%) of the USPIO+/Gd- lesions, USPIO enhancement preceded Gd enhancement by 1 month. Assuming that USPIO enhancement reflects macrophages in inflammatory lesions, these results suggest that cellular inflammation can both precede and persist longer than BBB leakage. The reverse question however, how often BBB breakdown precedes cellular infiltration, cannot be answered in this study. Due to study design, patients were screened for Gd-DTPA enhancement of lesions, followed by USPIO injection if Gd-DTPA enhancement was observed. Therefore, by definition, Gd+ lesions were never present 1 month prior to USPIO injection. Future studies are warranted to address the exact temporal relationship between BBB breakdown and cellular infiltration.

The lack of signal decrease on post-USPIO T_2*W images was interesting, as this is the most commonly described form of USPIO enhancement. In previous studies, both T_2*-hypointense and T_1-hyperintense enhancement were seen (Neuwelt et al., 2004; Manninger et al., 2005; Dousset et al., 2006). T_2* signal decrease is a susceptibility effect caused by clustering of USPIO particles, as demonstrated in EAE experiments (Dousset et al., 1999b; Floris et al., 2004). The lack of T_2* effects may be explained by results of our in vitro experiments, which demonstrated that T_1 hyperintensity without T_2* hypointensity is observed for low concentrations of labeled cells. This reflects the in vivo situation, as in the described patients USPIO enhancement occurred as hyperintense enhancement on T_1W images without T_2* signal changes (Fig 1). Concentration and cellular incorporation dependent effects have been described previously using other USPIO particles (Corot et al., 2006; Simon et al., 2006).

In conclusion, we have demonstrated that USPIO-enhanced brain MRI in MS shows patterns distinct from Gd enhancement. These patterns provide complementary insight into the underlying pathology and are therefore clinically relevant as potential MRI markers for disease severity and possibly treatment efficacy. Further investigation should elucidate how sensitivity and specificity of MRI in MS can be improved using USPIO.

REFERENCES

Barkhof F, Bruck W, De Groot CJ, Bergers E, Hulshof S, Geurts J et al. Remyelinated lesions in multiple sclerosis: magnetic resonance image appearance. Arch Neurol 2003; 60: 1073-1081.

Bendszus M, Bartsch A, Stoll G. Is the disruption of the blood-brain barrier a prerequisite for cellular infiltration in autoimmune encephalitis? Brain 2005; 128: E25.

Brochet B, Deloire MS, Touil T, Anne O, Caille JM, Dousset V et al. Early macrophage MRI of inflammatory lesions predicts lesion severity and disease development in relapsing EAE. Neuroimage 2006; 32: 266-274.

Corot C, Robert P, Idee JM, Port M. Recent advances in iron oxide nanocrystal technology for medical imaging. Adv Drug Deliv Rev 2006; 58: 1471-1504.

Dousset V, Ballarino L, Delalande C, Coussemacq M, Canioni P, Petry KG et al. Comparison of ultrasmall particles of iron oxide (USPIO)-enhanced T2-weighted, conventional T2-weighted, and gadolinium-enhanced T1-weighted MR images in rats with experimental autoimmune encephalomyelitis. AJNR Am J Neuroradiol 1999a; 20: 223-227.

Dousset V, Brochet B, Deloire MS, Lagoarde L, Barroso B, Caille JM et al. MR imaging of relapsing multiple sclerosis patients using ultra-small-particle iron oxide and compared with gadolinium. AJNR Am J Neuroradiol 2006; 27: 1000-1005.

Dousset V, Delalande C, Ballarino L, Quesson B, Seilhan D, Coussemacq M et al. In vivo macrophage activity imaging in the central nervous system detected by magnetic resonance. Magn Reson Med 1999b; 41: 329-333.

Floris S, Blezer EL, Schreibelt G, Dopp E, van der Pol SM, Schadee-Eestermans IL et al. Blood-brain barrier permeability and monocyte infiltration in experimental allergic encephalomyelitis: a quantitative MRI study. Brain 2004; 127: 616-627.

Grossman RI, Braffman BH, Brorson JR, Goldberg HI, Silberberg DH, Gonzalez-Scarano F. Multiple sclerosis: serial study of gadolinium-enhanced MR imaging. Radiology 1988; 169: 117-122.

Hohlfeld R. Does inflammation stimulate remyelination? J Neurol 2007; 254 Suppl 1: I47-I54.

Jander S, Schroeter M, Saleh A. Imaging inflammation in acute brain ischemia. Stroke 2007; 38: 642-645.

Kappos L, Moeri D, Radue EW, Schoetzau A, Schweikert K, Barkhof F et al. Predictive value of gadolinium-enhanced magnetic resonance imaging for relapse rate and changes in disability or impairment in multiple sclerosis: a meta-analysis. Gadolinium MRI Meta-analysis Group. Lancet 1999; 353: 964-969.

Kooi ME, Cappendijk VC, Cleutjens KB, Kessels AG, Kitslaar PJ, Borgers M et al. Accumulation of ultrasmall superparamagnetic particles of iron oxide in human atherosclerotic plaques can be detected by in vivo magnetic resonance imaging. Circulation 2003; 107: 2453-2458.

Kurtzke JF. Rating neurologic impairment in multiple sclerosis: an expanded disability status scale (EDSS). Neurology 1983; 33: 1444-1452.

Manninger SP, Muldoon LL, Nesbit G, Murillo T, Jacobs PM, Neuwelt EA. An exploratory study of ferumoxtran-10 nanoparticles as a blood-brain barrier imaging agent targeting phagocytic cells in CNS inflammatory lesions. AJNR Am J Neuroradiol 2005; 26: 2290-2300.

Metz S, Bonaterra G, Rudelius M, Settles M, Rummeny EJ, Daldrup-Link HE. Capacity of human monocytes to phagocytose approved iron oxide MR contrast agents in vitro. Eur Radiol 2004; 14: 1851-1858.

Neuwelt EA, Varallyay P, Bago AG, Muldoon LL, Nesbit G, Nixon R. Imaging of iron oxide nanoparticles by MR and light microscopy in patients with malignant brain tumours. Neuropathol Appl Neurobiol 2004; 30: 456-471.

Nighoghossian N, Wiart M, Cakmak S, Berthezene Y, Derex L, Cho TH et al. Inflammatory response after ischemic stroke: a USPIO-enhanced MRI study in patients. Stroke 2007; 38: 303-307.

Oude Engberink RD, van der Pol SM, Dopp EA, de Vries HE, Blezer EL. Comparison of SPIO and USPIO for in vitro labeling of human monocytes: MR detection and cell function. Radiology 2007; 243: 467-474.

Rausch M, Hiestand P, Baumann D, Cannet C, Rudin M. MRI-based monitoring of inflammation and tissue damage in acute and chronic relapsing EAE. Magn Reson Med 2003; 50: 309-314.

Rausch M, Hiestand P, Foster CA, Baumann DR, Cannet C, Rudin M. Predictability of FTY720 efficacy in experimental autoimmune encephalomyelitis by in vivo macrophage tracking: clinical implications for ultrasmall superparamagnetic iron oxide-enhanced magnetic resonance imaging. J Magn Reson Imaging 2004; 20: 16-24.

Rovira A, Alonso J, Cucurella G, Nos C, Tintore M, Pedraza S et al. Evolution of multiple sclerosis lesions on serial contrast-enhanced T1-weighted and magnetization-transfer MR images. AJNR Am J Neuroradiol 1999; 20: 1939-1945.

Saleh A, Schroeter M, Jonkmanns C, Hartung HP, Modder U, Jander S. In vivo MRI of brain inflammation in human ischaemic stroke. Brain 2004; 127: 1670-1677.

Schreibelt G, Musters RJ, Reijerkerk A, de Groot LR, van der Pol SM, Hendrikx EM et al. Lipoic acid affects cellular migration into the central nervous system and stabilizes blood-brain barrier integrity. J Immunol 2006; 177: 2630-2637.

Silver NC, Good CD, Sormani MP, MacManus DG, Thompson AJ, Filippi M et al. A modified protocol to improve the detection of enhancing brain and spinal cord lesions in multiple sclerosis. J Neurol 2001; 248: 215-224.

Simon GH, Bauer J, Saborovski O, Fu Y, Corot C, Wendland MF et al. T1 and T2 relaxivity of intracellular and extracellular USPIO at 1.5T and 3T clinical MR scanning. Eur Radiol 2006; 16: 738-745.

van Waesberghe JH, van Walderveen MA, Castelijns JA, Scheltens P, Nijeholt GJ, Polman CH et al. Patterns of lesion development in multiple sclerosis: longitudinal observations with T1-weighted spin-echo and magnetization transfer MR. AJNR Am J Neuroradiol 1998; 19: 675-683.

van Walderveen MA, Barkhof F, Hommes OR, Polman CH, Tobi H, Frequin ST et al. Correlating MRI and clinical disease activity in multiple sclerosis: relevance of hypointense lesions on short-TR/short-TE (T1-weighted) spin-echo images. Neurology 1995; 45: 1684-1690.

Vos CM, Geurts JJ, Montagne L, van Haastert ES, Bo L, van der Valk P et al. Blood-brain barrier alterations in both focal and diffuse abnormalities on postmortem MRI in multiple sclerosis. Neurobiol Dis 2005; 20: 953-960.

Xu S, Kay Jordan E, Brocke S, Bulte JW, Quigley L, Tresser N et al. Study of relapsing remitting experimental allergic encephalomyelitis SJL mouse model using MION-46L enhanced in vivo MRI: Early histopathological correlation. J Neurosci Res 1998; 52: 549-558.

ACKNOWLEDGEMENTS

The contrast agent was kindly provided free of charge by Bayer Schering Pharma, Berlin, Germany. This work was supported by the Dutch MS research Foundation, grant no. 02-358b

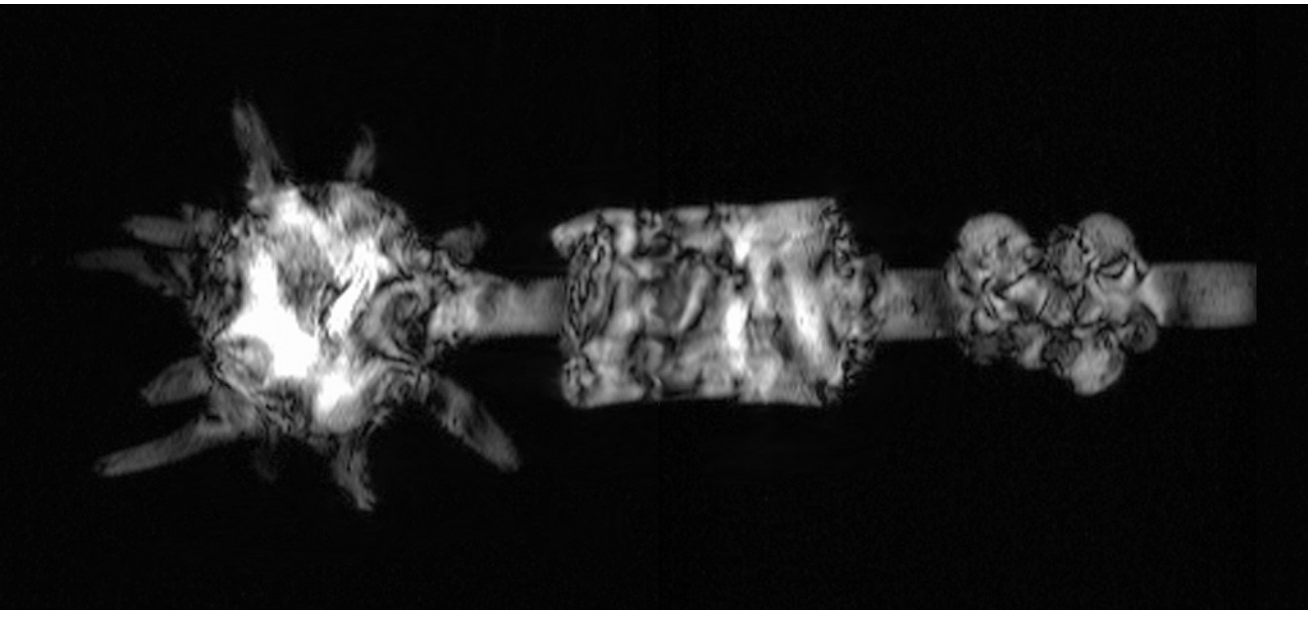

General Discussion

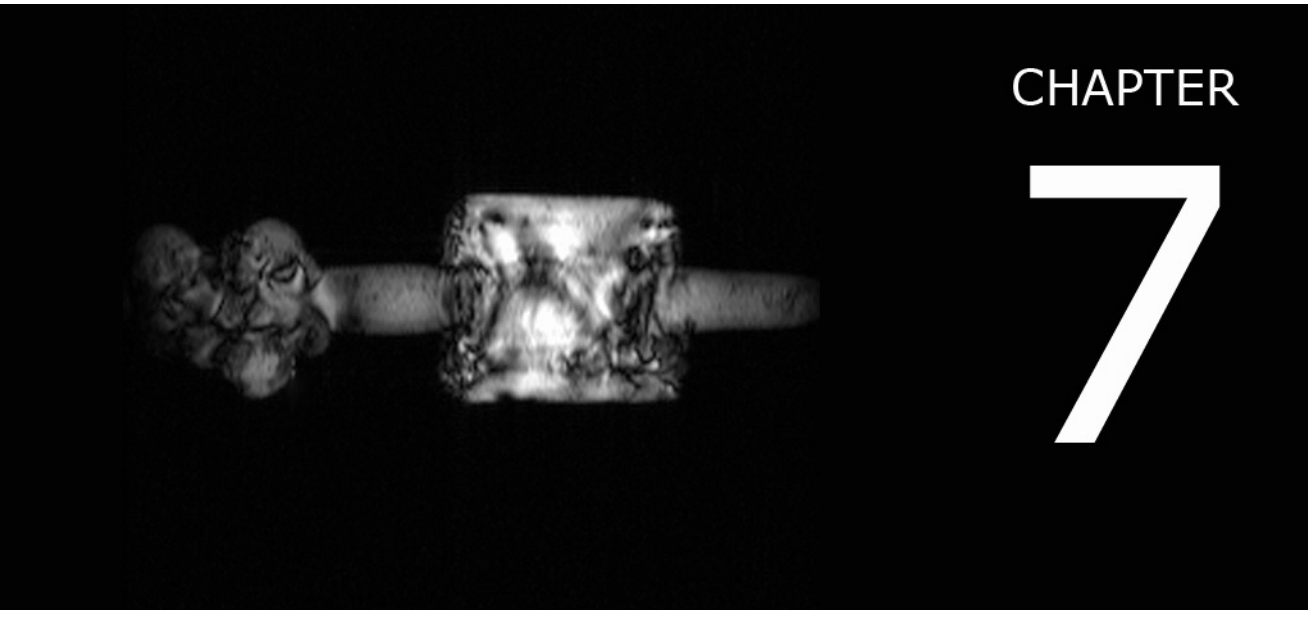

The research described in this thesis focused on the use of magnetic resonance imaging (MRI) as non-invasive imaging modality to visualize monocyte infiltration in the CNS during neuroinflammatory conditions. In central nervous system (CNS) pathologies, like multiple sclerosis (MS), the infiltration of monocytes into the brain is a critical step in the inflammatory process. Inside the brain, monocyte derived macrophages are involved in phagocytosis of myelin and induction of cell damage resulting in the formation of new lesions in MS. The main goal of this research project was to visualize the migration of monocytes non-invasively in experimental autoimmune encephalomyelitis (EAE), the animal model of MS, using MRI. This thesis describes the design of cellular imaging experiments that are composed of several steps. First of all, an efficient cell labeling strategy has to be developed and optimized with respect to cell type and choice of MR contrast agent. Key factors that determine successful application of cellular MRI are the MR detection limit and preservation of cell function. Secondly, proof of principle has to be established concerning MR visualization of labeled cells in vivo. Subsequently, labeled cells can be applied in a disease model of interest to investigate their migration longitudinally. In the following sections, our results on monocyte imaging will be discussed for each step, concluded by a future view on clinical implementation.

1 Cell labeling strategies

1.1 Choice of contrast agents

To enhance the contrast in MR images, two distinct groups of contrast agents are commonly used. The paramagnetic agents, like Gadolinium (Gd), shorten the T_1 relaxation time of tissue and will appear as bright contrast in T_1-weighted (T_1W) images. Conversely, the superparamagnetic agents, like iron oxide particles shorten the $T_2^{(*)}$ relaxation time of tissue resulting in regions of low signal intensity on $T_2^{(*)}$W images. Special MR contrast agents were developed containing iron oxides, classified as superparamagnetic particles of iron oxide (SPIO). SPIO were introduced as MR contrast agents shortly after the use of gadolinium compounds (Mendonca Dias and Lauterbur, 1986; Renshaw et al., 1986), and appeared to have ideal physical properties for cell labeling studies. They are (1) composed of biodegradable iron, (2) give rise to a substantial change in signal intensity (compared to Gd), (3) can easily be detected by light microscopy and (4) their dextran surface coating provides the opportunity for chemical synthesis of functional groups and ligands (Bulte and Kraitchman, 2004; Corot et al., 2006).

Given the favorable properties of iron oxide particles, we initially designed

a labeling strategy for human monocytes to optimize the labeling protocol with respect to cell function and MR detection (chapter 2). We used commercially available iron oxide particles with two different sizes: ferumoxide (trade name Endorem®) with a mean diameter of 150nm classified as SPIO and fermoxtran (trade name Sinerem®) classified as ultra small SPIO (USPIO) with a mean diameter of 30nm. Freshly isolated monocytes were incubated with different (U)SPIO concentrations in the medium for several hours. Results demonstrated that monocytes are labeled more efficiently using SPIO compared to USPIO. Previously, it was shown by competition/inhibition experiments that the mechanism of SPIO uptake by monocytes involves scavenger receptor SR-A-mediated endocytosis (Raynal et al., 2004). The larger diameter of SPIO particles as compared to USPIO may trigger this pathway and explains the preferred incorporation by monocytes. In this view, the recently developed micron-sized particles of iron oxide (MPIO, diameter of 1□m) may be of interest in monocyte labeling studies. Earlier, it was reported that these particles are taken up by several cell types and their high T_2 relaxivity (that is a larger change in MR signal intensity as a result of the large iron oxide core) further improves detection by MRI (Hinds et al., 2003; Shapiro et al., 2004). However, in addition to efficient incorporation of contrast agents, the effect of high amounts of intracellular iron has to be considered.

1.2 Effect of iron oxide particles on cell function

An important aspect in developing an efficient cell labeling strategy is maintaining the physiological status of the cell. With respect to monocyte imaging studies, the migratory capacity of monocytes is an important determinant for their function in vivo, especially during neuroinflammatory conditions (Lassmann, 1997).

Therefore, with a view to future in vivo tracking experiments, we investigated monocyte viability, the migratory capacity over brain endothelial cells and interleukin (IL)-1 and IL-6 production after the labeling procedure. The cytokines IL-1 and IL-6 were studied because their upregulation reflects monocyte activation (Gordon, 2003). In chapter 2, using the established SPIO concentration (1mg Fe/ml), we showed that the labeling procedure and the amount of intracellular iron had no effect on monocyte migration and cytokine production. Importantly, these findings suggest that SPIO-labeled monocytes could still migrate towards inflammatory sites, when applied in an in vivo situation. Other studies in different cell types similarly showed that SPIO labeling does not affect long-term viability, growth rate, and apoptotic indexes (Arbab et al., 2003a; Arbab et al., 2003b). However, it was also shown that iron oxide particle labeling can cause a transient increase in oxidative conditions in a rat macrophage cell line (Stroh et al., 2004). No long-term cytotoxic effects were observed.

Together with our data, it is shown that labeling monocytes with SPIO is efficient and safe.

1.3 Transfer of labeling protocol from human to rat monocytes

So far, the optimal SPIO concentration to label human monocytes was established and validated by in vitro MRI. To explore monocyte imaging in vivo, we adapted the protocol of human monocytes to label freshly isolated rat monocytes in chapter 3. Interestingly, labeling efficiency for rat monocytes was less than achieved for human monocytes using the same protocol (Fig 1). This may be explained by the smaller size of rat cells compared to human cells: a decreased volume of the cytoplasm implies that less contrast agent can be incorporated. Alternatively, the monocyte isolation procedure may influence SPIO uptake. Human monocytes were isolated and purified by positive selection using immunomagnetic beads, whereas rat monocytes were collected via a negative selection procedure. It can be argued that the positive selection procedure initiates a slightly activated state of the monocyte that drives the internalization of SPIO.

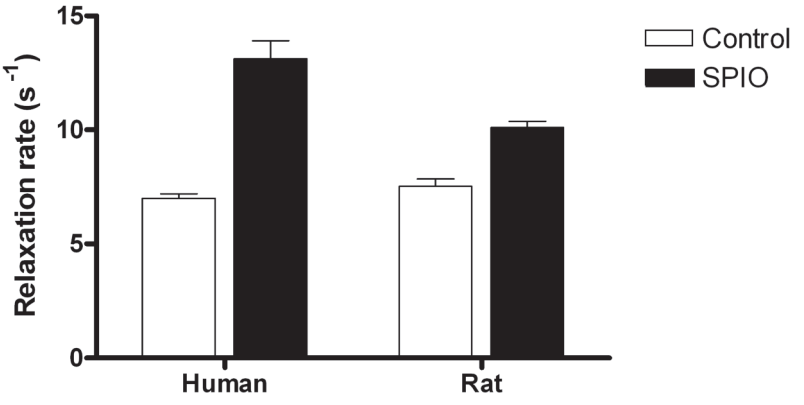

Figure 1: Comparison of T_2 relaxation rates for human versus rat monocytes. Monocytes were incubated in the presence of SPIO (1mg Fe/ml) for 1.5h and processed for in vitro MRI. Imaging was performed on agar-gel samples (n=3) containing 0.5 x10^6 monocytes.

To increase the labeling efficiency of rat monocytes, we increased the SPIO concentration in the medium. As a result, the T_2 relaxation rate of labeled rat monocyte was similar to the optimal results obtained for human monocytes. Identically, for this SPIO concentration we confirmed preservation of cell viability and migratory capacity. Alternatively, addition of transfection agents (TA) to the incubation medium is a method to increase labeling efficiency. TAs, like FuGene, Poly-L-Lysine and Superfect, can coat the surface of SPIO and by their lipophilic and/or charged nature facilitate cel-

lular incorporation. Previous studies have shown that low concentrations of SPIO complexed to TA enhanced labeling efficiency, even in case of non-phagocytic cell types (Arbab et al., 2003a; Arbab et al., 2004; Bulte et al., 2004). Although a lower concentration of contrast agents is a preferred condition, the long incubation period (24h – 48h) that is usually required by the use of TAs, is not beneficial. Moreover, we demonstrated in chapter 2 that labeling efficiency was not increased for human monocytes, using different TAs in combination with SPIO and an incubation time of 1.5h.

In summary, we have developed an efficient labeling procedure for monocytes and demonstrated SPIO internalization without affecting important biological parameters like cell viability, cytokine production and migratory capacity.

2 In vivo visualization of SPIO-labeled monocytes

2.1 Tracking ex vivo labeled monocytes

Initially in chapter 3, we explored the visualization of labeled monocytes in vivo with MRI using an intracerebral injection of SPIO-labeled monocytes in healthy rats. Imaging was performed directly after injection of $2x10^6$ labeled monocytes and resulted in a hypointense area in the brain parenchyma that diminished with time, but was still detected after 5 days. Important questions arise from these results: (1) how long does the label remain inside the cell and (2) do hypointense areas in MR images reflect the originally labeled cells? It cannot be excluded that monocytes die at the site of injection and deposit their SPIO that are then slowly degraded or taken up by other phagocytic cells, like microglia. Previously, it was shown that areas of signal loss are detected up to 14 days after an intracerebral injection of labeled monocytes in immunodeficient mice (Zelivyanskaya et al., 2003). Also, it was reported for non-dividing human mesenchymal stem cells in vitro, that SPIO could still be detected intracellularly after 7 weeks (Arbab et al., 2003b). Altogether, these findings indicate that SPIO labeling of monocytes is a suitable approach to perform in vivo monocyte imaging in a longitudinal fashion.

Secondly in chapter 3, to validate MR tracking of SPIO-labeled monocytes in vivo, we performed our first cell transfusion experiments in rats with a cortical lesion, induced by photothrombosis (Watson et al., 1985). In this animal model of neuroinflammation, focal illumination of the brain after intravenous injection of a photosensitive dye induces a well-defined inflammatory infarct (Hoff et al., 2005). This model was chosen for its

reproducible lesion size and predictable timing of cellular events, that is predominantly characterized by the infiltration of monocytes in the lesion, 3 to 10 days after induction (Lee et al., 1996). In our experiments, labeled monocytes were injected at day 5 after lesion induction. Areas of low signal intensity were detected in the lesion not earlier than 72h after injection of labeled monocytes. Histological analysis revealed the presence of intracellular iron clusters in ED1+ (marker for infiltrated monocytes) regions. We thus demonstrated the migration of intravenously injected, ex vivo labeled monocytes into areas of neuroinflammation, visualized longitudinally and non-invasively. Earlier, in a different study, spleen-derived-mononuclear cells labeled with iron oxide particles were injected intravenously in splenectomised mice after middle cerebral artery occlusion (Stroh et al., 2006). In agreement with our results, labeled cells were detected in the lesion within 2 to 4 days after injection. It has only been recently recognized that neuroinflammation and especially the recruitment of monocytes may cause secondary damage in ischaemic stroke and contribute to lesion development, days after the initial infarct (Dirnagl et al., 1999; Price et al., 2003). To investigate this process in detail, the use of ex vivo labeled monocytes may be an interesting tool.

2.2 Ex vivo or in vivo labeling?

As opposed to imaging of ex vivo labeled monocytes, an alternative approach for monocyte imaging is the injection of free iron oxide particles in circulation. It is generally assumed that circulating monocytes incorporate the iron oxide particles and subsequently migrate into inflammatory tissue. This is classified as the 'in vivo labeling' technique. SPIO have a relative large diameter and are rapidly taken up by liver Kupffer cells. This results in a blood half-life of approximately 6 minutes in rats (Saini et al., 1987; Weissleder et al., 1989). Subsequently, USPIO particles were developed with a smaller diameter (Weissleder et al., 1990). Less readily recognized by the mononuclear phagocytic system, their blood half-life is prolonged which makes them suitable for in vivo labeling of monocytes/macrophages at other locations. This approach has been studied in animal models of ischemia, i.e. photothrombosis and middle cerebral artery occlusion model (Kleinschnitz et al., 2003; Rausch et al., 2002; Rausch et al., 2001; Saleh et al., 2004). In these studies, USPIO accumulation was observed in damaged brain areas and co-localized with the distribution of ED1+ cells. Clearly, the presence of USPIO is a marker for macrophage activity. However, knowledge on USPIO uptake in the CNS is limited and USPIO may enter the CNS passively by leakage over an impaired blood-brain barrier (BBB) or by transcytosis across the brain endothelial cells (Xu et al., 1998). Moreover, it has also been suggested that USPIO incorporation may occur outside the vasculature by activated microglia (Dousset et al., 1999b).

To specifically address this issue, we directly compared imaging patterns after injection of free as opposed to intracellular iron oxide particles in the photothrombotic rat model. In chapter 3, we showed that transfused SPIO-labeled monocytes were visualized in the lesion not earlier than after 72h whereas injected USPIO resulted in a strong signal decrease in the lesion as soon as 2h after injection. Within this short time period, it is unlikely that circulating monocytes incorporate USPIO, as we have shown in chapter 2 that labeling efficiency using USPIO is very low. With respect to USPIO injections, this suggests that other mechanisms such as BBB leakage and possibly endothelial trapping are important determinants for the observed change in signal intensity 24h later. Further implications and novel insights of the 'in vivo labeling' approach are discussed in the next sections in the context of EAE.

In summary, we have successfully delivered proof of principle that ex vivo labeled monocytes can be detected by MRI, migrating into inflammatory sites after being administered intravenously. It emphasizes the fact that SPIO-labeled monocytes are a powerful tool to specifically address the time window of monocyte infiltration.

3 Imaging monocyte infiltration in experimental autoimmune encephalomyelitis

3.1 Transfusion of ex vivo labeled monocytes in EAE: The limitations

The major goal in this research project was the non-invasive visualization of monocyte recruitment in EAE animals. Initial experiments were performed using procedures and protocols described in chapters 2 and 3. However, upon injection of SPIO-labeled monocytes in the tail vein (5 to 10 million cells per animal), no hypointense areas were detected in the CNS of EAE rats. Labeled monocytes were injected at onset and at peak of the disease and animals were scanned up to 5 days after injection. General limitations exist that apply to all cell transfusion experiments: (1) the biodistribution of labeled cells in vivo is a major factor that decreases the chance that labeled cells reach the target organ. After intravenous administration, cells will accumulate in liver, spleen and lungs as has been previously reported in a study using dendritic cells labeled with fluorine compounds (Ahrens et al., 2005). No data exist on the number of blood-derived monocytes that will infiltrate the CNS of EAE animals. However, in other studies, the cerebral concentrations of T-cells labeled with radio active ^{111}Indium were measured in EAE animals following intravenous administration (Hickey, 1999; Yeager et al., 2000). It was reported that

about 0.03% (total of lumbar cord, cervical cord and cerebrum) of the injected T-cells reached the CNS in EAE rats. Likewise, from these data, it can be argued that a small percentage of our SPIO-labeled monocytes will infiltrate the CNS. (2) Another consideration reflects the fact that the SPIO-labeled monocytes have to compete with the population of endogeneous monocytes that may be better targeted towards the CNS. This may decrease the opportunity for labeled cells to enter inflammatory sites.
On the other hand, despite these considerations, we achieved visualization of CNS infiltration in the photothrombotic infarct model as shown in chapter 3. Compared to the relatively large (1-2cm in diameter) focal lesion induced in this model, the EAE model is characterized by multiple small lesions (in the order of microns) throughout brain and spinal cord. Likely, MR detection is hampered by the relative small size of the lesions and, consequently, an accumulation of a low number of labeled monocytes. Therefore, the iron load per cell may not be sufficient to detect a few labeled monocytes present in EAE lesions. So far, no study has described the successful detection of monocyte recruitment in EAE using ex vivo labeled monocytes with iron oxide particles. There is a pressing need to develop a labeling strategy that brings single cell detection by MRI within reach.

3.2 Magneto-electroporation

Imaging of monocyte infiltration in CNS pathologies with multiple small lesions, as in case of MS, is still a major challenge. To further enhance MR detection for individual monocytes that infiltrate the CNS, a high load of contrast agent per cell is crucial. The use of a novel labeling technique, magneto-electroporation (MEP) that labels cells within a few milliseconds (Walczak et al., 2005b) may be a promising method for labeling and tracking monocytes by MRI in the EAE model. Earlier, this technique was used to transfect cells and shuttle DNA products and chemotherapeutic drugs across the cell membrane (Neumann et al., 1982). Not until recently this method has been recognized as a fast and effective method to label cells with iron oxide particles (Walczak et al., 2005a). In contrast to cell labeling by incubation, electroporation is a voltage based method causing a temporarily loss of cell membrane integrity, which drives the uptake of contrast agents present in the medium.
In chapter 4, important electroporation parameters, like voltage, pulse length and number of pulses were optimized to label rat monocytes with respect to the amount of internalized iron and cell function. MEP was found to increase the intracellular iron concentration compared to conventional incubation procedures. Labeling efficiency was dependent on the choice of iron oxide particle. Iron staining and quantification revealed that Supravist was the preferred USPIO for cellular incorporation. Supravist is

a charged nano-particle and previous reports have also shown an increased uptake compared to non-charged particles (Metz et al., 2004). Likely, the ionic surface properties attract the nano-particles to the cell surface that are then easily internalized upon the temporarily loss of membrane integrity by an electrical current. This may also explain the different labeling efficiencies using Sinerem, a similar-sized non-ionic iron oxide particle that was not internalized.
A major concern that has to be addressed is the effect of the electroporation procedure on cell viability and other functions. Previously, it was shown for stem cells that MEP was not toxic for the cells and no adverse effects on proliferation were reported (Walczak et al., 2005b). We showed that with our optimized MEP protocol for labeling monocytes, cell viability and metabolic activity was not altered. However, long-term effects have not yet been determined.
Ultimately in chapter 4, we tested if monocytes labeled with Supravist by MEP could be tracked in EAE animals with MRI. Therefore, we injected labeled monocytes at different stages of the disease to reveal the temporal pattern of monocyte infiltration. Results demonstrated that electroporation of monocytes significantly improved their visualization as focal hypointensities in the CNS were detected 24h and 72h after injection. Moreover, quantification of these contrast effects revealed an important difference between disease onset and peak: monocyte migration into the CNS was increased at disease peak, confirming results obtained with histological analyses (Floris et al., 2004). No data exist on the use of MEP for monocyte labeling and tracking in vivo. We have identified this novel technique as a powerful labeling strategy to monitor the process of monocyte migration in CNS pathologies. Since this technique is ultra-fast and allows the use of clinically approved contrast agents, it may be suitable for clinical trials in the near future.

3.3 USPIO injection in EAE: considerations and novel insights

The alternative approach, 'in vivo labeling' by an injection of free iron oxide particles has been extensively studied in EAE rats (Dousset et al., 1999a; Dousset et al., 1999b; Rausch et al., 2003). We previously showed that maximal Gd-DTPA enhancement (reflecting BBB damage) precedes the maximal USPIO load in the CNS of EAE rats (Floris et al., 2004). USPIO were detected by histology and co-localized with ED1+ cells, demonstrating that USPIO can be used as a marker for cellular infiltrates in EAE. Generally in these studies, imaging was always performed 18 -24h after USPIO injection.
Whereas Gd-DTPA is a small molecule and has a relatively short tissue half-life (minutes), little is known about USPIO kinetics and the mechanisms responsible for their presence in the brain parenchyma. Since the

BBB is compromised during the course of EAE, intravenously injected USPIO may have various ways of entering the CNS, as discussed previously for the photothrombotic model. Therefore, we investigated in chapter 5 the USPIO dynamics in more detail and imaged EAE rats directly upon USPIO administration repetitively up to 6h and again 24h and 72h later. Our findings were two-fold and each will have major implications for future application of USPIO: (1) Upon USPIO injection, hypointense areas were detected in the cerebellum within 1h and histological analysis after 6h revealed the presence of extracellular iron clusters in the brain parenchyma. These results suggest that BBB leakage is the most important physiological mechanism responsible for USPIO entry. It is important to consider this mechanism when interpreting post-USPIO MR images in EAE and possibly also in MS patients as it contributes to the contrast effects frequently reported after 24h. (2) Surprisingly, hypointensities in the EAE brain were no longer apparent at later time points (72h). In chapter 3, we showed that iron oxide (loaded cells) implanted in the rat brain remain detectable for at least 5 days. Clearly, other processes may play a role in the loss of USPIO detection in the inflammatory brain.

To explore a possible efflux mechanism, in chapter 5 we imaged the cervical lymph nodes (CLN) of EAE rats at similar time points and demonstrated USPIO accumulation at 72h. This indicates that USPIO in the brain parenchyma of EAE rats are partly drained by the CLN. Interestingly, in EAE it is suggested that the CLN play a pivotal role as a site for presentation of myelin components and the priming of T-cells (de Vos et al., 2002; Phillips et al., 1997). USPIO accumulation in CLN was predominantly found in the medulla, co-localizing with ED1+ cells and in a sharp rim lining the cortex, suggesting internalization by macrophages of the subcapsular sinuses. Specifically these macrophages have recently been shown to capture lymph-borne viruses and translocate viral particles for presentation to follicular B-cells (Junt et al., 2007). Over the years of extensive research to potential causal factors of MS, several infectious agents have been proposed. Recent advances in this area have associated the Epstein-Barr virus infection to the incidence of MS (Serafini et al., 2007). It is compelling to speculate that a novel application for USPIO is to non-invasively study antigen translocation in the pathology of MS.

Summarizing our achievements concerning in vivo imaging of monocyte recruitment in the animal model of MS, we have shown that conventional cell labeling techniques are not effective enough for MR visualization purposes in EAE. To effectively monitor monocyte infiltration in the CNS of EAE rats, MEP is a crucial labeling strategy. Additionally, we discussed novel insights on the use of free USPIO injections. Since several of these

particles have been FDA approved, clinical applications in CNS disorders are emerging.

4 Iron oxide particles in the clinic

4.1 USPIO imaging in multiple sclerosis patients

The non-toxic and biodegradable properties of USPIO have facilitated the application in clinical trials. Earlier, as discussed before, we and others have shown the presence of USPIO in EAE lesions (Floris et al., 2004; Xu et al., 1998) providing the evidence that USPIO-enhanced MRI can detect ongoing inflammation in vivo. Therefore, USPIO injections may be clinically relevant as potential MRI marker not only for detection of inflammation but also for prediction and follow-up of treatment efficacy in MS patients.

To explore the relevance of USPIO in MS pathology, in chapter 6 we administered the iron oxide particle Supravist to 19 relapsing-remitting MS patients and imaging was performed 24h later. Our main findings were: (1) Different patterns of USPIO enhancement were observed (2) the amount of USPIO-positive lesions outnumbered the Gd-DTPA enhanced lesions and (3) enhancement patterns were exclusively detected as bright contrast on T_1W images and no signal decrease was observed in T_2W images. This latter finding is intriguing for it is known that USPIO have a stronger effect on the T_2 relaxation time of the surrounding tissue, resulting in areas of decreased signal intensity on T_2W images (Weissleder et al., 1990). USPIO compartmentalization may offer an explanation that has been described earlier to change the T_1 and T_2-proton relaxivity (Simon et al., 2006). Therefore, we investigated the effects of intracellular versus extracellular USPIO in agar-gel phantoms using similar human MR protocols. Results demonstrated that low concentrations of labeled monocytes caused an increase in signal intensity on T_1W images without decreasing the signal intensity on T_2W images. Judged by our in vitro results, the patterns of bright contrast observed in MS brains may reflect the presence of small amounts of phagocytic cells that have incorporated USPIO.

Previous studies, that evaluated USPIO injections in MS patients, reported on both hypointense areas on T_2W images as hyperintensities on T_1W images (Dousset et al., 2006; Manninger et al., 2005). There, patients were administered ferumoxtran-10 (Sinerem) to reveal the presence of phagocytic cells in the CNS. Compared to these studies, our study design had two major advantages: (1) Patients were screened monthly by Gd-DTPA enhanced MRI and only if a newly Gd-DTPA enhancing lesion was detected, USPIO were administered. This ensured data collection predominantly during ongoing inflammation. (2) We were the first to apply the novel USPIO particle Supravist in MS patients. As discussed earlier, the charged sur-

face properties will facilitate incorporation by monocytes. Previously, a higher uptake of Supravist by activated monocytes has been reported in vitro (Metz et al., 2004). Based upon these results it can be argued that Supravist is the preferred USPIO to study macrophage activity in CNS pathologies. Importantly, it has become evident that USPIO-enhanced MRI provides additional insights in the underlying pathology of MS and will contribute to the development of therapeutic strategies in the near future.

4.2 Cellular MRI: Tracking the future

Non-invasive imaging of immune cells using iron oxide particles in vivo is a potent technique to study neuropathology in MS patients and to test promising therapeutics. An urgent need in the development of therapies, that limit cell infiltration in MS, is to proof the migration of transplanted immune cells towards inflammatory sites in the CNS. This is especially important when administering cells intravenously, awaiting several passages in blood circulation. In this thesis, we have shown proof of concept for tracking ex vivo labeled monocytes in the animal model for MS. However, application of ex vivo labeled cells in a clinical setting warrants further research concerning long-term effects of intracellular iron oxide particles and labeling strategies on cell viability and proliferation. We suggest that MEP is an interesting technique to apply in the clinic since it is performed ultrafast just prior to transfusion and works with clinically approved iron oxide particles. Importantly, our data suggest that a small number of migrating monocytes can be visualized which is critical in CNS pathologies with multiple small lesions, as in case of MS. Recently, SPIO-labeled dendritic cells have been injected intranodally in melanoma patients and were successfully tracked by MRI (de Vries et al., 2005). Non-invasive imaging of the migration of dendritic cells is of major importance in the development of cancer vaccines. The results suggest that cell labeling using iron oxide particles is clinically safe and is a promising technique to monitor cell-based therapies in humans.

In addition to cell labeling and tracking purposes, the iron oxide particles may also be of great interest for imaging the presence of important molecules in vivo(Bulte and Kraitchman, 2004). Molecular imaging has been driven by the ability to attach a specific label to the surface coatings of nano-particles. Iron oxide particles conjugated to antibodies may provide the opportunity to visualize upregulation of molecules, like VCAM-1 and ICAM that are key mediators in monocyte recruitment in the CNS (Dosquet et al., 1992; Gonzalez-Amaro and Sanchez-Madrid, 2002). Recently, this concept was reported in a mice model for acute brain inflammation using micron-sized particles of iron oxide targeted for VCAM (McAteer et al., 2007). This approach may be promising in the future to complement cel-

lular tracking studies and provide information on molecular pathology in an early disease stage of MS.

Iron oxide particles possess a variety of beneficial properties that facilitate clinical implementation. However, one of the major limitations is the negative contrast they provide in the MR image, resulting in 'black holes'(Bulte and Kraitchman, 2004). It limits accurate interpretation of the underlying anatomical structure and more importantly it can be easily mistaken with susceptibility artifacts like air-tissue transitions or hemorrhagic transformations. Since the MR contrast of iron oxide particles is provided by the indirect effect upon surrounding protons, cellular and molecular MRI would benefit from contrast agents that can be imaged directly. The development of fluorine compounds has provided this opportunity. Previously, this approach was demonstrated for tracking dendritic cells labeled by perfluoropolyether in mice (Ahrens et al., 2005). Although clinical grade fluorine compounds are already available, the high amount of contrast agent that is essential for a significant MR signal limits immediate application. With the recent emergence of high field clinical scanners this issue might be overcome and fluorine compounds may be a valuable immune cell-tracking agent in the near future.

5 Conclusion

Altogether, in this thesis we showed that monocytes can be labeled efficiently with iron oxide particles without compromising physiological function. Optimizing the labeling strategy with respect to intracellular iron and cell function is a key factor for the success of cellular MRI. We demonstrated that labeled monocytes can be tracked by MRI, migrating towards areas of ongoing inflammation. Specifically in the case of EAE, we showed that MEP is an essential labeling strategy that allows the visualization of monocyte migration towards multiple small CNS lesions. Application of labeled monocytes elucidates the spatio-temporal pattern of monocyte migration and will be a valuable tool to timely administer and monitor the effectiveness of therapies that target monocyte infiltration in the CNS.
Furthermore, important aspects of free USPIO injections during neuroinflammation have been discovered which may contribute to the interpretation of post-USPIO images. In EAE, we showed that USPIO are capable of penetrating the brain parenchyma within a short time period acting as a marker for BBB breakdown. At later time points, USPIO presence was no longer detected in the brain whereas accumulation in the CLN was observed. This suggests a unique possibility for USPIO-enhanced MRI to study brain drainage pathways. Moreover, in MS patients USPIO-enhanced

MRI was able to detect more lesions compared to the conventional Gd-DTPA. Results underline the strength of USPIO-enhanced MRI to study the pluriformity of CNS inflammation in MS patients.

References

Ahrens ET, Flores R, Xu H, Morel PA. In vivo imaging platform for tracking immunotherapeutic cells. Nat Biotechnol 2005; 23: 983-7.

Arbab AS, Bashaw LA, Miller BR, Jordan EK, Bulte JW, Frank JA. Intracytoplasmic tagging of cells with ferumoxides and transfection agent for cellular magnetic resonance imaging after cell transplantation: methods and techniques. Transplantation 2003a; 76: 1123-30.

Arbab AS, Bashaw LA, Miller BR, Jordan EK, Lewis BK, Kalish H, et al. Characterization of biophysical and metabolic properties of cells labeled with superparamagnetic iron oxide nanoparticles and transfection agent for cellular MR imaging. Radiology 2003b; 229: 838-46.

Arbab AS, Yocum GT, Kalish H, Jordan EK, Anderson SA, Khakoo AY, et al. Efficient magnetic cell labeling with protamine sulfate complexed to ferumoxides for cellular MRI. Blood 2004; 104: 1217-23.

Bulte JW, Arbab AS, Douglas T, Frank JA. Preparation of magnetically labeled cells for cell tracking by magnetic resonance imaging. Methods Enzymol 2004; 386: 275-99.

Bulte JW, Kraitchman DL. Iron oxide MR contrast agents for molecular and cellular imaging. NMR Biomed 2004; 17: 484-99.

Corot C, Robert P, Idee JM, Port M. Recent advances in iron oxide nanocrystal technology for medical imaging. Adv Drug Deliv Rev 2006; 58: 1471-504.

de Vos AF, van Meurs M, Brok HP, Boven LA, Hintzen RQ, van der Valk P, et al. Transfer of central nervous system autoantigens and presentation in secondary lymphoid organs. J Immunol 2002; 169: 5415-23.

de Vries IJ, Lesterhuis WJ, Barentsz JO, Verdijk P, van Krieken JH, Boerman OC, et al. Magnetic resonance tracking of dendritic cells in melanoma patients for monitoring of cellular therapy. Nat Biotechnol 2005; 23: 1407-13.

Dirnagl U, Iadecola C, Moskowitz MA. Pathobiology of ischaemic stroke: an integrated view. Trends Neurosci 1999; 22: 391-7.

Dosquet C, Weill D, Wautier JL. Molecular mechanism of blood monocyte adhesion to vascular endothelial cells. Nouv Rev Fr Hematol 1992; 34 Suppl: S55-9.

Dousset V, Ballarino L, Delalande C, Coussemacq M, Canioni P, Petry KG, et al. Comparison of ultrasmall particles of iron oxide (USPIO)-enhanced T2-weighted, conventional T2-weighted, and gadolinium-enhanced T1-weighted MR images in rats with experimental autoimmune encephalomyelitis. AJNR Am J Neuroradiol 1999a; 20: 223-7.

Dousset V, Brochet B, Deloire MS, Lagoarde L, Barroso B, Caille JM, et al. MR imaging of relapsing multiple sclerosis patients using ultra-small-particle iron oxide and compared with gadolinium. AJNR Am J Neuroradiol 2006; 27: 1000-5.

Dousset V, Delalande C, Ballarino L, Quesson B, Seilhan D, Coussemacq M, et al. In vivo macrophage activity imaging in the central nervous system detected by magnetic resonance. Magn Reson Med 1999b; 41: 329-33.

Floris S, Blezer EL, Schreibelt G, Dopp E, van der Pol SM, Schadee-Eestermans IL, et al. Blood-brain barrier permeability and monocyte infiltration in experimental allergic encephalomyelitis: a quantitative MRI study. Brain 2004; 127: 616-27.

Gonzalez-Amaro R, Sanchez-Madrid F. [Intercellular adhesion molecules and chemotaxic factors in the pathogenesis of multiple sclerosis]. Rev Neurol 2002; 35: 985-93.

Gordon S. Alternative activation of macrophages. Nat Rev Immunol 2003; 3: 23-35.

Hickey WF. Leukocyte traffic in the central nervous system: the participants and their roles. Semin Immunol 1999; 11: 125-37.

Hinds KA, Hill JM, Shapiro EM, Laukkanen MO, Silva AC, Combs CA, et al. Highly efficient endosomal labeling of progenitor and stem cells with large magnetic particles allows magnetic resonance imaging of single cells. Blood 2003; 102: 867-72.

Hoff EI, oude Egbrink MG, Heijnen VV, Steinbusch HW, van Oostenbrugge RJ. In vivo visualization of vascular leakage in photochemically induced cortical infarction. J Neurosci

Methods 2005; 141: 135-41.
Junt T, Moseman EA, Iannacone M, Massberg S, Lang PA, Boes M, et al. Subcapsular sinus macrophages in lymph nodes clear lymph-borne viruses and present them to antiviral B cells. Nature 2007; 450: 110-4.
Kleinschnitz C, Bendszus M, Frank M, Solymosi L, Toyka KV, Stoll G. In vivo monitoring of macrophage infiltration in experimental ischemic brain lesions by magnetic resonance imaging. J Cereb Blood Flow Metab 2003; 23: 1356-61.
Lassmann H. Basic mechanisms of brain inflammation. J Neural Transm Suppl 1997; 50: 183-90.
Lee VM, Burdett NG, Carpenter A, Hall LD, Pambakian PS, Patel S, et al. Evolution of photochemically induced focal cerebral ischemia in the rat. Magnetic resonance imaging and histology. Stroke 1996; 27: 2110-8; discussion 2118-9.
Manninger SP, Muldoon LL, Nesbit G, Murillo T, Jacobs PM, Neuwelt EA. An exploratory study of ferumoxtran-10 nanoparticles as a blood-brain barrier imaging agent targeting phagocytic cells in CNS inflammatory lesions. AJNR Am J Neuroradiol 2005; 26: 2290-300.
McAteer MA, Sibson NR, von Zur Muhlen C, Schneider JE, Lowe AS, Warrick N, et al. In vivo magnetic resonance imaging of acute brain inflammation using microparticles of iron oxide. Nat Med 2007; 13: 1253-8.
Mendonca Dias MH, Lauterbur PC. Ferromagnetic particles as contrast agents for magnetic resonance imaging of liver and spleen. Magn Reson Med 1986; 3: 328-30.
Metz S, Bonaterra G, Rudelius M, Settles M, Rummeny EJ, Daldrup-Link HE. Capacity of human monocytes to phagocytose approved iron oxide MR contrast agents in vitro. Eur Radiol 2004; 14: 1851-8.
Neumann E, Schaefer-Ridder M, Wang Y, Hofschneider PH. Gene transfer into mouse lyoma cells by electroporation in high electric fields. Embo J 1982; 1: 841-5.
Phillips MJ, Needham M, Weller RO. Role of cervical lymph nodes in autoimmune encephalomyelitis in the Lewis rat. J Pathol 1997; 182: 457-64.
Price CJ, Warburton EA, Menon DK. Human cellular inflammation in the pathology of acute cerebral ischaemia. J Neurol Neurosurg Psychiatry 2003; 74: 1476-84.
Rausch M, Baumann D, Neubacher U, Rudin M. In-vivo visualization of phagocytotic cells in rat brains after transient ischemia by USPIO. NMR Biomed 2002; 15: 278-83.
Rausch M, Hiestand P, Baumann D, Cannet C, Rudin M. MRI-based monitoring of inflammation and tissue damage in acute and chronic relapsing EAE. Magn Reson Med 2003; 50: 309-14.
Rausch M, Sauter A, Frohlich J, Neubacher U, Radu EW, Rudin M. Dynamic patterns of USPIO enhancement can be observed in macrophages after ischemic brain damage. Magn Reson Med 2001; 46: 1018-22.
Raynal I, Prigent P, Peyramaure S, Najid A, Rebuzzi C, Corot C. Macrophage endocytosis of superparamagnetic iron oxide nanoparticles: mechanisms and comparison of ferumoxides and ferumoxtran-10. Invest Radiol 2004; 39: 56-63.
Renshaw PF, Owen CS, McLaughlin AC, Frey TG, Leigh JS, Jr. Ferromagnetic contrast agents: a new approach. Magn Reson Med 1986; 3: 217-25.
Saini S, Stark DD, Hahn PF, Wittenberg J, Brady TJ, Ferrucci JT, Jr. Ferrite particles: a superparamagnetic MR contrast agent for the reticuloendothelial system. Radiology 1987; 162: 211-6.
Saleh A, Wiedermann D, Schroeter M, Jonkmanns C, Jander S, Hoehn M. Central nervous system inflammatory response after cerebral infarction as detected by magnetic resonance imaging. NMR Biomed 2004; 17: 163-9.
Serafini B, Rosicarelli B, Franciotta D, Magliozzi R, Reynolds R, Cinque P, et al. Dysregulated Epstein-Barr virus infection in the multiple sclerosis brain. J Exp Med 2007; 204: 2899-912.
Shapiro EM, Skrtic S, Sharer K, Hill JM, Dunbar CE, Koretsky AP. MRI detection of single particles for cellular imaging. Proc Natl Acad Sci U S A 2004; 101: 10901-6.

Simon GH, Bauer J, Saborovski O, Fu Y, Corot C, Wendland MF, et al. T1 and T2 relaxivity of intracellular and extracellular USPIO at 1.5T and 3T clinical MR scanning. Eur Radiol 2006; 16: 738-45.

Stroh A, Zimmer C, Gutzeit C, Jakstadt M, Marschinke F, Jung T, et al. Iron oxide particles for molecular magnetic resonance imaging cause transient oxidative stress in rat macrophages. Free Radic Biol Med 2004; 36: 976-84.

Stroh A, Zimmer C, Werner N, Gertz K, Weir K, Kronenberg G, et al. Tracking of systemically administered mononuclear cells in the ischemic brain by high-field magnetic resonance imaging. Neuroimage 2006.

Walczak P, Kedziorek D, Gilad AA, Lin S, Bulte JW. Magnetoelectroporation: ultrafast, one-step magnetic labeling of non-phagocytic cells without the need for transfection agents. 13th Annual Meeting of ISMRM. Miami:

, 2005a: 132617.

Walczak P, Kedziorek DA, Gilad AA, Lin S, Bulte JW. Instant MR labeling of stem cells using magnetoelectroporation. Magn Reson Med 2005b; 54: 769-74.

Watson BD, Dietrich WD, Busto R, Wachtel MS, Ginsberg MD. Induction of reproducible brain infarction by photochemically initiated thrombosis. Ann Neurol 1985; 17: 497-504.

Weissleder R, Elizondo G, Wittenberg J, Rabito CA, Bengele HH, Josephson L. Ultrasmall superparamagnetic iron oxide: characterization of a new class of contrast agents for MR imaging. Radiology 1990; 175: 489-93.

Weissleder R, Stark DD, Engelstad BL, Bacon BR, Compton CC, White DL, et al. Superparamagnetic iron oxide: pharmacokinetics and toxicity. AJR Am J Roentgenol 1989; 152: 167-73.

Xu S, Jordan EK, Brocke S, Bulte JW, Quigley L, Tresser N, et al. Study of relapsing remitting experimental allergic encephalomyelitis SJL mouse model using MION-46L enhanced in vivo MRI: early histopathological correlation. J Neurosci Res 1998; 52: 549-58.

Yeager MP, DeLeo JA, Hoopes PJ, Hartov A, Hildebrandt L, Hickey WF. Trauma and inflammation modulate lymphocyte localization in vivo: quantitation of tissue entry and retention using indium-111-labeled lymphocytes. Crit Care Med 2000; 28: 1477-82.

Zelivyanskaya ML, Nelson JA, Poluektova L, Uberti M, Mellon M, Gendelman HE, et al. Tracking superparamagnetic iron oxide labeled monocytes in brain by high-field magnetic resonance imaging. J Neurosci Res 2003; 73: 284-95.

Summary

In this thesis, the use of magnetic resonance imaging (MRI) is described as a tool to study neuroinflammatory processes and more specifically the infiltration of monocytes in the central nervous system (CNS) in an animal model of multiple sclerosis (MS). The non-invasive character of MRI together with recent developments in the synthesis of contrast agents, provide the opportunity to perform cell tracking studies. Cellular MRI will improve our knowledge on the dynamic process of monocyte migration and may lead to effective treatment protocols for drugs that limit monocyte entry during neuroinflammation. Here, we summarize our main findings of the research described in this thesis.

In **chapter 1** the consequences of neuroinflammation with respect to MS are explained. Especially monocytes play a key role in the underlying cellular pathology, and the study of monocyte migration in vivo would benefit from a non-invasive imaging strategy. Here, the concept of cellular MRI is introduced using superparamagnetic particles of iron oxide (SPIO), which allow visualisation of monocytes by MRI.

Chapter 2 describes the initial labeling experiments for human monocytes with SPIO and ultra small SPIO (USPIO). Histological analysis and MR validation showed that monocytes are labeled more efficiently using the larger SPIO compared to USPIO. We optimized the protocol for monocytes with respect to incubation time and iron concentration. Results indicated that ex vivo labeling of human monocytes with SPIO allows detection by MRI without compromising important physiological cell functions like cell viability, migratory capacity and cytokine production.

In **chapter 3,** we used the monocyte labeling technique described in chapter 2 to label freshly isolated rat monocytes. Cell tracking experiments were performed in a rat model for neuroinflammation and we directly compared two main approaches of in vivo monocyte imaging: (1) Intravenous injection of monocytes that were labeled ex vivo with SPIO versus (2) the administration of free iron oxide particles. We demonstrated the proof of principle using method 1 for longitudinal MR detection of SPIO-labeled monocytes that migrate towards an inflammatory site in the brain. Moreover, the use of free iron oxide particles, method 2, resulted in an early decrease of signal intensity in the lesion (2 hours) and pointed to the detection of blood-brain barrier (BBB) leakage instead of monocyte migration.

For optimal detection and tracking of monocytes by MRI in rats with experimental autoimmune encephalomyelitis (EAE, animal model for MS), in **chapter 4** we introduced a novel labeling strategy: Magneto-Electroporation (MEP). Best labeling results were obtained using small and charged iron oxide particles. Importantly, intravenous injection of monocytes labeled with USPIO using MEP resulted in multiple foci of signal loss, predominantly in the white matter of the cerebellum in EAE rats. Our study indicated that MEP is essential to visualize the dynamic process of monocyte infiltration in pathologies with multiple small lesions in the CNS, as in case of MS.

Complementary to our previous studies, in **chapter 5** we focused on the administration of free USPIO in EAE rats to gain a better insight in the pathological processes in the CNS, as detected by the presence of USPIO. We found that USPIO enter the brain parenchyma of EAE rats within 1 hour whereas at 72 hours after injection, MR abnormalities were no longer present in the CNS. Subsequent imaging of the cervical lymph nodes revealed USPIO accumulation. Our data emphasizes the fact that the process of leakage over the BBB has to be considered next to cellular infiltration when interpreting post-USPIO MR images. Moreover, in this study we identified the potential use of USPIO-enhanced MRI to study non-invasively drainage in the inflammatory brain.

A major advantage of the use of iron oxide particles as MR contrast agents is that a number of USPIO is clinically approved. Ultimately in **chapter 6**, changing from an experimental to a clinical setting, we administered a novel USPIO to MS patients and compared enhancement patterns in the brain with enhancement obtained after conventional Gd-DTPA injections. We showed that USPIO enhancements were more frequently observed and several types of enhancement patterns could be distinguished and correlated to certain stages of lesion development. USPIO-enhanced MRI is a valuable tool to study the multiple aspects of inflammation in MS patients and may be applied as a diagnostic tool in the near future.

Visualisatie van Monocyten Infiltratie in een Diermodel van Multiple Sclerose met Magnetic Resonance Imaging

Het onderzoek beschreven in dit proefschrift richt zich op de ontwikkeling van technieken voor de visualisatie van monocyten (immuuncellen) tijdens ontstekingsprocessen in de hersenen. Monocyten zijn verantwoordelijk voor weefselschade aan het centrale zenuwstelsel (CZS) in neurologische aandoeningen zoals multiple sclerose (MS). Het is van groot belang inzicht te krijgen waar en wanneer deze cellen het CZS binnenkomen tijdens de ziekte. Het blootleggen van dit schadelijke proces in MS zal uiteindelijk bijdragen aan de ontwikkeling van ontstekingsremmende medicijnen waarmee gericht en op het juiste moment ingegrepen kan worden.
Om deze cellen te visualiseren wordt er gebruik gemaakt van de techniek magnetic resonance imaging (MRI) en procedures om monocyten te labelen met specifieke MRI-contrastmiddelen. Het non-invasieve karakter van MRI maakt het mogelijk om de infiltratie van monocyten op verschillende plaatsen in het CZS en in de tijd te bestuderen.

De monocyt als ontstekingscel
MS is een aandoening van het CZS waarbij ontstekingen in de hersenen en het ruggenmerg resulteren in verlammingsverschijnselen. Onderzoek in autopsie breinen van MS patiënten heeft uitgewezen dat op meerdere plekken de myeline schede is aangetast (demyelinisatie). Deze isolerende laag beschermt normaliter de uitlopers van zenuwcellen en is onmisbaar voor een goede geleiding van zenuwimpulsen. Demyelinisatie is het gevolg van een verstoring van het immuunsysteem waarbij bepaalde bestanddelen van het myeline als lichaamsvreemd worden beschouwd en afgebroken. Aandoeningen waarbij het afweersysteem van het lichaam zich tegen lichaamseigen structuren richt, wordt een autoimmuunziekte genoemd. Het is nog onbekend wat de autoimmuniteit in MS veroorzaakt, maar mogelijke factoren zijn van genetische aard of vinden hun oorsprong in virus infecties. Het is wel aangetoond dat de aanwezigheid van witte bloedcellen, en voornamelijk monocyten en T-cellen, een grote rol speelt in de ontwikkeling van deze ontstekingshaarden (laesies) in het CZS. In de laesies van MS patiënten zijn macrofagen (geactiveerde monocyten) aangetoond die afgebroken stukjes myeline bevatten. Dit benadrukt de rol van monocyten tijdens een ontsteking als effectorcel die het weefsel schade berokkent.
Een belangrijke gebeurtenis tijdens de vorming van laesies in MS patiënten, is het binnendringen van monocyten in het CZS vanuit de bloedbaan. Hiertoe moeten monocyten een gespecialiseerde grenslaag van cellen

oversteken, de bloed-hersen-barrière (BHB). In gezonde toestand voorkomt de BHB dat bepaalde bestanddelen uit de bloedcirculatie het CZS kunnen betreden. Tijdens MS is de BHB op verschillende plaatsen aangetast en kunnen cellen vanuit de bloedbaan het CZS binnendringen. Het bestuderen van monocyten infiltratie levert belangrijke aanknopingspunten op voor het ontrafelen van het ontstekingsmechanisme. Zo is uit voorgaand onderzoek gebleken dat specifieke eiwitten (adhesiemolekulen) op de BHB het binnendringen van circulerende monocyten vergemakkelijkt. Tot op heden is informatie over de rol van monocyten voornamelijk gebaseerd op histologisch onderzoek. Het grote nadeel van dit soort onderzoek is dat het een momentopname op één locatie betreft van de ontsteking zonder duidelijkheid te verschaffen over het verloop. De migratie van monocyten is een dynamisch proces en om dit goed in kaart te brengen is de ontwikkeling van een non-invasieve visualisatie techniek van groot belang.

Doel van het onderzoek

- Ontwikkeling en optimalisering van een labelingstechniek voor monocyten zodat deze cellen gedetecteerd kunnen worden met MRI.
- Toepassing van deze strategie in een diermodel van MS om de migratie van monocyten tijdens het verloop van deze ziekte te bestuderen.

Beeldvorming op cel niveau

In de kliniek wordt MRI voornamelijk gebruikt als beeldvormingstechniek om afwijkingen in de hersenen te detecteren op weefsel niveau. Zo kunnen bijvoorbeeld de laesies in de hersenen van MS patiënten worden opgespoord. De verantwoordelijke ontstekingscellen zijn echter onmogelijk waar te nemen met standaard MRI technieken. Dankzij de recente ontwikkeling binnen het MRI onderzoek is het nu ook mogelijk om cellen met MRI te onderscheiden. Hierbij worden cellen gelabeld met ijzeroxide bevattende contrastmiddelen. Deze ijzerhoudende deeltjes worden 'superparamagnetic particles of iron oxide' (SPIO; als hun diameter groter is dan 50nm) genoemd of 'ultra small SPIO' (USPIO; diameter tot 50nm). Het binnenste van deze deeltjes is opgebouwd uit ijzeroxide molekulen die lokaal het magneetveld kunnen verstoren en daarmee het MRI signaal verlagen. Cellen die ijzeroxide deeltjes bevatten zullen daarom een signaalverandering veroorzaken en zichtbaar worden op een MRI scan als donkere vlekjes.

Om monocyten te visualiseren met MRI is het van belang dat de cellen deze ijzerdeeltjes opnemen, een proces dat cellabeling wordt genoemd. In **hoofdstuk 2** beschrijven wij een labelingsprocedure voor humane monocyten en wordt de labelingsefficiëntie van verschillende ijzeroxide deeltjes bestudeerd. Voor een optimaal MRI detectie niveau moeten monocyten zo efficiënt mogelijk gelabeld worden met ijzeroxide deeltjes zonder dat dit

ten koste gaat van het 'normale' functioneren van de cel. In vitro MRI in combinatie met celkleuringen van de gelabelde monocyten toonden aan dat de labelingsefficiëntie met SPIO vele malen hoger ligt dan met USPIO. Een evenzo belangrijke bevinding is dat deze labelingsconditie geen nadelig effect heeft op (1) cel viabiliteit, (2) migratie capaciteit en (3) de activatie status van monocyten. Concluderend hebben we in **hoofdstuk 2** laten zien dat monocyten efficiënt gelabeld kunnen worden met ijzeroxide deeltjes zonder dat dit ten koste gaat van de fysiologische functie. Deze strategie biedt de mogelijkheid om de migratie van monocyten in vivo te bestuderen.

Visualisatie van monocyten in de hersenen

'Proof of principle'

Om te testen of gelabelde monocyten in vivo gedetecteerd kunnen worden, hebben wij in eerste instantie in **hoofdstuk 3** gebruik gemaakt van ratten met een photothrombotisch (PT) herseninfarct. Dit diermodel van neuroinflammatie wordt gekenmerkt door een grote laesie in de cortex waarin een massale invasie van monocyten plaatsvindt. De labelingsprocedure, uitgewerkt in **hoofdstuk 2,** is hier toegepast om monocyten uit de rat te labelen met SPIO. Vervolgens zijn de SPIO-geladen monocyten intraveneus geïnjecteerd in PT ratten 5 dagen na laesie inductie. Een preinjectie MRI scan van de ratten hersenen is gevolgd door scans 24 en 72 uur later. Pas 72 uur na injectie van gelabelde monocyten werd een duidelijke verlaging van signaalintensiteit in de corticale laesie waargenomen. Histologisch onderzoek naderhand wees uit dat het aangetaste stukje hersenen een aantal SPIO-geladen cellen bevatte. Een belangrijke boodschap van deze studie is dat we SPIO-geladen monocyten non-invasief met MRI kunnen detecteren zodra zij vanuit de bloedbaan de hersenen binnentreden.

Ex vivo versus in vivo labeling strategie

Naast het terugspuiten van ex vivo gelabelde monocyten, zoals beschreven in de vorige paragraaf, is het 'in vivo labelen' een alternatieve strategie om monocyten activiteit te bestuderen met MRI. Hierbij worden ijzeroxide deeltjes (voornamelijk USPIO) direct in de bloedbaan gespoten waarna opname door circulerende monocyten kan plaatsvinden. Hoewel dit een aantrekkelijke labelingsprocedure lijkt, kleven er een aantal nadelen aan. De mogelijkheid bestaat dat de ijzerdeeltjes in ongebonden staat de laesie in lekken over een aangetaste BHB. Feitelijk verschaffen ze dan geen informatie over de migratie van cellen. Anderzijds bestaat het risico dat de partikels opgenomen worden door andere cellen. Tot op heden is er weinig bekend over acute USPIO kinetiek en in vivo opname in diermo-

dellen van neuroinflammatie.
Daarom hebben wij in **hoofdstuk 3** deze in vivo labelingsmethode (USPIO injectie) rechtstreeks vergeleken met de ex vivo labelingsmethode (SPIO-geladen monocyten injectie) in PT ratten. Op MRI scans die elk half uur werden uitgevoerd na USPIO injectie ontdekten wij dat de signaalintensiteit in de corticale laesie al veranderde na 2 uur, wat duidt op lekkage van ijzeroxide deeltjes over de BHB. Dit in tegenstelling tot de bevindingen na de injectie van SPIO-gelabelde monocyten waarbij er pas na 72 uur 'donkere vlekken' in de laesie werden geregistreerd. De boodschap van **hoofdstuk 3** is tweeledig: (1) na intraveneuze toediening migreren SPIO-gelabelde monocyten naar een ontsteking in de hersenen en dit proces kan gevolgd worden met MRI. (2) Bij intraveneuze toediening van vrije USPIO moet rekening gehouden worden met een substantiële bijdrage van lekkende ijzeroxide partikels aan de verandering van het MRI signaal in ontstekingsgebieden. Dit laatste aspect is in **hoofdstuk 5** nader bestudeerd in het licht van het MS diermodel.

Het volgen van gelabelde monocyten in een diermodel voor MS
Om de migratie van monocyten te bestuderen tijdens het ziekteverloop van MS hebben we vervolgens de strategie uit **hoofdstuk 3** toegepast in een diermodel voor MS, experimental autoimmune encephalomyelitis (EAE). Op weefsel niveau wordt EAE gekenmerkt door BHB beschadigingen en de aanwezigheid van celinfiltraten in de hersenen welke resulteren in verlammingsverschijnselen. Zowel aan het begin van de ziekte als op de piek van de ziekte zijn in ratten met EAE, monocyten geïnjecteerd die ex vivo gelabeld waren met SPIO. Op geen van de MRI scans die volgden in de tijd zijn gebieden met verlaagde signaalintensiteit waargenomen in de hersenen van deze EAE ratten. Een mogelijke verklaring voor de negatieve resultaten is de aanwezigheid van meerdere kleine laesies verspreid door het CZS in dit model (in vergelijking met één locale grotere laesie in PT ratten), waarover de gelabelde monocyten zich moeten verdelen. Dit houdt in dat mogelijk slechts enkele gelabelde monocyten zich ophopen in een klein ontstekingsgebied en als gevolg daarvan is de verandering in MRI signaal te klein om te detecteren. Waarschijnlijk is de efficiëntie van de toegepaste labeling strategie niet goed genoeg om monocyten infiltratie in het EAE model te bestuderen.
Om de monocyten effectiever te labelen en daarmee de MRI detectie limiet te verhogen, is in **hoofdstuk 4** een nieuwe labeling strategie voor monocyten toegepast: magneto-electroporatie (MEP). Deze techniek is gebaseerd op het gegeven dat een elektrische stroom stoot, die heel kort aan de cellen wordt gegeven, de celmembraan korte tijd doorlaatbaar maakt voor contrastmiddelen in het medium. Onze resultaten hebben uitgewezen dat met de juiste parameters (voltage, pulsduur) en het gebruik van kleine

geladen ijzeroxide deeltjes, monocyten uit de rat binnen afzienbare tijd (milliseconden) gelabeld kunnen worden zonder de cel viabiliteit aan te tasten. Injectie van deze gelabelde monocyten in ratten met EAE resulteerde op de MRI scans, 24 en 72 uur later, in de aanwezigheid van kleine donkere vlekjes verspreid door het CZS. Quantificatie van deze signaalafwijkingen liet zien dat er een duidelijke toename was na injectie tijdens de piek van de ziekte in vergelijking met injecties aan de start van de ziekteverschijnselen. De belangrijkste boodschap van deze studie is dat MEP een waardevolle labelingstechniek is en daarbij essentieel om de migratie van monocyten als dynamisch proces te visualiseren in neurologische aandoeningen met een diffuus laesie patroon, zoals in MS.

Injectie van vrije ijzeroxide deeltjes: van rat naar mens
Uit eerder onderzoek naar USPIO injecties in ratten met EAE is gebleken dat deze partikels na 24 uur gedetecteerd worden in het CZS. De aanwezigheid van deze USPIO positieve gebieden correleerde met de activiteit van immuuncellen en laesie vorming. Om MRI beelden na USPIO injecties juist te interpreteren is het van groot belang om de achterliggende USPIO dynamiek in vivo te bestuderen. Daartoe hebben wij in hoofdstuk 5 gekeken naar USPIO effecten in het CZS van EAE ratten direct na injectie (0 – 6 uur) en op de langere termijn (24 en 72 uur). Hieruit kwamen een aantal belangrijke zaken aan het licht: (1) MRI scans direct na inspuiten lieten de donkere vlekken al 1 uur na USPIO injectie zien in het CZS en er werden grote overeenkomsten geconstateerd met Gd-DTPA lekkage, een conventionele MRI marker voor BHB schade. (2) Op MRI beelden 72 uur na injectie werd geen enkel USPIO effect meer in het CZS gedetecteerd, wat zou kunnen duiden op een afvoermechanisme van ijzeroxide partikels in de hersenen. (3) MRI van de cervicale lymfe-klieren toonde een accumulatie van USPIO voornamelijk 72 uur na injectie aan de start van de ziekte. Uit eerder onderzoek is gebleken dat cervicale lymfe-klieren een belangrijke rol spelen in het ontwikkelen van een autoimmuun reactie in EAE ratten en mogelijk ook in MS patiënten. Ons resultaat wijst erop dat USPIO in de hersenen mogelijk gedraineerd worden door de cervicale lymfe-klieren en dat dit proces non-invasief gevolgd kan worden met MRI. Samenvattend voor USPIO in de dierexperimentele setting, kunnen we zeggen dat USPIO in de acute fase zich voornamelijk gedragen als marker voor BHB schade. Daarnaast zouden USPIO heel goed van pas kunnen komen om andere facetten in de MS pathogenese te bestuderen, zoals antigeen presentatie in lymfe-klieren.

Een groot voordeel van het gebruik van USPIO in het onderzoek naar neurologische aandoeningen is dat een aantal ijzeroxide deeltjes zijn goedgekeurd om aan mensen toe te dienen. Zo hebben wij in **hoofdstuk 6**

recentelijk ontwikkelde en goedgekeurde USPIO intraveneus toegediend aan MS patiënten en onderzoek gedaan naar de samenhang van USPIO aankleuring en laesie ontwikkeling. Uit dit onderzoek is gebleken dat USPIO meer gebieden in hersenen van MS patiënten aankleurden dan het conventionele contrastmiddel Gd-DTPA. Een andere belangrijke ontdekking was dat de USPIO aankleuringen in verschillende patronen verschenen die gedeeltelijk gecorreleerd konden worden aan het verdere verloop van de laesie ontwikkeling. Uit deze studie komt duidelijk naar voren dat USPIO MRI in MS patiënten een waardevol instrument is om het ontstekingsmechanisme te onderzoeken en zou in de toekomst mogelijk ingezet kunnen worden als diagnose en prognose techniek.

List of publications

Papers

Raoul D. Oude Engberink, Susanne M.A. van der Pol, Ed A. Dopp, Helga E. de Vries, Erwin L.A. Blezer. Comparison of SPIO and USPIO for in vitro labeling of human monocytes: MR detection and cell function. *Radiology 2007; 243(2):467-74.*

Raoul D. Oude Engberink, Erwin L.A. Blezer, Erik I. Hoff, Susanne M.A. van der Pol, Annette van der Toorn, Rick M. Dijkhuizen, Helga E. de Vries. MRI of monocyte infiltration in an animal model of neuroinflammation using SPIO-labeled monocytes or free USPIO. *J Cereb Blood Flow Metab. 2007 Nov 14th; In press.*

Raoul D. Oude Engberink, Erwin L.A. Blezer, Susanne M.A. van der Pol, Annette van der Toorn, Christine D. Dijkstra, Helga E. de Vries. Dynamics and fate of USPIO in the central nervous system in experimental autoimmune encephalomyelitis. *Submitted.*

Raoul D. Oude Engberink, Piotr Walczak, Susanne M.A. van der Pol, Jeff W.M. Bulte, Helga E. de Vries, Erwin L.A. Blezer. Magnetic Resonance Imaging of Monocytes Labeled with USPIO using Magneto Electroporation in an Animal Model of Multiple Sclerosis. *In preparation.*

Machteld M. Vellinga, **Raoul D. Oude Engberink**, Alexandra Seewann, Petra J.W. Pouwels, Michael P.Wattjes, Susanne M.A. van der Pol, Christiane Pering, Chris H. Polman, Helga E. de Vries HE, Jeroen J.G. Geurts, Frederik Barkhof. Pluriformity of inflammation in multiple sclerosis shown by ultra small iron oxide enhancement. *Brain 2008 Feb 1st; In press.*

International Conference Proceedings (first author only)

Ex vivo labeling of primary monocytes with ultra small particles of iron oxide using different transfection agents. **Raoul D. Oude Engberink**, Susanne M.A. van der Pol, Ed A. Dopp, Chantal Renardel de Lavalette, Helga E. de Vries, Erwin L.A. Blezer. *7th International Congress of Neuroimmunology: Journal of Neuroimmunology, 2004.*

Ex vivo labeling of monocytes for in vivo cell tracking using MR imaging. **Raoul D. Oude Engberink**, Susanne M.A. van der Pol, Ed A. Dopp, Chantal Renardel de Lavalette, Helga E. de Vries, Erwin L.A. Blezer. *VII. European Meeting on Glial Cell Functions in Health and Disease, 2005.*

MR imaging of rat monocytes homing towards an area of cerebral infarction. **Raoul D. Oude Engberink**, Erik I. Hoff, Susanne M.A. van der Pol, Chantal Renardel, Erwin L.A. Blezer, Helga E. de Vries. *Proceedings Annual Meeting ISMRM 2006*.

Comparison of SPIO and USPIO for in vitro labelingof human monocytes with respect to MR detection and cellular activation status. **Raoul D. Oude Engberink**, Susanne M.A. van der Pol, Ed A. Dopp, Helga E. de Vries, Erwin L.A. Blezer. *Proceedings Annual Meeting ISMRM 2006*.

MR imaging of monocyte infiltration into the central nervous system in animal models of neuroinflammation. **Raoul D. Oude Engberink**, Erwin L.A. Blezer, Erik I. Hoff, Susanne M.A. van der Pol, Helga E. de Vries. *8th International Congress of Neuroimmunology. Journal of Neuroimmunology*, 2006

Iron oxide labeling of primary rat monocytes using magneto electroporation. **Raoul D. Oude Engberink**, Piotr Walczak, Helga E. de Vries, Erwin L.A. Blezer, Jeff, W.M. Bulte. *Proceedings Annual Meeting ISMRM 2007*.

Cellular MRI of monocyte infiltration: In vitro versus in vivo labeling. **Raoul D. Oude Engberink**, Erwin L.A. Blezer, Erik I. Hoff, Susanne M.A. van der Pol, Helga E. de Vries. *Proceedings Annual Meeting ISMRM 2007*.

USPIO dynamics in an animal model of multiple sclerosis. **Raoul D. Oude Engberink**, Susanne M.A. van der Pol, Helga E. de Vries, Erwin L.A. Blezer. *Proceedings Annual Meeting ISMRM 2007*.

Dankwoord

...'t komt allemaal goed. Een mooie uitspraak die ik de afgelopen jaren vaak heb gedaan en waar ik uiteindelijk ook zelf in ben gaan geloven. Dat er nu een goed proefschrift ligt, heb ik te danken aan een heleboel mensen om mij heen. Ik ben blij dat ik mij nu tot jullie kan richten; iedereen die mijn promotietraject tot een succesvolle en onvergetelijke tijd heeft gemaakt, muchas gracias! En natuurlijk wil ik graag aan een aantal mensen wat regels in het bijzonder wijden.

Veel dank gaat zeker uit naar mijn twee begeleiders, Erwin en Elga. Wie had dat ooit gedacht Erwin, een toevallige ontmoeting in de rij voor de saucijzenbroodjes die uiteindelijk heeft geleid tot een laudatio in het academiegebouw. Bedankt voor alle MRI-expertise, praktische vaardigheden en tijd (en dat was nogal wat he!) die je in me hebt gestoken. Bijkomend voordeel was dat ik meestal niet meer bijkwam van je grappen, we een gedeelde passie voor mobiele telefoons hadden en we allebei heel goed zwart van grijs konden onderscheiden (op een schaal van 1 op 10 een dikke 10 dus). In één woord: Prachtig!
Elga, aan Amsterdamse zijde en binnen de wondere wereld van 'cell labeling' heb je mij op een fijne manier begeleid. Mede dankzij jouw goede focus en richtlijnen hebben we mooie resultaten geboekt. Nooit gedacht dat een zweepje in de wetenschap nog van pas zou komen. Dank voor alle goede aanwijzingen en motiverende gesprekken! Naast mijn twee toegewijde begeleiders mag ik mij ook gelukkig prijzen met twee promotoren, Max en Christine. In jullie beide groepen heb ik met veel plezier gewerkt.

Werkplek 1: In vivo NMR, Utrecht.
JEDI, m'n favoriete collega! Vanaf het allereerste uur vormden wij toch wel het aio-fundament van de afdeling. Ik zal het allemaal missen, je ochtendhumeur, de middelvingers en al het aio-lief-en-leed dat we gedeeld hebben tijdens talloze senseo-sessies. Nu we het toch over leed hebben, kom ik al snel bij Maurits terecht. Van Meer: Ik ben blij dat wij elkaar begrijpen en goed kunnen genieten van elkaars ellende en rampspoed. Dank voor alle inspirerende momenten, wie weet treffen wij elkaar echt nog eens om 08:45. Voor de zekerheid blijf ik de schoorsteen checken. Gerard, jij bent een uitstekende collega en ik kon altijd met vanalles bij je terecht, van gecrashte computersystemen tot vervelende maagklachten. Jij hebt een fijne positieve kijk op het leven en dat is precies wat ik soms nodig had. Annette, het is niet niks om twee state of the art MRI-scanners draaiende te houden en daarnaast ook nog eens in te gaan op onze last-minute verzoekjes die veelal de strekking hadden van '... hij doet 't niet meer'. Dank voor alle hulp. Beste Rick, Ona, Kajo, Mark, Wim, Kim, Li-

sette, Ivo, Angga, Pieter, Casper, de cardio's en alle studenten: De In vivo NMR is allang geen klein clubje meer! Ik heb veel gehad aan alle wetenschappelijke input, software, taal en godsdienst lessen, flauwekul-opmerkingen, micro- dan wel macro-borrels en overbodige wandversieringen (fijn dat mijn altaar er nog staat). Erik, jou zou ik graag even apart noemen. Maastricht ligt namelijk ook niet naast de deur. Ik wil je bedanken voor onze geweldige marathon aan photothrombose-laser operaties, gevolgd door nachtelijke port-sessies. Een winnende combinatie, dat blijkt wel uit die top-paper die eruit is voortgekomen. Verder wil ik een aantal mensen noemen die altijd erg behulpzaam waren bij het soepel verlopen van dierexperimenten als ik weer eens wat wijzigingen had die vrij acuut (hoe kan het ook anders) doorgevoerd moesten worden. Planning is nooit m'n sterkste punt geweest, Romy, Harry, Harut en alle GDL medewerkers, bedankt.
Aan de andere kant van de busbaan, het UMC Utrecht waarbinnen ik nog een aantal mensen wil bedanken. Jan-Henry, jammer dat je zover weg gaat, maar zwarte vlekken kunnen ook zeker mooi wit worden. Nicky, Lisa, Annemarieke, Seevinck, Wilbert, Wouter en nog een heleboel anderen binnen het ISI, dank voor het luisteren naar mijn presentaties over zwarte vlekken (ze zijn er echt), de small talk, zwetende spinsessies en natuurlijk onze ISMRM-nachten.

Werkplek 2: MCBI, VU, Amsterdam.
Voor veel van het belangrijke celwerk en histologische validatie, of gewoon als ik even genoeg had van al het ge-MRI, was ik vaak op de VU te vinden. Susanne, jouw naam staat op alle papers... en dat is natuurlijk niet voor niks. Dank voor al je inspanningen bij al onze experimenten; ik denk dat we een prachtige balans hebben gevonden tussen jouw strakke planning en mijn chaotische flexibiliteit! Mijn aio-kamer, vrijstaat J296 en zijn inwoners, daar kan ik nog hele boekwerken over schrijven. Ik voelde me daar meteen thuis tussen alle (an)aerobe processen op de vloer en al het bestek in het plafond. Esther en Irene, hoewel jullie nu beregezellig bij mij op het GDL zitten, was het al op de VU met jullie één groot feest. Ireen, ik vind je niet meer eng en Esther, wij gaan er inderdaad deze zomer erg goed uitzien! Gerben, jij hebt me fantastisch geholpen met veel computer en plaatjes geshizzle (zie pag. 11) in de afgelopen jaren, muchas gracias. Die lauwe halve liters in het Vondelpark doen we zeker nog een keer. Marijn en Ruben, zonder jullie geen gezelligheid, aan jullie de eer om deze kamer in zijn huidige staat te behouden.

Ik wil graag ook de hele blauwe groep bedanken voor alle kritische vragen en bruikbare tips in het onderzoek, maar voornamelijk voor de relaxte en laagdrempelige sfeer die het voor mij een stuk makkelijker maakten. Gijs

jongen, we hebben er een mooie tijd van gemaakt... en hij is nog lang niet voorbij. Succes met jouw afronding, enne ik wacht op je Nature-publicatie. Jack, jij bent een must-have voor elk congres, en natuurlijk niet alleen voor je wetenschappelijke kwaliteiten. Arie, Sipke en alle anderen bedankt voor de fijne tijd.
Als we verder de afdeling oplopen, stonden ook daar altijd mensen voor me klaar bij het uitvoeren van experimenten, zowel 's ochtends als 's avonds. Ed, Eelco, Nico en Tom, dank voor de ondersteuning bij alle ratten-perfusies en onze ellenlange sort-sessies. Naast al het labwerk en besprekingen is DE koffie in de loop der jaren ook uitgegroeid tot een verplicht wetenschappelijk onderdeel van de dag. Dat was altijd lekker bijkomen en bijkletsen met veel collega's. Daarbij wil ik Mascha, Manja en Tanja bedanken voor alle aanstekelijke levendigheid of het nou overdag of 's nachts was, in het lab of uit het lab (of op zolder) en natuurlijk niet te vergeten in het Bruin Cafe. Lisa, Jasper, Rosalie, Mark, Marielle, de aio-weekenden waren fantastisch (de ochtend erna wat minder). Dat bowlen en boarden houden we er ook in! In mijn laatste jaar heb ik, aan de andere kant van de trambaan deze keer, erg fijn samengewerkt met een aantal mensen op het VUmc. Machteld, Jeroen, Petra, ik heb met veel plezier achter de humane scanner gezeten. Veel mensen uit het MS onderzoeks wereldje in binnen en buitenland, wil ik graag bedanken voor de vruchtbare discussies tijdens congressen, diners en (dansvloer) activiteiten.

Een deel van mijn onderzoek heb ik gedaan aan het Johns Hopkins in Baltimore. Een super ervaring! Dear Piotr, Dorota, Hanneke, Jesus, Chris, Jeff, thank you for showing me around and helping me out in the lab. I have had a wonderful time and I hope to see you guys again. Then, I will definitely eat some more crabs and we will finish that bottle of tequila!

Dit proefschrift kan natuurlijk niet verdedigd worden zonder de aanwezigheid van mijn twee goede vrienden en geweldige paranimfen, Victor en Sander. Victor, de avondjes Stockholm, het skaten en het stappen waren een noodzakelijke afwisseling in het onderzoek. Sander, voor jou staan de slavinken altijd klaar en we zijn nog lang niet uitgespeeld. Dank voor alle motiverende onderonsjes en ik ben onwijs blij dat jullie achter me staan! Voor de lay-out van mijn proefschrift wil ik hier graag Fred en Mea in het bijzonder noemen, die hier ook bijzonder veel tijd in hebben gestoken. Ik ben trots op het resultaat.

Buiten het onderzoekswereldje om wil ik ook nog een aantal mensen bedanken met wie ik altijd graag wijze woorden wissel, biertjes dan wel cocktails drink en andere buitenschoolse evenementen bezoek. Mara, wat kennen wij elkaar lang! Ik ben blij dat ik je nog vaak spreek en zie. We

moeten echt samen een keer een feest gaan geven. Wie weet kom ik ook wel naar het Zuiden. Jannes, Roy en Bas, verspreid door Nederland zie ik jullie veel te weinig, maar ik kijk zeker uit naar het volgende mannen-etentje. M'n oud-huisgenoten, Wilbert en Daan, prachtige gasten zijn jullie en het was altijd relaxed thuiskomen in m'n eerste aio-jaren. Liesbeth, Volkert, Simone, Jeanine en daarnaast mijn grenzeloze oud-bestuur en de oudledencommissie, bedankt!

Tot slot wil ik het woord richten aan mijn allerdierbaarsten. Pa, ma, ik kan niet onder woorden brengen hoe belangrijk jullie voor mij zijn. Dankzij jullie steun, vertrouwen en wijze raad heb ik het ooit zover kunnen schoppen. Ik hou van jullie en jullie kunnen op me rekenen. Zusje, ondanks dat ik je maar weinig spreek, waardeer ik alles wat je doet enorm en ben ik gewoon super blij dat jij er bent.
Lieve Janneke, hoe jij het met mij hebt uitgehouden is me nog steeds een groot raadsel. Samen zijn, samen wonen, samen eten, dat is niet altijd even makkelijk met een aio (zeker niet als die een presentatie moet geven de volgende ochtend). Dank voor al je liefde, warmte, begrip en ontspanningsoefeningen. Er is geen proefschrift dik genoeg om te beschrijven wat ik voor je voel. Je bent een prachtvrouw!

CURRICULUM VITAE

Raoul David Oude Engberink was born on June 11th 1978 in Leiden. He spent his childhood in Oud-Beijerland and attended the Erasmiaans Gymnasium in Rotterdam, graduating in 1996. He studied Chemistry at the Utrecht University and obtained his master degree at the department of Molecular Cell Biology studying the regulation of radical induced responses during the cell cycle. In 2003 he started a challenging PhD project combining two research areas at the Image Sciences Institute, University Medical Center Utrecht in de group of Prof.dr.ir. M.A. Viergever and at the department of Molecular Cell Biology and Immunology, VU medical center in de group of Prof.dr. C.D. Dijkstra. Under supervision of Dr.ir. E.L.A. Blezer and Dr. H.E. de Vries, he successfully optimized and applied cellular imaging in an animal model for Multiple Sclerosis. In this period he made a short research visit to the lab of Dr. J.W.M. Bulte at Johns Hopkins University School of Medicine, Baltimore, USA. The results of his research have been described in this thesis.